FROM GODUNOV TO A UNIFIED HYBRIDIZED DISCONTINUOUS GALERKIN FRAMEWORK FOR PARTIAL DIFFERENTIAL EQUATIONS

TAN BUI-THANH †

Abstract. By revisiting the basic Godunov approach for linear system of hyperbolic Partial Differential Equations (PDEs) we show that it is hybridizable. As such, it is a natural recipe for us to constructively and systematically establish a unified HDG framework for a large class of PDEs including those of Friedrichs' type. The unification is fourfold. First, it provides a single constructive procedure to devise HDG schemes for elliptic, parabolic and hyperbolic PDEs. Second, it reveals the nature of the trace unknowns as the Riemann solutions. Third, it provides a parameter-free HDG framework, and hence eliminating the "usual complaint" that HDG is a parameter-dependent method. Fourth, it allows us to construct the existing HDG methods in a natural manner. In particular, using the unified framework we can rediscover most of the existing HDG methods and furthermore discover new ones.

We apply the proposed unified framework to three different PDEs: the convection-diffusion-reaction equation, the Maxwell equation in both frequency and time domains, and the Stokes equation. The purpose is to present a step-by-step construction of various HDG methods, including the most economic ones with least trace unknowns, by exploiting the particular structure of the underlying PDEs. The well-posedness of the resulting HDG schemes, i.e. the existence and uniqueness of the HDG solutions, are proved. The well-posedness results are also extended and proved for abstract Friedrichs' systems. We also discuss variants of the proposed unified framework and extend them to the popular Lax-Friedrichs flux and to nonlinear PDEs. Numerical results for transport equation, convection-diffusion equation, compressible Euler equation, and shallow water equation are presented to support the unification of the HDG methods.

Key words. discontinuous Galerkin methods; hybridized discontinuous Galerkin methods; upwind hybridized discontinuous Galerkin methods; Godunov method; Riemann flux; Lax-Friedrichs flux; Friedrichs' system; upwind; well-posedness; compressible Euler equation; shallow water equation; Newton method;

AMS subject classifications. 65N30, 65N12, 65N15, 65N22.

1. Introduction.

The discontinuous Galerkin (DG) method was originally developed by Reed and Hill [50] for the neutron transport equation, first analyzed in [35, 33], and then has been extended to other problems governed by partial differential equations (PDEs) [13]. Roughly speaking, DG combines advantages of classical finite volume and finite element methods. In particular, it has the ability to treat solutions with large gradients including shocks, it provides the flexibility to deal with complex geometries, and it is highly parallelizable due to its compact stencil. As such, it has been adopted to solve large-scale forward [4, 54] and inverse [5] problems. However, it is has so many (coupled) unknowns compared to the other existing numerical methods for PDEs, and hence more expensive in general.

Recently, Cockburn, his coworkers, and others have introduced a hybridizable (also known as hybridized) discontinuous Galerkin (HDG) methods for various type of PDEs including Poisson equation [10,12,34], convection-diffusion equation [42,43,8, 18], Stokes equation [15,9,44], Euler and Navier-Stokes equations [47,48,40], Maxwell equation [46, 37, 38], acoustics and elastodynamics [45], Helmholtz equation [27, 17], and eigenvalue problem [14], to name a few. The beauty of the HDG method is that it reduces the number of coupled unknowns substantially while retaining all other attractive properties of the DG method. The coupled unknowns are in fact

†Department of Aerospace Engineering and Engineering Mechanics, and Institute for Computational Engineering & Sciences, The University of Texas at Austin, Austin, TX 78712, USA.

new unknown traces introduced on the mesh skeleton to hybridize the DG method. Once they are solved for the usual DG unknowns can be recovered in an element-by-element fashion, completely independent of each other. Existing HDG constructions however vary from one type of PDE to another, though they do share some similarities. Moreover, they are parameter-dependent method. Consequently, practitioners may be wary of deriving/applying the HDG approach to a new PDE.

Our aim is to construct a unified HDG framework that can be applied to any PDEs and that rediscovers most, if not all, the existing HDG methods when applied to aforementioned PDEs. More importantly, the unified framework should be able to provide a constructive approach to discover new HDG methods. It should be pointed out that similar efforts for constructing a unified DG framework have been done recently in [32, 20, 21, 22]. We have also successful devised a unified framework for the discontinuous Petrov-Galerkin method [6]. Following this light, this paper is an attempt provide a unified framework for the HDG approach.

In the following we summarize the contributions of this article. We start by revisiting the Godunov approach for solving a general system of linear PDEs in Section 2. This reveals the fact that the Godunov upwind flux on a face/edge can be hybridized so that it can be computed using information of either of elements sharing that face/edge and the single-valued Riemann solution. This motivates us to replace the Riemann solution by a trace unknown living on the mesh skeleton and solve for it as part of the solution. At the first sight, this seems to be more expensive than the standard (upwind) DG. However, by a Schur complement approach ("static condensation") we show that the actual coupled unknowns is the trace, and hence the number of globally coupled unknowns are substantially reduced. In other words, instead of evaluating the Riemann solution first and then the Godunov flux as usually done, we propose to treat Riemann solutions as unknowns and compute it as part of solution. We essentially suggest to redesign or, equivalently, to hybridize numerical methods using the Godunov approach.

The purpose of above systematic construction of the upwind HDG framework is threefold. First, we have shown that the basic Godunov approach can be used as a natural recipe to constructively derive the HDG numerical fluxes. Thus, Godunov flux is hybridizable. However, unlike the Godunov approach that was designed and mainly used for hyperbolic PDEs, we first generalize it to abstract linear systems of PDEs and then carry out the hybridization. Second, we provide a better understanding of the trace unknown, that is, it is nothing more than the solution of the Riemann problem. Third, our upwind HDG is parameter free by construction. Nevertheless, from the upwind HDG we will show how one can naturally and constructively derive families of parameter-dependent HDG methods in the literature.

We next apply our abstract upwind HDG framework to convection-diffusion-reaction equation in Section 3, Maxwell's equations in both time and frequency domains in Section 4, and Stokes equation in Section 5. The purpose of these sections is to show that by exploiting the structure of the underlying PDEs, one can systematically construct HDG method with minimal number of trace unknowns. In these sections, we show the power of the unified framework in rediscovering most, if not all, of the existing HDG methods and in discovering new ones. In each section (or its subsections) we provide an analysis of the devised HDG method including the well-posedness of the HDG global and local systems.

Section 6 is our attempt to generalize the analysis in Sections 3, 4, and 5 to a large class of PDEs of Friedrichs' type. It will be shown that one can indeed do so under

certain conditions which will be stated clearly. In Section 7 we show how to extend our upwind HDG idea to hybridize the popular Lax-Friedrichs flux. The advantages and disadvantages of the latter compared to the former are also discussed. After that we show in Section 8 how to construct variants of the upwind HDG that recover a popular class of HDG schemes. It is then followed by an extension of the upwind HDG framework in Section 9 to accommodate cases in which the coefficient of the PDEs are discontinuous across element boundaries. Section 10 presents an extrapolation of the proposed framework to nonlinear PDEs. To validate our HDG framework we presents numerical results in Section 11 for various types of PDE including transport equation, convection-diffusion equation, compressible Euler equation, and shallow water equation. Finally, Section 12 concludes the paper.

2. A constructive derivation of a unified HDG framework by hybridizing the Godunov's flux. In this section we are interested in constructing a single HDG framework for general linear system of PDEs of the following form

$$\mathcal{T}\mathbf{u} := \sum_{k=1}^{d} \partial_k \mathbf{F}_k(\mathbf{u}) + \mathbf{C}\mathbf{u} := \sum_{k=1}^{d} \partial_k \left(\mathbf{A}^k \mathbf{u}\right) + \mathbf{C}\mathbf{u} = \mathbf{f}, \quad \text{in } \Omega, \tag{2.1}$$

where d is the spatial dimension (which, for clarity in the exposition, is assumed to be $d = 3$ whenever a particular value of dimension is of concern though our theory is valid for any dimension), $\mathbf{F}_k$ the kth component of the flux vector (or tensor) $\mathbf{F}$, $\mathbf{u}$ the unknown solution with values in $\mathbb{R}^m$, and $\mathbf{f}$ the forcing term. The matrices $\mathbf{A}^k$ and $\mathbf{C}$ are assumed to be constant and continuous across the domain of interest Ω (the continuity will be relaxed later). Here, ∂_k is understood as the kth partial derivative. Since the boundary condition plays no role in the basic construction and understanding of our unified framework, it is ignored until the well-definedness is concerned. At the point we will provide the boundary condition and show how to incorporate it through the trace unknown..

We are going to solve (2.1) using the discontinuous Galerkin finite element method. To begin, let us partition the domain Ω into N_{el} non-overlapping elements $K_j, j = 1, \ldots, N_{\text{el}}$ with Lipschitz boundaries such that $\Omega_h := \cup_{j=1}^{N_{\text{el}}} K_j$ and $\overline{\Omega} = \overline{\Omega}_h$. Here, h is defined as $h := \max_{j\in\{1,\ldots,N_{\text{el}}\}} diam\,(K_j)$. We denote the skeleton of the mesh by $\mathcal{E}_h := \cup_{j=1}^{N_{\text{el}}} \partial K_j$; it is the set of all (uniquely defined) faces e, each of which comes with a normal vector $\mathbf{n}^e$. We conventionally identify the normal vector $\mathbf{n}^-$ on the boundary ∂K of the element K under consideration (also denoted as K^-) and $\mathbf{n}^+ = -\mathbf{n}^-$ as the normal of the boundary of a neighboring element (also denoted as K^+). On the other hand, we use $\mathbf{n}$ to denote either $\mathbf{n}^-$ or $\mathbf{n}^+$ in an expression that is valid for both cases, and this convention is also used for other quantities (restricted) on $e \in \mathcal{E}_h$. For the sake of convenience, we denote by $\mathcal{E}_h^\partial$ the sets of all boundary faces and define $\mathcal{E}_h^o := \mathcal{E}_h \setminus \mathcal{E}_h^\partial$ the set of all interior faces. We also need $\partial\Omega_h := \{\partial K : K \in \Omega_h\}$.

For simplicity in writing we define $(\cdot,\cdot)_K$ as the L^2-inner product on a domain $K \in \mathbb{R}^d$ and $\langle\cdot,\cdot\rangle_K$ as the L^2-inner product on a domain K if $K \in \mathbb{R}^{d-1}$. We shall use $\|\cdot\|_K = \|\cdot\|_{L^2(K)}$ as the induced norm for both cases and the particular value K in context will indicate which inner product the norm is coming from. We also denote the ε-weighted norm of a function u as $\|u\|_{K,\varepsilon} = \|\sqrt{\varepsilon}u\|_K$ for any positive ε. We shall use bold-face lowercase letters for vector-valued functions and in that case the inner product is defined as $(\mathbf{u},\mathbf{v})_K = \sum_{i=1}^m (\mathbf{u}_i,\mathbf{v}_i)_K$, and similarly as $\langle\mathbf{u},\mathbf{v}\rangle_K = \sum_{i=1}^m \langle\mathbf{u}_i,\mathbf{v}_i\rangle_K$, where m is the number of components $(\mathbf{u}_i, i = 1,\ldots,m)$ of $\mathbf{u}$. Moreover, we define $(\mathbf{u},\mathbf{v})_\Omega := \sum_{K\in\Omega_h} (\mathbf{u},\mathbf{v})_K$ and $\langle\mathbf{u},\mathbf{v}\rangle_{\mathcal{E}_h^o} := \sum_{e\in\mathcal{E}_h^o} \langle\mathbf{u},\mathbf{v}\rangle_e$ whose induced (weighted)

norms are clear, and hence their definitions are omitted. We also employ bold upper case letter, e.g. $\mathbf{L}$, to denote both matrices and tensors. It is our convention that subscripts are used to denote the components of vector, matrix, and tensor.

We define $\mathcal{P}^p(K)$ as the space of polynomial of degree at most p on the domain K. Next, we introduce three discontinuous piecewise polynomial spaces

$$\mathbf{V}_h(\Omega_h) := \left\{\mathbf{v} \in \left[L^2(\Omega)\right]^m : \mathbf{v}|_K \in \left[\mathcal{P}^p(K)\right]^m, \forall K \in \Omega_h\right\},$$
$$\mathbf{\Lambda}_h(\mathcal{E}_h) := \left\{\boldsymbol{\lambda} \in \left[L^2(\mathcal{E}_h)\right]^m : \boldsymbol{\lambda}|_e \in \left[\mathcal{P}^p(e)\right]^m, \forall e \in \mathcal{E}_h\right\},$$

and similarly for $\mathbf{V}_h(K)$, and $\mathbf{\Lambda}_h(e)$ by replacing Ω_h with K and $\mathcal{E}_h$ with e. If $m = 1$, i.e. scalar-valued functions, we denote these spaces as

$$V_h(\Omega_h) := \left\{v \in L^2(\Omega) : v|_K \in \mathcal{P}^p(K), \forall K \in \Omega_h\right\},$$
$$\Lambda_h(\mathcal{E}_h) := \left\{\lambda \in L^2(\mathcal{E}_h) : \lambda|_e \in \mathcal{P}^p(e), \forall e \in \mathcal{E}_h\right\}.$$

From now on to the rest of the paper we conventionally use $\mathbf{u}$ as the numerical solution and $\mathbf{u}^e$ for the exact solution. We would like to find local finite element solution $\mathbf{u} \in \mathbf{V}_h(K)$ on each element $K \in \Omega_h$. To that end, multiplying (2.1) by $\mathbf{v}$ and integrating by parts we have

$$(\mathbf{F}(\mathbf{u}), \nabla\mathbf{v})_K - \langle \mathbf{F}(\mathbf{u}) \cdot \mathbf{n}, \mathbf{v}\rangle_{\partial K} + (\mathbf{C}\mathbf{u}, \mathbf{v})_K = (\mathbf{f}, \mathbf{v})_K, \quad \forall \mathbf{v} \in \mathbf{V}_h(K). \tag{2.2}$$

At this point, the flux $\mathbf{F}(\mathbf{u}) \cdot \mathbf{n}$ on $e \in \partial K$ is not well-defined since the traces of both $\mathbf{u}^-$ of element K^- and $\mathbf{u}^+$ of element K^+ co-exist on e. Godunov's type methods [26] resolves this by first solving, either exactly or approximately, the Riemann problem at the interface e and then introducing some (typically upwind) numerical flux $\mathbf{F}^*(\mathbf{u}^-, \mathbf{u}^+)$ to replace $\mathbf{F}(\mathbf{u})$ on the boundary term in (2.2) so that (2.2) becomes

$$(\mathbf{F}(\mathbf{u}), \nabla\mathbf{v})_K - \left\langle \mathbf{F}^*\left(\mathbf{u}^-, \mathbf{u}^+\right) \cdot \mathbf{n}, \mathbf{v}\right\rangle_{\partial K} + (\mathbf{C}\mathbf{u}, \mathbf{v})_K = (\mathbf{f}, \mathbf{v})_K, \quad \forall \mathbf{v} \in \mathbf{V}_h(K). \tag{2.3}$$

It is this numerical flux that couples local unknowns on elements K^+ and K^- that share a face $e \in \partial K$. Consequently, the local unknowns on all elements are coupled, and they must be solved together. This leads to the "usual complaint" that DG has so many coupled unknowns, and hence is expensive, though it has many attractive properties.

The chief goal of this paper is to remove this coupling by introducing new trace unknowns that live on the mesh skeleton. The beauty of this approach is that the actual globally coupled unknowns are those newly introduced trace unknowns, and hence the resulting system is substantially smaller and sparser. Once the trace unknowns are computed, the usual local DG unknown $\mathbf{u}$ are computed locally element-by-element independent of each other. In other words, by introducing the trace unknowns, we essentially transform the usual global DG system into much smaller global system and many little local systems. In the following, we will show that this is possible by revisiting the basic and classical Godunov flux.

The numerical flux is typically constructed by solving the Riemann problem locally along the normal coordinate n of ∂K: find $\mathbf{u}(n, t)$ such that

$$\frac{\partial \mathbf{u}}{\partial t} + \frac{\partial(\mathbf{A}\mathbf{u})}{\partial n} = \mathbf{0}, \tag{2.4}$$

with the initial condition $\mathbf{u}(n, 0) = \mathbf{u}^-$ for $n < 0$, $\mathbf{u}(n, 0) = \mathbf{u}^+$ for $n \geq 0$, and $\mathbf{A} = \sum_{k=1}^d \mathbf{A}^k \mathbf{n}_k$. Here, the time t is introduced to facilitate the understanding of (the

physics of) the Riemann problem and Godunov flux, but it is otherwise not necessary in the following development. The detailed solution of the Riemann's problem can be found in [53] for example. For completeness, we however review the main points here. We begin with the eigenvalue decomposition of $\mathbf{A}$

$$\mathbf{A} := \sum \mathbf{A}^k \mathbf{n}_k = \mathbf{R}\mathbf{S}\mathbf{R}^{-1}, \tag{2.5}$$

where $\mathbf{S} := \text{diag}\,(\theta_1, \ldots, \theta_m)$ and θ_i are eigenvalues of $\mathbf{A}$. To the end of this section we assume that $\mathbf{A}$ has real eigenvalues and independent eigenvectors, i.e., the system of linear PDEs (2.1) is hyperbolic [53].

Since $\mathbf{R}$ forms a complete basis of $\mathbb{R}^m$, we can decompose the initial condition as

$$\mathbf{u}^- = \sum_{i=1}^{m} \alpha_i^- \mathbf{R}_i, \text{ and } \mathbf{u}^+ = \sum_{i=1}^{m} \alpha_i^+ \mathbf{R}_i.$$

The solution of the Riemann problem (2.4) for small time t can be shown to be

$$\mathbf{u}^* = \sum_{i=1}^{I} \alpha_i^- \mathbf{R}_i + \sum_{i=I+1}^{m} \alpha_i^+ \mathbf{R}_i, \tag{2.6}$$

where I is such that $\theta_I \leq 0$ and $\theta_{I+1} \geq 0$. In terms of the "left" (-) and the "right" (+) states, we have

$$\mathbf{u}^* = \mathbf{u}^- + \sum_{i=1}^{I} \left(\alpha_i^+ - \alpha_i^-\right) \mathbf{R}_i, \tag{2.7}$$

and

$$\hat{\mathbf{u}} = \mathbf{u}^+ - \sum_{i=I+1}^{m} \left(\alpha_i^+ - \alpha_i^-\right) \mathbf{R}_i. \tag{2.8}$$

The Godunov flux $\mathbf{F}^* \cdot \mathbf{n}^-$ on the boundary of element K^- is found by multiplying both sides of (2.7) by $\mathbf{A}$, i.e.,

$$\mathbf{F}^* \cdot \mathbf{n}^- := \mathbf{A}\mathbf{u}^- + \mathbf{A} \sum_{i=1}^{I} \left(\alpha_i^+ - \alpha_i^-\right) \mathbf{R}_i. \tag{2.9}$$

Since the positive spectrum of $\mathbf{A}$ has no contribution to the second term in (2.9), we can write

$$\mathbf{F}^* \cdot \mathbf{n}^- = \mathbf{A}\mathbf{u}^- - |\mathbf{A}| \sum_{i=1}^{I} \left(\alpha_i^+ - \alpha_i^-\right) \mathbf{R}_i, \tag{2.10}$$

where $|\mathbf{A}| := \mathbf{R}\,|\mathbf{S}|\,\mathbf{R}^{-1}$. Now substituting (2.7) into (2.10) gives

$$\mathbf{F}^* \cdot \mathbf{n}^- = \mathbf{F}\left(\mathbf{u}^-\right) \cdot \mathbf{n}^- + |\mathbf{A}|\left(\mathbf{u}^- - \hat{\mathbf{u}}\right). \tag{2.11}$$

Similarly, the Godunov's flux for the neighboring element K^+ on the same face e is given by

$$\mathbf{F}^* \cdot \mathbf{n}^+ := \mathbf{F}\left(\mathbf{u}^+\right) \cdot \mathbf{n}^+ + |\mathbf{A}|\left(\mathbf{u}^+ - \hat{\mathbf{u}}\right). \tag{2.12}$$

The following identity obviously holds

$$[\![\mathbf{F}^* \cdot \mathbf{n}]\!] = \mathbf{0}, \tag{2.13}$$

where we have defined the "jump" operator $[\![(\cdot)]\!] := (\cdot)^- + (\cdot)^+$.

Next, combining (2.11) and (2.12) we have the usual "symmetric" form of the Godunov's flux

$$\mathbf{F}^* \cdot \mathbf{n}^- = \frac{1}{2}\left[\mathbf{F}\left(\mathbf{u}^-\right) + \mathbf{F}\left(\mathbf{u}^+\right)\right] \cdot \mathbf{n}^- + \frac{1}{2}\left|\mathbf{A}\right|\left(\mathbf{u}^- - \mathbf{u}^+\right), \tag{2.14}$$

which is usually used in upwind numerical methods such as upwind DG. It is this nicely symmetric form that couples the unknowns of the neighboring elements, and hence the unknowns of all elements. This leads to the "usual complaint" that DG has so many (coupled) unknowns.

Can we avoid this "standard" global coupling? The above re-derivation of the Godunov flux with two new expressions in (2.11) and (2.12) in fact provides an answer. These new formulas are unnecessary and not useful in the standard Godunov approach since the symmetric form (2.14) is the final product that is actually used in numerical methods. However, they are the key leading us to a unified HDG framework, as we now show. We first observe that the Godunov numerical fluxes (2.11) and (2.12) depend on the DG unknowns of only one side of a face $e \in \partial K$ and the single-valued solution $\mathbf{u}^*$ of the Riemann problem. The numerical flux is then completely determined using only information from either side (left or right) of the face $e \in \partial K$, as long as $\mathbf{u}^*$ is (either exactly or approximately) provided. More importantly, this in turn shows that we can solve equation (2.3) for $\mathbf{u}$ element-by-element independent of each other.

The above discussion suggests that we should treat $\mathbf{u}^*$ as the extra unknown and solve for it on the skeleton of the mesh instead of using the Riemann solution which couples the local unknown $\mathbf{u}$. To signify this step, let us rename $\mathbf{u}^*$ to $\hat{\mathbf{u}}$ and $\mathbf{F}^*$ to $\hat{\mathbf{F}}$. Conventionally, "hatted" quantities are computed using the trace unknown $\hat{\mathbf{u}}$ while "starred" quantities are associated with the Riemann solution $\mathbf{u}^*$. An immediate question that arises is how to compute $\hat{\mathbf{u}}$. To answer this question, we note that $\hat{\mathbf{u}}$ is a new unknown that is introduced on ∂K so that (2.3) can be solved in an element-by-element fashion. To ensure the well-posedness of our formulation, we need to introduce an extra equation on ∂K. Clearly, at this point $\hat{\mathbf{u}}$ is not the solution of the Riemann problem and hence the identity (2.13) is no longer satisfied in general. It is therefore natural to use (2.13) as the extra equation. This additional algebraic equation ensures that what coming out from element K through its boundary ∂K must enter the neighboring elements that share (part of) the boundary ∂K. This is the statement of conservation and it is exactly conveyed by (2.13).

In summary, for each element K, the DG local unknown $\mathbf{u}$ and the extra "trace" unknown $\hat{\mathbf{u}}$ need to satisfy

$$\left(\mathbf{F}\left(\mathbf{u}\right), \nabla \mathbf{v}\right)_K - \left\langle \hat{\mathbf{F}}\left(\mathbf{u}, \hat{\mathbf{u}}\right) \cdot \mathbf{n}, \mathbf{v} \right\rangle_{\partial K} + \left(\mathbf{C}\mathbf{u}, \mathbf{v}\right)_K = \left(\mathbf{f}, \mathbf{v}\right)_K, \quad \forall \mathbf{v} \in \mathbf{V}_h\left(K\right), \tag{2.15a}$$

$$\left\langle [\![\hat{\mathbf{F}}\left(\mathbf{u}, \hat{\mathbf{u}}\right) \cdot \mathbf{n}]\!], \boldsymbol{\mu} \right\rangle_{\partial K} = \mathbf{0}, \quad \forall \boldsymbol{\mu} \in \boldsymbol{\Lambda}_h, \tag{2.15b}$$

where we have enforced the uniqueness of the numerical flux weakly which is sufficient for local conservation. Here, the HDG flux has exactly the same form as the Godunov one, i.e.

$$\hat{\mathbf{F}} \cdot \mathbf{n} = \mathbf{F}\left(\mathbf{u}\right) \cdot \mathbf{n} + \left|\mathbf{A}\right|\left(\mathbf{u} - \hat{\mathbf{u}}\right), \tag{2.16}$$

but $\hat{\mathbf{u}}$ is now an extra unknown to be solved for.

By revisiting derivation of the Godunov flux we have constructively derived the HDG method for a general linear system of PDEs. The procedure for computing HDG solution requires three steps. We first solve (2.15a) for the local solution $\mathbf{u}$ as a function of $\hat{\mathbf{u}}$. It is then substituted into the conservative algebraic equation (2.15b) on the mesh skeleton to solve for the unknown $\hat{\mathbf{u}}$. Finally, the local unknown $\mathbf{u}$ is computed, as in the first step, using $\hat{\mathbf{u}}$ solved from the second step. To signify the nature of each step, we conventionally name the element-by-element elimination in the first and the third step as the local solver, and solving for the trace on the mesh skeleton in the second step as the global solver.

Let us emphasize some other crucial points. First, we have shown that the Godunov method is hybridizable. Second, the trace unknown in our upwind HDG, once computed, is no thing more than the Riemann solution; we will verify this fact for various linear PDEs in the following. Third, the appearance of $|\mathbf{A}|$, and hence $|\mathbf{A}|(\mathbf{u}-\hat{\mathbf{u}})$, is to ensure the upwinding mechanism, and hence stability. In the HDG literature $|\mathbf{A}|$ is a free stabilization parameter that must be appropriately chosen for stability, whereas in our upwind HDG framework $|\mathbf{A}|$ arises explicitly from the hybridization of the Godunov method. Thus, it automatically ensures the stability of the upwind HDG method if the original Godunov is stable.

At this level of generality, it appears that we have m trace unknowns $\hat{\mathbf{u}}_i, i = 1,\dots,m$ to solve for on the skeleton. However, when we apply our general HDG method for a particular PDE—including convection-diffusion-reaction equation in Section 3, Maxwell equation in Section 4, and Stokes equation in Section 5—we can eliminate most of them so that there are in fact only a few trace unknowns that need to be solved for. For all examples considered, we will assume that all the boundary conditions are homogeneous for the clarity of the exposition. The extension to non-homogeneous boundary conditions are straightforward and hence omitted.

3. HDG schemes for convection-diffusion-reaction equation. In this section we will apply the general HDG methodology in Section 2 to convection-diffusion-reaction equation and its subsets. As shall be shown, we recover several existing HDG methods and discover new ones.

The problem of interest in this section is the convection-diffusion-reaction equation written in the first order form

$$\varepsilon^{-1}\boldsymbol{\sigma} + \nabla u = 0 \quad \text{in } \Omega, \tag{3.1a}$$

$$\nabla\cdot\boldsymbol{\sigma} + \boldsymbol{\beta}\cdot\nabla u + \nu u = f \quad \text{in } \Omega \tag{3.1b}$$

where we assume $\boldsymbol{\beta} \in [L^\infty(\Omega)]^d$, $\nabla\cdot\boldsymbol{\beta} \in L^\infty(\Omega)$. Simple algebraic manipulation shows that

$$|\mathbf{A}| = \frac{1}{\alpha}\begin{bmatrix} 2\mathbf{n}_1^2 & 2\mathbf{n}_1\mathbf{n}_2 & 2\mathbf{n}_1\mathbf{n}_3 & \boldsymbol{\beta}\cdot\mathbf{n}\mathbf{n}_1 \\ 2\mathbf{n}_1\mathbf{n}_2 & 2\mathbf{n}_2^2 & 2\mathbf{n}_2\mathbf{n}_3 & \boldsymbol{\beta}\cdot\mathbf{n}\mathbf{n}_2 \\ 2\mathbf{n}_1\mathbf{n}_3 & 2\mathbf{n}_2\mathbf{n}_3 & 2\mathbf{n}_3^2 & \boldsymbol{\beta}\cdot\mathbf{n}\mathbf{n}_3 \\ \boldsymbol{\beta}\cdot\mathbf{n}\mathbf{n}_1 & \boldsymbol{\beta}\cdot\mathbf{n}\mathbf{n}_2 & \boldsymbol{\beta}\cdot\mathbf{n}\mathbf{n}_3 & \gamma \end{bmatrix},$$

with $\alpha := \sqrt{|\boldsymbol{\beta}\cdot\mathbf{n}|^2 + 4}$ and $\gamma = |\boldsymbol{\beta}\cdot\mathbf{n}|^2 + 2$. If we order the Riemann solution in

(2.6) as $\mathbf{u}^* := (u^*, \sigma_1^*, \sigma_2^*, \sigma_3^*) = (u^*, \boldsymbol{\sigma}^*)$, the Godunov flux (2.16) becomes

$$\mathbf{F}^* \cdot \mathbf{n} = \frac{1}{\alpha} \begin{bmatrix} \alpha u \mathbf{n}_1 + 2\left(\boldsymbol{\sigma} - \boldsymbol{\sigma}^*\right) \cdot \mathbf{n} \mathbf{n}_1 + \boldsymbol{\beta} \cdot \mathbf{n} \left(u - u^*\right) \mathbf{n}_1 \\ \alpha u \mathbf{n}_2 + 2\left(\boldsymbol{\sigma} - \boldsymbol{\sigma}^*\right) \cdot \mathbf{n} \mathbf{n}_2 + \boldsymbol{\beta} \cdot \mathbf{n} \left(u - u^*\right) \mathbf{n}_2 \\ \alpha u \mathbf{n}_3 + 2\left(\boldsymbol{\sigma} - \boldsymbol{\sigma}^*\right) \cdot \mathbf{n} \mathbf{n}_3 + \boldsymbol{\beta} \cdot \mathbf{n} \left(u - u^*\right) \mathbf{n}_3 \\ \alpha \boldsymbol{\beta} \cdot \mathbf{n} u + \alpha \boldsymbol{\sigma} \cdot \mathbf{n} + \boldsymbol{\beta} \cdot \mathbf{n} \left(\boldsymbol{\sigma} - \boldsymbol{\sigma}^*\right) \cdot \mathbf{n} + \gamma \left(u - u^*\right). \end{bmatrix} \tag{3.2}$$

If we stop here and construct an HDG method by replacing starred quantities by hatted ones as in the abstract setting presented in Section 2, we see that there are four trace unknowns: three from $\boldsymbol{\sigma}^*$ and one from u^*. However, as can be seen from (3.2), there are only two independent quantities, namely, the traces $|\boldsymbol{\sigma}^* \cdot \mathbf{n}|$ and u^* that are needed to compute the upwind flux. In fact, even these two quantities are not independent of each other, as will be shown, and hence either of them can be eliminated. This is the key leading to the most economic HDG methods: first removing all the dependencies, and then constructing HDG methods.

3.1. Constructing HDG scheme by eliminating $\boldsymbol{\sigma}^* \cdot \mathbf{n}$. We first show that the Godunov flux can be written as a function of only u^*.

LEMMA 3.1. *The following hold true:*

i) The Riemann solution $\mathbf{u}^*$ *satisfies*

$$u^* = \{\{u\}\} + \frac{\boldsymbol{\beta} \cdot \mathbf{n}}{2\alpha} [\![u\mathbf{n}]\!] \cdot \mathbf{n} + \frac{1}{\alpha} [\![\boldsymbol{\sigma} \cdot \mathbf{n}]\!], \tag{3.3a}$$

$$\boldsymbol{\sigma}^* \cdot \mathbf{n} = \{\{\boldsymbol{\sigma}\}\} \cdot \mathbf{n} + \frac{1}{\alpha} [\![u\mathbf{n}]\!] \cdot \mathbf{n} - \frac{\boldsymbol{\beta} \cdot \mathbf{n}}{2\alpha} [\![\boldsymbol{\sigma} \cdot \mathbf{n}]\!], \tag{3.3b}$$

ii) The Godunov flux is given by

$$\mathbf{F}^* \cdot \mathbf{n} = \begin{bmatrix} \hat{u} \mathbf{n}_1 \\ \hat{u} \mathbf{n}_2 \\ \hat{u} \mathbf{n}_3 \\ \boldsymbol{\beta} \cdot \mathbf{n} u + \boldsymbol{\sigma} \cdot \mathbf{n} + \frac{1}{2}\left(\alpha - \boldsymbol{\beta} \cdot \mathbf{n}\right)\left(u - u^*\right) \end{bmatrix}, \tag{3.4}$$

where

$$u^* = u + \frac{2}{\alpha}\left(\boldsymbol{\sigma} - \hat{\boldsymbol{\sigma}}\right) \cdot \mathbf{n} + \frac{\boldsymbol{\beta} \cdot \mathbf{n}}{\alpha}\left(u - u^*\right). \tag{3.5}$$

Proof. To prove the first assertion we can use popular techniques such as those in [53]. Here, we take a different approach using the conservation equation. Specifically, we note that for the convection-diffusion-reaction problem, the conservation (2.13) gives us four equations for the Riemann solution $\mathbf{u}^*$. Solving for u^* and $\boldsymbol{\sigma}^* \cdot \mathbf{n}$ in terms of u and $\boldsymbol{\sigma}$ we obtain the desired result. The second assertion immediately follows by substituting (3.3) into (3.2) and inspecting that (3.5) is true. ∎

Up to this point, we have used the exact Riemann solution and the Godunov flux to derive identities in Lemma 3.1. These simple results are important since they immediately pave the way for constructing a HDG method with single trace unknown. In particular, we start by replacing the starred quantities with hatted ones in (3.4), and then defining resulting expression as the HDG flux with $\hat{u}$ as the trace unknown, i.e.,

$$\hat{\mathbf{F}} \cdot \mathbf{n} = \begin{bmatrix} \hat{u} \mathbf{n}_1 \\ \hat{u} \mathbf{n}_2 \\ \hat{u} \mathbf{n}_3 \\ \boldsymbol{\beta} \cdot \mathbf{n} u + \boldsymbol{\sigma} \cdot \mathbf{n} + \frac{1}{2}\left(\alpha - \boldsymbol{\beta} \cdot \mathbf{n}\right)\left(u - \hat{u}\right) \end{bmatrix}. \tag{3.6}$$

That is, we do not assume that $\hat{u}$ satisfies (3.3) and (3.5). It is clear that the first three components of our HDG flux (3.6) automatically satisfy the conservation condition (2.15b), and thus we need to weakly enforce only the fourth one according to (2.15b), i.e.,

$$\left\langle [\![\boldsymbol{\beta}\cdot\mathbf{n}u+\boldsymbol{\sigma}\cdot\mathbf{n}+\frac{1}{2}(\alpha-\boldsymbol{\beta}\cdot\mathbf{n})(u-\hat{u})]\!],\mu\right\rangle_e=0,\quad \forall\mu\in\Lambda_h(e),\quad \forall e\in\mathcal{E}_h^o. \tag{3.7}$$

Taking $\mathbf{v}=(\boldsymbol{\kappa},v)\in\mathbf{V}_h(K)\otimes V_h(K)$ as the test function, the local equation (2.15a) when applied to (3.1) becomes: find $(\boldsymbol{\sigma},u)\in\mathbf{V}_h(K)\otimes V_h(K)$ such that

$$\left(\varepsilon^{-1}\sigma_i,\kappa_i\right)_K-(u,\partial_i\kappa_i)_K+\left\langle\left(\hat{\mathbf{F}}\cdot\mathbf{n}\right)_i,\kappa_i\right\rangle_{\partial K}=0\quad i=1,2,3, \tag{3.8a}$$

$$-(\boldsymbol{\sigma},\nabla v)_K-(u,\nabla\cdot(\boldsymbol{\beta}v))_K+(\nu u,v)_K+\left\langle\left(\hat{\mathbf{F}}\cdot\mathbf{n}\right)_4,v\right\rangle_{\partial K}=(f,v)_K, \tag{3.8b}$$

with $\left(\hat{\mathbf{F}}\cdot\mathbf{n}\right)_i, i=1,\ldots,4$ denoting the ith component of numerical flux (3.6).

In summary, we have proposed an HDG scheme consisting of local equations (3.8), numerical flux (3.6), and conservation condition (3.7). A question immediately arises is whether the trace solution $\hat{u}$ of the HDG method is identical to the Riemann solution (3.3a) and the HDG flux (3.6) is in fact the Godunov one. The answer is, not surprisingly, affirmative.

LEMMA 3.2. *The trace solution $\hat{u}$ of the HDG scheme (3.8), (3.6), and (3.7) coincides with the Riemann solution. Furthermore, the HDG flux (3.6) is identical to the Godunov upwind flux (3.2).*

Proof. We proceed with the conservation condition (3.7) which shows that

$$\langle\alpha\hat{u},\mu\rangle_e=\left\langle\alpha\{\{u\}\}+\frac{\boldsymbol{\beta}\cdot\mathbf{n}}{2}[\![u\mathbf{n}]\!]\cdot\mathbf{n}+[\![\boldsymbol{\sigma}\cdot\mathbf{n}]\!],\mu\right\rangle_e=\langle\alpha u^*,\mu\rangle_e,\quad\forall\mu\in\Lambda_h(e),$$

where we have used (3.3a) to obtain the second equality. Now, taking $\mu=\hat{u}-u^*$ yields

$$\|\hat{u}-u^*\|_{e,\alpha}^2=0,$$

which in turn shows that $\hat{u}$ is exactly the same as the Riemann solution u^*. The second assertion is clear by defining $\hat{\boldsymbol{\sigma}}\cdot\mathbf{n}$ in place of $\boldsymbol{\sigma}^*\cdot\mathbf{n}$ in (3.3b) and substituting $\hat{u}$ from (3.3a) into (3.6). ∎

As pointed out in the general case in Section 2, the HDG method involves three steps. First, we solve the local problem (3.8) for $(\boldsymbol{\sigma},u)$ as a function of $\hat{u}$, which are then substituted in (3.7) to have a sparse system of equation to solve for $\hat{u}$ on the mesh skeleton. Finally, repeating step 1 element-by-element with the just-computed $\hat{u}$ gives the local solution $(\boldsymbol{\sigma},u)$.

3.2. Constructing HDG scheme by eliminating u^*. To achieve the goal of eliminating u^*, let us define the unique flux θ^* such that

$$\theta^*\ \mathrm{sgn}(\mathbf{n}):=\boldsymbol{\beta}\cdot\mathbf{n}u+\boldsymbol{\sigma}\cdot\mathbf{n}+\frac{\boldsymbol{\beta}\cdot\mathbf{n}}{\alpha}(\boldsymbol{\sigma}-\boldsymbol{\sigma}^*)\cdot\mathbf{n}+\frac{\gamma}{\alpha}(u-u^*), \tag{3.9}$$

so that the fourth component of the Godunov flux (3.2) can be written simply as

$$(\mathbf{F}^*\cdot\mathbf{n})_4=\theta^*\ \mathrm{sgn}(\mathbf{n}).$$

Here, we have defined, $\forall e \in \mathcal{E}_h$,

$$\text{sgn}(\mathbf{n}) := \begin{cases} 1 & \text{if } \mathbf{n} = \mathbf{n}^e \\ -1 & \text{if } \mathbf{n} = -\mathbf{n}^e \end{cases}$$

Then, we have a result parallel to Lemma 3.1.

PROPOSITION 3.3. *The Godunov flux* (3.2) *is equivalent to*

$$\mathbf{F}^* \cdot \mathbf{n} = \begin{bmatrix} \tilde{u}\mathbf{n}_1 \\ \tilde{u}\mathbf{n}_2 \\ \tilde{u}\mathbf{n}_3 \\ \theta^* \ sgn(\mathbf{n}) \end{bmatrix}, \tag{3.10}$$

where

$$\tilde{u} = \left(1 + \frac{2\alpha\boldsymbol{\beta}\cdot\mathbf{n}}{\alpha - \boldsymbol{\beta}\cdot\mathbf{n}}\right) u + \frac{2\alpha}{\alpha - \boldsymbol{\beta}\cdot\mathbf{n}}\boldsymbol{\sigma}\cdot\mathbf{n} - \frac{2\alpha}{\alpha - \boldsymbol{\beta}\cdot\mathbf{n}}\theta^* \ sgn(\mathbf{n})\,. \tag{3.11}$$

Proof. Combining (3.5) and (3.9) gives

$$(\boldsymbol{\sigma} - \boldsymbol{\sigma}^*)\cdot\mathbf{n} = -\frac{\alpha}{2}\left(1 + \frac{\boldsymbol{\beta}\cdot\mathbf{n}}{2}\right)(u - u^*)\,, \tag{3.12a}$$

$$(u - u^*) = \frac{2}{\alpha - \boldsymbol{\beta}\cdot\mathbf{n}}\left[\theta^* \ \text{sgn}(\mathbf{n}) - \boldsymbol{\beta}\cdot\mathbf{n} - \boldsymbol{\sigma}\cdot\mathbf{n}\right]. \tag{3.12b}$$

Substituting (3.12) and (3.9) into (3.2) ends the proof. ∎

Proposition 3.3 shows that the upwind flux (3.2) can be written as a function of only θ^* instead of u^* and $\boldsymbol{\sigma}^*$. This suggests that we can construct a new HDG scheme consisting of local solver (3.8) with numerical flux $\hat{\mathbf{F}}\cdot\mathbf{n}$ and $\hat{\theta}$ defined in place of $\mathbf{F}^*\cdot\mathbf{n}$ and θ^*, respectively, in (3.10), where $\hat{\theta}$ is now the single unknown trace. As can be seen, the fourth equation in the conservation condition (2.15b) is automatically satisfied since $\hat{\theta}$ is single-valued. We need to weakly enforce the conservation for the first three components, but they are the same up to a constant $\mathbf{n}_i$. Consequently, only one conservation condition on the skeleton is necessary and this ensures that the number of equations is the same as the number of unknowns, i.e.,

$$\langle [\![\tilde{u}\ \text{sgn}(\mathbf{n})]\!], \mu\rangle_e = 0, \quad \forall \mu \in \Lambda_h(e)\,, \quad \forall e \in \mathcal{E}_h^o. \tag{3.13}$$

Similar to Lemma 3.2, we can show that the new HDG scheme with $\hat{\theta}$ as the trace unknown is equivalent to the standard upwind DG scheme for the convection-diffusion-reaction (3.1).

LEMMA 3.4. *The HDG flux* $\hat{\mathbf{F}}\cdot\mathbf{n}$ (3.10) *is identical to the Godunov upwind flux.*

Proof. The proof is similar to that of Lemma 3.2. ∎

3.3. HDG method for convection-reaction equation. This is a special case of (3.1) in which the diffusion coefficient is zero, i.e. $\varepsilon = 0$. The construction of the HDG method following the general procedure in Section 2 is substantially simplified. In particular, we have

$$|\mathbf{A}| = |\boldsymbol{\beta}\cdot\mathbf{n}|\,,$$

and the HDG flux (2.14) turns out to be very simple

$$\hat{\mathbf{F}}\cdot\mathbf{n} = \boldsymbol{\beta}\cdot\mathbf{n}u + |\boldsymbol{\beta}\cdot\mathbf{n}|\,(u - \hat{u})\,. \tag{3.14}$$

The local HDG equation (2.15a) on each element K now becomes: find $u \in V_h(K)$ such that

$$-(u, \nabla \cdot (\boldsymbol{\beta} v))_K + (\nu u, v)_K + \left\langle \hat{\mathbf{F}} \cdot \mathbf{n}, v \right\rangle_{\partial K} = (f, v)_K, \quad \forall v \in V_h(K) \tag{3.15}$$

with the HDG flux given in (3.14), and the conservation equation (2.15b) is simply

$$\langle [\![\boldsymbol{\beta} \cdot \mathbf{n} u + |\boldsymbol{\beta} \cdot \mathbf{n}| (u - \hat{u})]\!], \mu \rangle_e = 0, \quad \forall \mu \in \Lambda_h(e), \quad \forall e \in \mathcal{E}_h^o. \tag{3.16}$$

LEMMA 3.5. *The trace solution $\hat{u}$ of the HDG scheme (3.15), (3.14), and (3.16) coincides with the Riemann solution. Furthermore, the HDG flux $\hat{\mathbf{F}} \cdot \mathbf{n}$ (3.14) is identical to the standard Godunov upwind flux for convection-reaction problem.*

Proof. To begin, we note that, similar to Lemma 3.1, we can use the conservation equation to deduce that

$$\hat{u} = \frac{1}{2} [\![u \operatorname{sgn}(\boldsymbol{\beta} \cdot \mathbf{n})]\!] + \{\{u\}\}, \tag{3.17}$$

which is exactly the solution of the Riemann problem. Next, $\hat{u}$ can can be substituted into the HDG flux (3.14) to give

$$\hat{\mathbf{F}} \cdot \mathbf{n} = \boldsymbol{\beta} \cdot \mathbf{n} \{\{u\}\} + \frac{1}{2} \operatorname{sgn}(\boldsymbol{\beta} \cdot \mathbf{n}) [\![\boldsymbol{\beta} \cdot \mathbf{n} u]\!], \tag{3.18}$$

which is exactly the usual upwind flux [50, 53] for the convection equation. Clearly, we can also bypass the computation of $\hat{u}$ to compute the upwind flux directly by

$$2\hat{\mathbf{F}} \cdot \mathbf{n}^- = \hat{\mathbf{F}} \cdot \mathbf{n}^- - \hat{\mathbf{F}} \cdot \mathbf{n}^+ = 2\boldsymbol{\beta} \cdot \mathbf{n} \{\{u\}\} + \operatorname{sgn}(\boldsymbol{\beta} \cdot \mathbf{n}) [\![\boldsymbol{\beta} \cdot \mathbf{n} u]\!],$$

and hence obtaining the same result. ∎

The HDG procedure is the same as before. We first solve (3.15) for u as a function of $\hat{u}$. We then substitute u into (3.16) to solve for the trace unknown $\hat{u}$ on the mesh skeleton. Finally we recover the local solution u on each element by repeating step one with known $\hat{u}$. The next result shows that our upwind HDG method is the same as the standard upwind scheme [33, 50, 35]. This is not surprising since the former is constructed from the latter by hybridizing the upwind flux.

COROLLARY 3.6. *The HDG scheme (3.15), (3.14), and (3.16) is equivalent to the standard upwind DG scheme.*

Proof. We first show that the HDG solution u is a solution of the DG scheme. But this is clear from the proof of Lemma 3.5. In particular, by substituting (3.18) into (3.15), the latter becomes the standard upwind DG [33, 50, 35].

Conversely, let u be the solution of the upwind DG method, i.e., u satisfies (3.15) with the upwind flux (3.18). Now, first defining $\hat{u}$ as in (3.17), then expressing the upwind flux (3.18) as a function of $\hat{u}$ we recover (3.15). We also observe that the upwind flux satisfies the conservation equation (3.16), and this concludes the proof. ∎

3.4. HDG method for Poisson equation. This is a special case of the HDG scheme in Section 3.1 in which the velocity field $\boldsymbol{\beta}$ is zero, i.e. $\boldsymbol{\beta} = \mathbf{0}$. In particular, the HDG flux (3.6) now simplifies to

$$\hat{\mathbf{F}} \cdot \mathbf{n} = \begin{bmatrix} \hat{u}\mathbf{n}_1 \\ \hat{u}\mathbf{n}_2 \\ \hat{u}\mathbf{n}_3 \\ \boldsymbol{\sigma} \cdot \mathbf{n} + (u - \hat{u}) \end{bmatrix}.$$

As shown above, $\hat{u}$ is the Riemann solution and hence approximating the trace of the exact solution on the skeleton. This implies that the discrepancy/error $u-\hat{u}$ converges to zero as the mesh (or solution order) is refined for PDE with smooth solution. This observation suggests that one can penalize $u-\hat{u}$ by introducing a penalty parameter τ so that the HDG flux now reads

$$\hat{\mathbf{F}}\cdot\mathbf{n} = \begin{bmatrix} \hat{u}\mathbf{n}_1 \\ \hat{u}\mathbf{n}_2 \\ \hat{u}\mathbf{n}_3 \\ \boldsymbol{\sigma}\cdot\mathbf{n}+\tau\left(u-\hat{u}\right) \end{bmatrix}, \tag{3.19}$$

which becomes our upwind HDG when the penalty parameter is unity. On the other hand, if τ approaches infinity the trace unknown $\hat{u}$ is forced to match the trace of the DG solution u. One can realize that, by hybridizing the Godunov flux, we have constructively and intuitively recovered the HDG methods for elliptic equations proposed in [11].

REMARK 3.7. *It is important to point out that since the differential part of the Helmholtz equation is the same as that of the Poisson equation, the development of the HDG method for the former is straightforward. In particular, the upwind HDG flux, or its penalized variant, for the Helmholtz equation is identical to* (3.19). *That is, we have also recovered the HDG scheme for Helmholtz equation in [27, 17].*

3.5. Analysis. In this section, we discuss the relation of the our proposed HDG schemes to the existing ones. This is advantageous since we can recycle the results that have been proved for existing HDG methods. Since the upwind HDG scheme with (3.8), (3.10), and (3.13) is equivalent to that with (3.8), (3.6), and (3.7), we study only the latter. We will also discuss the HDG schemes for transport and Poisson equations.

It is important to point out that our upwind HDG scheme for convection-diffusion-reaction problem (3.1) is different from that proposed in [42]. In particular, their HDG flux $\hat{\boldsymbol{\sigma}}^{NPC}\cdot\mathbf{n}$ is

$$\hat{\boldsymbol{\sigma}}^{NPC}\cdot\mathbf{n} := \boldsymbol{\beta}\cdot\mathbf{n}\hat{u}+\boldsymbol{\sigma}\cdot\mathbf{n}+\tau\left(u-\hat{u}\right),$$

where τ is the so-called stabilization parameter. On the other hand, by hybridizing the Godunov's upwind method, ours is

$$\hat{\boldsymbol{\sigma}}\cdot\mathbf{n} := \boldsymbol{\beta}\cdot\mathbf{n}u+\boldsymbol{\sigma}\cdot\mathbf{n}+\frac{1}{2}\left(\alpha-\boldsymbol{\beta}\cdot\mathbf{n}\right)\left(u-\hat{u}\right).$$

Nevertheless, we can rewrite our upwind HDG flux as

$$\hat{\boldsymbol{\sigma}}\cdot\mathbf{n} := \boldsymbol{\beta}\cdot\mathbf{n}\hat{u}+\boldsymbol{\sigma}\cdot\mathbf{n}+\frac{1}{2}\left(\alpha+\boldsymbol{\beta}\cdot\mathbf{n}\right)\left(u-\hat{u}\right),$$

and if we take $\tau = \frac{1}{2}\left(\alpha+\boldsymbol{\beta}\cdot\mathbf{n}\right)$ the two fluxes are identical. Moreover, in this case $\tau-\boldsymbol{\beta}\cdot\mathbf{n}/2 = \alpha > 0$, and therefore all results in [42] hold for our upwind HDG method as well. Let us summarize some important points for mixed Dirichlet-Neumann boundary condition (enforcing boundary condition via the trace unknown is straightforward and can be found in [42]).

THEOREM 3.8. *Assume* $\nu-\frac{1}{2}\nabla\cdot\boldsymbol{\beta}\geq 0$. *Then:*

- *There exists a unique solution for the local solver* (3.8) *of the upwind HDG scheme* (3.8), (3.6), *and* (3.7).

- *The trace solution $\hat{u}$ of the upwind HDG scheme (3.8), (3.6), and (3.7) exists and it is unique.*

Proof. See [42] for a proof. ∎

When $\boldsymbol{\beta} = \mathbf{0}$ the HDG scheme is much simplified as shown in Section 3.4. Consequently, more results can be obtained for this case. Indeed, the work in [12] presents a complete analysis, including optimal convergent rate, of the HDG method for the Poisson equation with Dirichlet boundary condition . Thus our upwind HDG method also converges optimally. A question that immediately arises is whether it is consistent with the local discontinuous Galerkin (LDG) approach proposed [16] in which the upwinding is done in the opposite direction, i.e. upwinding for (3.8a) and downwinding for (3.8b) or the other way around. For clarity in the exposition, we present the answer for the Poisson equation.

Due to Lemma 3.2, we see that since $\hat{u} = u^*$, and hence $\hat{\boldsymbol{\sigma}} = \boldsymbol{\sigma}^*$, they also satisfy (3.5), i.e.,

$$\hat{u} - u = -\left(\hat{\boldsymbol{\sigma}} \cdot \mathbf{n} - \sigma \cdot \mathbf{n}\right), \tag{3.20}$$

which says that the unbalanced (or mismatched) components of the flux due to our upwind HDG/DG discretization of the system (3.1) are opposite. More specifically, $\hat{u} - u$ and $\hat{\boldsymbol{\sigma}} \cdot \mathbf{n} - \sigma \cdot \mathbf{n}$ are the flux mismatch of quantities u and $\boldsymbol{\sigma}$, respectively, per unit area/length. The identity (3.20) implies that the mismatches are opposite. In particular, if $\hat{u} = u^{\mp}$ then from (3.3a)–(3.3b) one can easily sees that $\hat{\boldsymbol{\sigma}} \cdot \mathbf{n} = \boldsymbol{\sigma}^{\pm} \cdot \mathbf{n}$, i.e., they are upwind fluxes in opposite directions. *In other words, we have rediscovered the LDG method from our upwind HDG/DG approach.* More generally, (3.20) says that the amount of out-going mismatched flux for u is exactly the amount of in-going one for $\boldsymbol{\sigma}$ and vice versa. This is always true unless h approaches 0 (or p approaches ∞), for which both sides of (3.20), namely both mismatches, vanish.

We next discuss the upwind HDG scheme for transport equation in Section 3.3. From Corollary 3.6, the upwind HDG scheme is equivalent to the standard upwind DG method and hence all the results in [33] hold for the former as well. Let us present some results that are special for our HDG scheme. These are simpler versions of the results in Section 6, and hence we postpone the boundary condition enforcement until then.

LEMMA 3.9. *If $\nu - \frac{1}{2}\nabla \cdot \boldsymbol{\beta} > 0$, there exists a unique solution for the local solver (3.15).*

Proof. Since the local problem is in finite dimensional space, it is sufficient to show that $u = 0$ when $f = 0$ and $\hat{u} = 0$. Indeed, testing (3.15) with $v = u$ we have

$$-\left(u, \nabla \cdot (\boldsymbol{\beta} u)\right)_K + \left(\nu u, u\right)_K + \left\langle \left(|\boldsymbol{\beta} \cdot \mathbf{n}| + \boldsymbol{\beta} \cdot \mathbf{n}\right) u, u \right\rangle_{\partial K} = 0,$$

which, after integrating the first term by parts gives

$$\left(u, \boldsymbol{\beta} \cdot \nabla u\right)_K + \left(\nu u, u\right)_K + \left\langle |\boldsymbol{\beta} \cdot \mathbf{n}| \, u, u \right\rangle_{\partial K} = 0.$$

Finally adding the above two equations gives

$$\left(\left(2\nu - \nabla \cdot \boldsymbol{\beta}\right) u, u\right)_K + \left\langle \left(2\,|\boldsymbol{\beta} \cdot \mathbf{n}| + \boldsymbol{\beta} \cdot \mathbf{n}\right) u, u \right\rangle_{\partial K} = 0.$$

Since $\nu - \frac{1}{2}\nabla \cdot \boldsymbol{\beta} > 0$ and $2\,|\boldsymbol{\beta} \cdot \mathbf{n}| + \boldsymbol{\beta} \cdot \mathbf{n} \geq 0$, we conclude that $u = 0$. ∎

LEMMA 3.10. *If $\nu - \frac{1}{2}\nabla \cdot \boldsymbol{\beta} > 0$, there exists a unique solution $(u, \hat{u})$ for the upwind HDG scheme.*

Proof. Similar to the proof of Lemma 3.9, it is sufficient to show that $f = 0$ and $g = 0$ imply $u = 0$ and $\hat{u} = 0$. Indeed, eliminating $\hat{u}$ as in the proof of the Lemma 3.5 we recover the standard upwind DG scheme [33] which shows that $u = 0$ since $f = 0$ and $g = 0$. This in turn implies that $\hat{u} = 0$. ∎

We have used the equivalence (Corollary 3.6) between our upwind HDG method and the standard upwind HDG to obtain the uniqueness of $\hat{u}$ with no effort. Going one step further we can immediately show the convergence rate of our upwind HDG method.

THEOREM 3.11. *Suppose the exact solution u^e is sufficiently smooth, i.e. $u^e|_K \in H^{p+1}(K)$, then the solution pair $(u, \hat{u})$ satisfy the following error bounds*

$$\|u - u^e\|_{L^2(\Omega_h)} \leq ch^{p+\frac{1}{2}} \|u^e\|_{H^{k+1}(\Omega_h)},$$
$$\|\hat{u} - u^e\|_{L^2(\mathcal{E}_h^o)} \leq ch^{p+\frac{1}{2}} \|u^e\|_{H^{k+1}(\Omega_h)},$$

Proof. Since the upwind HDG is equivalent to the upwind DG scheme, the first assertion is immediate by the existing convergence theory of the latter (see, e.g., [33, 49]). For the second assertion, subtracting u^e from both sides of (3.17) yields

$$\|\hat{u} - u^e\|_{L^2(e)} \leq \left\| \frac{1}{2} [\![u - u^e]\!] \operatorname{sgn}(\boldsymbol{\beta} \cdot \mathbf{n}) \right\|_{L^2(e)} + \|\{\{u - u^e\}\}\|_{L^2(e)}$$
$$\leq c \|u - u^e\|_{L^2(e)} \leq ch^{p+\frac{1}{2}} \|u^e\|_{H^{k+1}(K)}.$$

where the last inequality is from the upwind DG (see [33, 49] and the references therein). Summing over all faces e, and hence elements, ends the proof. ∎

4. HDG schemes for the Maxwell equations. In this section, we apply our single abstract HDG framework in Section 2 to the Maxwell equation in both time and frequency (time harmonic) domains. We will show that by hybridizing the upwind DG for the first order Maxwell equation we can derive families of HDG schemes from which we recover many existing methods and discover new ones. The details of our constructive approach will be discussed at length in Section 4.1 for time domain equation and in Section 4.2 for the frequency domain counterpart.

4.1. Time domain Maxwell equation. Consider the following Maxwell equation in the time domain

$$\varepsilon \frac{\partial \mathbf{E}}{\partial t} - \nabla \times \mathbf{H} = \mathbf{f}_1 \text{ in } \Omega \tag{4.1a}$$
$$\nu \frac{\partial \mathbf{H}}{\partial t} + \nabla \times \mathbf{E} = \mathbf{f}_2 \text{ in } \Omega. \tag{4.1b}$$

Let us define $\mathbf{u} = (\mathbf{E}, \mathbf{H})^T$ and $\mathbf{f} = (\mathbf{f}_1, \mathbf{f}_2)^T$. We can rewrite (4.1) as

$$\mathbf{Q} \frac{\partial \mathbf{u}}{\partial t} + \nabla \cdot \mathbf{F}(\mathbf{u}) = \mathbf{f}, \tag{4.2}$$

where $\mathbf{Q} = \operatorname{diag}(\varepsilon, \varepsilon, \varepsilon, \nu, \nu, \nu)$ and the ith component of the flux tensor $\mathbf{F}(\mathbf{u})$ is given by

$$\mathbf{F}_i = \begin{bmatrix} -\mathbf{e}_i \times \mathbf{H} \\ \mathbf{e}_i \times \mathbf{E} \end{bmatrix},$$

with $\mathbf{e}_i$ as the ith canonical basis vector in $\mathbb{R}^d$.

Let us introduce some notations: define $c = 1/\sqrt{\nu\varepsilon}$, $Z = \sqrt{\nu/\varepsilon}$ and $Y = \sqrt{\varepsilon/\nu} = 1/Z$. One can easily see that $\mathbf{A}$ in (2.5) when applied to the Maxwell equation (4.1) can be written as

$$\mathbf{A} = \begin{bmatrix} \mathbf{0} & \frac{1}{\varepsilon}\mathbf{B} \\ \frac{1}{\nu}\mathbf{B} & \mathbf{0} \end{bmatrix}, \text{ where } \mathbf{B} = \begin{bmatrix} 0 & \mathbf{n}_3 & -\mathbf{n}_2 \\ -\mathbf{n}_3 & 0 & \mathbf{n}_1 \\ \mathbf{n}_2 & -\mathbf{n}_1 & 0 \end{bmatrix}.$$

Following the same exercise as above, one can show that $|\mathbf{A}|$ is given by

$$|\mathbf{A}| = \begin{bmatrix} \tilde{\mathbf{B}} & \mathbf{0} \\ \mathbf{0} & \tilde{\mathbf{B}} \end{bmatrix}, \text{ where } \tilde{\mathbf{B}} = c \begin{bmatrix} (1-\mathbf{n}_1^2) & -\mathbf{n}_1\mathbf{n}_2 & -\mathbf{n}_1\mathbf{n}_3 \\ -\mathbf{n}_1\mathbf{n}_2 & (1-\mathbf{n}_2^2) & -\mathbf{n}_2\mathbf{n}_3 \\ -\mathbf{n}_1\mathbf{n}_3 & -\mathbf{n}_2\mathbf{n}_3 & (1-\mathbf{n}_3^2) \end{bmatrix},$$

and the upwind Godunov fluxes (2.11) and (2.12), when applied to the Maxwell equation (4.1), read

$$\mathbf{F}^* \cdot \mathbf{n} = \begin{bmatrix} -\mathbf{n}\times\mathbf{H} + Y\mathbf{n}\times\mathbf{n}\times(\mathbf{E}^* - \mathbf{E}) \\ \mathbf{n}\times\mathbf{E} + Z\mathbf{n}\times\mathbf{n}\times(\mathbf{H}^* - \mathbf{H}) \end{bmatrix}, \tag{4.3}$$

where $\mathbf{E}^*$ and $\mathbf{H}^*$ are the Riemann solutions.

It can be observed that in order to compute the flux (4.3) only tangent components of $\mathbf{E}^*$ and $\mathbf{H}^*$, namely $-\mathbf{n}\times\mathbf{n}\times\mathbf{E}^*$ and $-\mathbf{n}\times\mathbf{n}\times\mathbf{H}^*$, are necessary. It implies that $\mathbf{E}^*$ and $\mathbf{H}^*$ are not independent of each other and this will be confirmed in the following. Again, this observation is the key to the hybridization in which we remove the redundancy. We start with the following result for the Godunov flux with exact Riemann solutions.

LEMMA 4.1. *Assuming ε and ν are positive and continuous across $e \in \mathcal{E}_h^o$, the following hold true:*

i) The Riemann solution $\mathbf{u}^* := (\mathbf{E}^*, \mathbf{H}^*)$ satisfies

$$\mathbf{n}\times\mathbf{n}\times\mathbf{E}^* = \mathbf{n}\times\mathbf{n}\times\{\{\mathbf{E}\}\} + \frac{Z}{2}[\![\mathbf{n}\times\mathbf{H}]\!], \tag{4.4a}$$

$$\mathbf{n}\times\mathbf{n}\times\mathbf{H}^* = \mathbf{n}\times\mathbf{n}\times\{\{\mathbf{H}\}\} - \frac{Y}{2}[\![\mathbf{n}\times\mathbf{E}]\!]. \tag{4.4b}$$

ii) The upwind Godunov flux (4.3) can be written either as

$$\mathbf{F}^* \cdot \mathbf{n} = \begin{bmatrix} -\mathbf{n}\times\mathbf{H} + Y\mathbf{n}\times\mathbf{n}\times(\mathbf{E}^* - \mathbf{E}) \\ \mathbf{n}\times\mathbf{E}^* \end{bmatrix}, \tag{4.5a}$$

or as

$$\mathbf{F}^* \cdot \mathbf{n} = \begin{bmatrix} -\mathbf{n}\times\mathbf{H}^* \\ \mathbf{n}\times\mathbf{E} + Z\mathbf{n}\times\mathbf{n}\times(\mathbf{H}^* - \mathbf{H}) \end{bmatrix}. \tag{4.5b}$$

Proof. The first assertion can be found using standard technique for solving the Riemann problem (see, e.g., [53, 29, 39]). Here, it is straightforward to obtain (4.4a)–(4.4b) from the conservation equation (2.13). Indeed, let us show (4.4a), and (4.4b) follows similarly. When applying (2.13) to flux (4.3), the first three equations read

$$-\mathbf{n}^-\times\mathbf{H}^- + Y\mathbf{n}^-\times\mathbf{n}^-\times\left(\mathbf{E}^* - \mathbf{E}^-\right) - \mathbf{n}^+\times\mathbf{H}^+ + Y\mathbf{n}^+\times\mathbf{n}^+\times\left(\mathbf{E}^* - \mathbf{E}^+\right) = 0,$$

which immediately becomes (4.4a) after dividing Y both sides and arranging terms appropriately.

In order to prove the second assertion, we start by rewriting (4.4a)–(4.4b) as

$$\mathbf{n}\times\mathbf{n}\times(\mathbf{E}^*-\mathbf{E}) = -\frac{1}{2}\mathbf{n}\times[\![\mathbf{n}\times\mathbf{E}]\!] + \frac{Z}{2}[\![\mathbf{n}\times\mathbf{H}]\!], \tag{4.6a}$$

$$\mathbf{n}\times\mathbf{n}\times(\mathbf{H}^*-\mathbf{H}) = -\frac{1}{2}\mathbf{n}\times[\![\mathbf{n}\times\mathbf{H}]\!] - \frac{Y}{2}[\![\mathbf{n}\times\mathbf{E}]\!]. \tag{4.6b}$$

Next, performing the cross product both sides of (4.6a) with $Y\mathbf{n}$ we obtain

$$-Y\mathbf{n}\times(\mathbf{E}^*-\mathbf{E}) = \frac{Y}{2}[\![\mathbf{n}\times\mathbf{E}]\!] + \frac{1}{2}\mathbf{n}\times[\![\mathbf{n}\times\mathbf{H}]\!],$$

which, together with (4.6b), yields

$$\mathbf{n}\times\mathbf{n}\times(\mathbf{H}^*-\mathbf{H}) = Y\mathbf{n}\times(\mathbf{E}^*-\mathbf{E}) \tag{4.7a}$$

$$\mathbf{n}\times\mathbf{n}\times(\mathbf{E}^*-\mathbf{E}) = -Z\mathbf{n}\times(\mathbf{H}^*-\mathbf{H}), \tag{4.7b}$$

where (4.7b) is obtained from (4.7a) by performing the cross product both sides with $\mathbf{n}$. The upwind fluxes (4.5a) and (4.5b) are readily available by substituting (4.7a) and (4.7b) into (4.3), respectively. □

We are now in the position to construct HDG methods and we start with the local solver. Taking $\mathbf{v} = (\mathbf{e}, \mathbf{h}) \in \mathbf{V}_h(K) \otimes \mathbf{V}_h(K)$ as the test function, the local equation (2.15a) when applied to (4.2) becomes: find $(\mathbf{E}, \mathbf{H}) \in \mathbf{V}_h(K) \otimes \mathbf{V}_h(K)$ such that

$$\left(\varepsilon\frac{\partial\mathbf{E}}{\partial t}, \mathbf{e}\right)_K - (\mathbf{H}, \nabla\times\mathbf{e})_K + \sum_{i=1}^{3}\left\langle\left(\hat{\mathbf{F}}\cdot\mathbf{n}\right)_i, \mathbf{e}_i\right\rangle_{\partial K} = 0, \tag{4.8a}$$

$$\left(\nu\frac{\partial\mathbf{H}}{\partial t}, \mathbf{h}\right)_K + (\mathbf{E}, \nabla\times\mathbf{h})_K + \sum_{i=4}^{6}\left\langle\left(\hat{\mathbf{F}}\cdot\mathbf{n}\right)_i, \mathbf{h}_i\right\rangle_{\partial K} = 0, \tag{4.8b}$$

with $\left(\hat{\mathbf{F}}\cdot\mathbf{n}\right)_i, i = 1,\ldots,6$ denoting the ith component of HDG flux.

It remains to construct the HDG flux $\hat{\mathbf{F}}\cdot\mathbf{n}$ and the conservation equation. To this end, we follow the same strategy presented in the abstract Section 2, namely, we simply replace the starred quantities, e.g. $\mathbf{E}^*$ and $\mathbf{H}^*$, in (4.5a)–(4.5b) with hatted ones, e.g. $\hat{\mathbf{E}}$ and $\hat{\mathbf{H}}$, but the latter are unknown traces that need to be solved for. Let us now present in details two (families of) HDG fluxes based on Godunov fluxes (4.5a)–(4.5b).

4.1.1. HDG schemes based on $\hat{\mathbf{E}}$. To define our first HDG method, we reverse the results in Lemma 4.1 by defining the HDG flux as in (4.5a), i.e.,

$$\hat{\mathbf{F}}\cdot\mathbf{n} = \begin{bmatrix} -\mathbf{n}\times\mathbf{H} + Y\mathbf{n}\times\mathbf{n}\times\left(\hat{\mathbf{E}}-\mathbf{E}\right) \\ \mathbf{n}\times\hat{\mathbf{E}} \end{bmatrix}. \tag{4.9}$$

However, now $\hat{\mathbf{E}}$, in fact its tangent component $\hat{\mathbf{E}}^t := -\mathbf{n}\times\mathbf{n}\times\hat{\mathbf{E}}$, is considered as the unknown. It is obvious that the last three components of the HDG flux (4.9) automatically satisfy the conservation constraint (2.15b). The task at hand is therefore to ensure the first three to obey the conservation condition as well. To that end, we

observe that since the flux $-\mathbf{n}\times\mathbf{H}+Y\mathbf{n}\times\mathbf{n}\times\left(\hat{\mathbf{E}}-\mathbf{E}\right)$ is a vector in the tangent plane orthogonal to $\mathbf{n}$, it is sufficient to enforce the continuity in the tangent plane only, i.e.,

$$\left\langle [\![-\mathbf{n}\times\mathbf{H}+Y\mathbf{n}\times\mathbf{n}\times\left(\hat{\mathbf{E}}-\mathbf{E}\right)]\!], \boldsymbol{\mu}^t\right\rangle_e = 0, \quad \forall \boldsymbol{\mu}^t \in \boldsymbol{\Lambda}_h^t(e), \quad \forall e\in\mathcal{E}_h^o, \tag{4.10}$$

where the tangent trace space $\boldsymbol{\Lambda}_h^t$ is defined as

$$\boldsymbol{\Lambda}_h^t(\mathcal{E}_h) := \left\{\boldsymbol{\lambda}\in\left[L^2(\mathcal{E}_h)\right]^m : \boldsymbol{\lambda}|_e \in [\mathcal{P}^p(e)]^m, \boldsymbol{\lambda}\cdot\mathbf{n}|_e = 0, \forall e\in\mathcal{E}_h\right\}.$$

Let us also define the tangent component of the electric field as $\mathbf{E}^t = -\mathbf{n}\times\mathbf{n}\times\mathbf{E}$. The HDG flux (4.9) and the conservation condition (4.10) can be written in terms of $\hat{\mathbf{E}}^t$ and $\mathbf{E}^t$ as follows

$$\hat{\mathbf{F}}\cdot\mathbf{n} = \begin{bmatrix} -\mathbf{n}\times\mathbf{H}+Y\left(\mathbf{E}^t-\hat{\mathbf{E}}^t\right) \\ \mathbf{n}\times\hat{\mathbf{E}}^t \end{bmatrix}, \tag{4.11}$$

and

$$\left\langle [\![-\mathbf{n}\times\mathbf{H}+Y\left(\mathbf{E}^t-\hat{\mathbf{E}}^t\right)]\!], \boldsymbol{\mu}^t\right\rangle_e = 0, \quad \forall \boldsymbol{\mu}^t \in \boldsymbol{\Lambda}_h^t(e), \quad \forall e\in\mathcal{E}_h^o, \tag{4.12}$$

where we have used the fact that $\mathbf{n}\times\mathbf{E} = \mathbf{n}\times\mathbf{E}^t$.

The first HDG method is defined by the local solver (4.8), where the HDG flux is defined in (4.11), and the conservation condition (4.12).

4.1.2. HDG schemes based on $\hat{\mathbf{H}}$. In this section, the HDG flux is constructed based on the Godunov flux (4.5b). More specifically, we define

$$\hat{\mathbf{F}}\cdot\mathbf{n} = \begin{bmatrix} -\mathbf{n}\times\hat{\mathbf{H}}^t \\ \mathbf{n}\times\mathbf{E}+Z\left(\mathbf{H}^t-\hat{\mathbf{H}}^t\right) \end{bmatrix}, \tag{4.13}$$

where the tangent components $\mathbf{H}^t := -\mathbf{n}\times\mathbf{n}\times\mathbf{H}$ of $\mathbf{H}$ and $\hat{\mathbf{H}}^t := -\mathbf{n}\times\mathbf{n}\times\hat{\mathbf{H}}$ of $\hat{\mathbf{H}}$ have been employed.

If we follow the same exercise as in Section 4.1.1 by defining the HDG flux as in (4.13), where the $\mathbf{H}^t$ is unknown on e, we see that the first three components automatically satisfy the conservation constraint (2.15b). Since the flux $\mathbf{n}\times\mathbf{E}+Z\left(\mathbf{H}^t-\hat{\mathbf{H}}^t\right)$ is a vector in the tangent plane orthogonal to $\mathbf{n}$, it is sufficient to enforce the continuity in the tangent plane only, i.e.,

$$\left\langle [\![\mathbf{n}\times\mathbf{E}+Z\left(\mathbf{H}^t-\hat{\mathbf{H}}^t\right)]\!], \boldsymbol{\mu}^t\right\rangle_e = 0, \quad \forall \boldsymbol{\mu}^t \in \boldsymbol{\Lambda}_h^t(e), \quad \forall e\in\mathcal{E}_h^o. \tag{4.14}$$

Our second HDG method for the Maxwell equation in the time domain consists of the local solver (4.8) with the HDG flux defined in (4.13) and the conservation condition (4.14).

Before diving into a detailed analysis, let us present a result parallel to Lemma 3.5 and Corollary 3.6. Since the result is almost the same for both HDG approaches, we present it for the first one only.

LEMMA 4.2.

i) Assume ε and ν are positive and continuous across $e \in \mathcal{E}_h^o$. Then, the tangent component of the trace solution $\hat{\mathbf{E}}^t$ of the first HDG scheme with (4.8), (4.11), and (4.12) coincides with that of the Riemann solution (4.4a). Furthermore, the HDG flux (4.11) is identical to the Godunov upwind flux (4.3).

ii) The first HDG scheme is equivalent to the standard upwind DG scheme.

Proof. Though there are differences in the details, the idea of the proof is similar to that of Lemma 3.5 and Corollary 3.6, and hence we omit the details. ∎

4.1.3. Analysis. In this section we will present some analysis for the first HDG method (those for the second HDG method follow similarly and hence omitted). As in Lemma 4.2, our HDG method is equivalent to the standard upwind DG for the Maxwell equation, and thus all the existing results on consistency, stability, and convergence [29, 30, 7] automatically hold. We therefore focus on results that are special for the HDG method. To that end, we need to equip the Maxwell equation (4.1) with an appropriate boundary condition. For simplicity, the perfect electric conduction (PEC) boundary condition is employed, namely the tangent component of the electric field is zero on $\partial\Omega$. We enforce the boundary condition through the tangent trace, i.e.,

$$\hat{\mathbf{E}}^t = \mathbf{0} \text{ on } \partial\Omega. \tag{4.15}$$

We next present a fully discrete HDG scheme using, for simplicity, the backward Euler approach. It is sufficient to present the results for one time step, so we will omit the time index for clarity. The backward Euler discretization of (4.8) with the HDG flux (4.11) reads

$$(\varepsilon\mathbf{E}, \mathbf{e})_K - (\mathbf{H}, \nabla\times\mathbf{e})_K + \left\langle -\mathbf{n}\times\mathbf{H} + Y\left(\mathbf{E}^t - \mathbf{1}_{\partial K\setminus\partial\Omega}\hat{\mathbf{E}}^t\right), \mathbf{e}\right\rangle_{\partial K} = (\mathbf{f}, \mathbf{e})_K, \tag{4.16a}$$

$$(\nu\mathbf{H}, \mathbf{h})_K + (\mathbf{E}, \nabla\times\mathbf{h})_K + \left\langle \mathbf{1}_{\partial K\setminus\partial\Omega}\mathbf{n}\times\hat{\mathbf{E}}^t, \mathbf{h}\right\rangle_{\partial K} = (\mathbf{g}, \mathbf{h})_K, \tag{4.16b}$$

where $\mathbf{f}$ and $\mathbf{g}$ contain quantities known from the previous time step and the forcing $\mathbf{f}_1, \mathbf{f}_2$. Here, $\mathbf{1}_{\partial K\setminus\partial\Omega}$ denotes the standard indicator function for the set $\partial K \setminus \partial\Omega$ and we have used it to enforce the PEC condition (4.15). We first study the well-posedness of the local solver (4.16), i.e. step one of the HDG method.

LEMMA 4.3. *Assume that $\varepsilon, \nu > 0$. For a given value of $\mathbf{f}, \mathbf{g}$ and $\hat{\mathbf{E}}^t$, the local solver (4.16) has a solution and it is unique.*

Proof. We observe that the local solver (4.16) is a finite dimensional square system. Thus, due to linearity, it is sufficient to show that $\mathbf{E} = \mathbf{H} = \mathbf{0}$ is the only solution when $\mathbf{f} = \mathbf{g} = \mathbf{0}$ and $\hat{\mathbf{E}}^t = \mathbf{0}$. Indeed, taking $\mathbf{e} = \mathbf{E}, \mathbf{h} = \mathbf{H}$, integrating the second term of (4.16a) by parts, adding the two equations, and using the fact that

$$\left\langle \mathbf{E}^t, \mathbf{E}\right\rangle_{\partial K} = \langle -\mathbf{n}\times\mathbf{n}\times\mathbf{E}, \mathbf{E}\rangle_{\partial K} = \|\mathbf{n}\times\mathbf{n}\times\mathbf{E}\|^2_{\partial K},$$

we obtain

$$\|\mathbf{E}\|^2_{K,\varepsilon} + \|\mathbf{H}\|^2_{K,\nu} + \|\mathbf{n}\times\mathbf{n}\times\mathbf{E}\|^2_{\partial K} = 0,$$

from which it follows that $\mathbf{H} = \mathbf{E} = \mathbf{0}$. ∎

We next consider the well-posedness of the global HDG system of determining the tangent trace unknown $\hat{\mathbf{E}}^t$, i.e. step two of the HDG method. We begin by setting

$\mathbf{e} = \mathbf{E}, \mathbf{h} = \mathbf{H}$ in (4.16), integrating the second term in (4.16a) by parts, adding the resulting equations, and then summing over all elements to obtain

$$\|\mathbf{E}\|^2_{\Omega_h,\varepsilon} + \|\mathbf{H}\|^2_{\Omega_h,\nu} + \sum_{K\in\Omega_h} \left\langle Y\left(\mathbf{E}^t - \hat{\mathbf{E}}^t\right), \mathbf{E}^t \right\rangle_{\partial K\setminus\partial\Omega} + \left\|\mathbf{E}^t\right\|^2_{\partial K\cap\partial\Omega,Y} + \sum_{K\in\Omega_h} \left\langle \mathbf{n}\times\hat{\mathbf{E}}^t, \mathbf{H}\right\rangle_{\partial K\setminus\partial\Omega} = 0, \quad (4.17)$$

where we have used the fact that $\mathbf{E}$ can be replaced by $\mathbf{E}^t$ in the third term on the left hand side of (4.16a). We next sum (4.12) over all faces $e \in \mathcal{E}^o_h$, set $\boldsymbol{\mu}^t = \hat{\mathbf{E}}^t$, and use the definition of the jump operator to arrive at

$$\sum_{K\in\Omega_h} \left\langle -\mathbf{n}\times\mathbf{H} + Y\left(\mathbf{E}^t - \hat{\mathbf{E}}^t\right), \hat{\mathbf{E}}^t \right\rangle_{\partial K\setminus\partial\Omega} = 0. \quad (4.18)$$

THEOREM 4.4. *Assume that $\varepsilon, \nu > 0$. For a given value of $\mathbf{f}$ and $\mathbf{g}$, there exists a unique solution for the tangent trace unknown $\hat{\mathbf{E}}^t$, $\mathbf{E}$, and $\mathbf{H}$.*

Proof. Since the system of linear equations (4.12) for determining $\hat{\mathbf{E}}^t$ is square, it is sufficient, by induction, to show that the solutions $\mathbf{E}, \mathbf{H}$ and $\hat{\mathbf{E}}^t$ of the HDG method for the first time step are zero with zero initial condition and zero forcing, i.e. $\mathbf{f} = \mathbf{g} = \mathbf{0}$. Subtracting (4.18) from (4.17) we have

$$\|\mathbf{E}\|^2_{\Omega,\varepsilon} + \|\mathbf{H}\|^2_{\Omega_h,\nu} + \left\|\mathbf{E}^t\right\|^2_{\partial K\cap\partial\Omega,Y} + \sum_{K\in\Omega_h} \left\|\mathbf{E}^t - \hat{\mathbf{E}}^t\right\|^2_{\partial K\setminus\partial\Omega,Y} = 0,$$

which shows that $\mathbf{E}, \mathbf{H}$, and hence $\mathbf{E}^t$, must vanish and so must $\hat{\mathbf{E}}^t$, and this concludes the proof. ∎

REMARK 4.5. *As in Theorem 3.11 we can further obtain the convergence rate for both the volume $\mathbf{E}, \mathbf{H}$ and the trace $\hat{\mathbf{E}}^t$ unknowns exploiting the equivalence (see Lemma 4.2) of our HDG schemes and the standard upwind DG in [29, 30, 7]. In particular, one can show that $\mathbf{E}, \mathbf{H}$ and the trace $\hat{\mathbf{E}}^t$ converge to the exact solution with the rate of $h^{p+\frac{1}{2}}$, but we leave out the details here.*

4.2. Frequency domain (time harmonic) Maxwell equation. Similar to [46] we consider the following time-harmonic equation

$$\nu\mathbf{E} - \nabla\times\mathbf{H} = \mathbf{0} \text{ in } \Omega, \quad (4.19a)$$

$$\nabla\times\mathbf{E} - \varepsilon\omega^2\mathbf{H} + \varepsilon\nabla q = \mathbf{f} \text{ in } \Omega, \quad (4.19b)$$

$$\nabla\cdot(\varepsilon\mathbf{H}) = 0 \text{ in } \Omega. \quad (4.19c)$$

As can be seen, $\mathbf{A}$ in this case has the structure of the time domain Maxwell equation (the first two equations with respect to $\mathbf{E}$ and $\mathbf{H}$) and the convection-diffusion (the last two equations with respect to $\mathbf{H}$ and q). Indeed, the explicit form of $\mathbf{A}$ reads

$$\mathbf{A} = \begin{bmatrix} \mathbf{0} & \mathbf{B} & \mathbf{0} \\ \mathbf{B} & \mathbf{0} & \mathbf{D} \\ \mathbf{0} & \mathbf{D}^T & 0 \end{bmatrix}, \text{ where } \mathbf{B} = \begin{bmatrix} 0 & \mathbf{n}_3 & -\mathbf{n}_2 \\ -\mathbf{n}_3 & 0 & \mathbf{n}_1 \\ \mathbf{n}_2 & -\mathbf{n}_1 & 0 \end{bmatrix}, \quad \mathbf{D} = \varepsilon \begin{bmatrix} \mathbf{n}_1 \\ \mathbf{n}_2 \\ \mathbf{n}_3 \end{bmatrix},$$

and $\mathbf{0}$ are zero matrices with appropriate size. After some simple algebraic manipulations one can show that $|\mathbf{A}|$ is given by

$$|\mathbf{A}| = \begin{bmatrix} \tilde{\mathbf{B}} & \mathbf{0} & \mathbf{0} \\ \mathbf{0} & \overline{\mathbf{B}} & \mathbf{0} \\ \mathbf{0} & \mathbf{0} & \varepsilon \end{bmatrix}, \text{ where } \tilde{\mathbf{B}} = \begin{bmatrix} \left(1-\mathbf{n}_1^2\right) & -\mathbf{n}_1\mathbf{n}_2 & -\mathbf{n}_1\mathbf{n}_3 \\ -\mathbf{n}_1\mathbf{n}_2 & \left(1-\mathbf{n}_2^2\right) & -\mathbf{n}_2\mathbf{n}_3 \\ -\mathbf{n}_1\mathbf{n}_3 & -\mathbf{n}_2\mathbf{n}_3 & \left(1-\mathbf{n}_3^2\right) \end{bmatrix},$$

and

$$\overline{\mathbf{B}} = \begin{bmatrix} (\varepsilon-1)\,\mathbf{n}_1^2+1 & (\varepsilon-1)\,\mathbf{n}_1\mathbf{n}_2 & (\varepsilon-1)\,\mathbf{n}_1\mathbf{n}_3 \\ (\varepsilon-1)\,\mathbf{n}_1\mathbf{n}_2 & (\varepsilon-1)\,\mathbf{n}_2^2+1 & (\varepsilon-1)\,\mathbf{n}_2\mathbf{n}_3 \\ (\varepsilon-1)\,\mathbf{n}_1\mathbf{n}_3 & (\varepsilon-1)\,\mathbf{n}_2\mathbf{n}_3 & (\varepsilon-1)\,\mathbf{n}_3^2+1 \end{bmatrix}.$$

Consequently, the Godunov fluxes (2.11)–(2.12) in this case read

$$\mathbf{F}^*\cdot\mathbf{n} = \begin{bmatrix} -\mathbf{n}\times\mathbf{H}+\mathbf{n}\times\mathbf{n}\times(\mathbf{E}^*-\mathbf{E}) \\ \mathbf{n}\times\mathbf{E}+\mathbf{n}\times\mathbf{n}\times(\mathbf{H}^*-\mathbf{H})+\varepsilon q\mathbf{n}+\varepsilon\left[(\mathbf{H}-\mathbf{H}^*)\cdot\mathbf{n}\right]\mathbf{n} \\ \varepsilon\mathbf{H}\cdot\mathbf{n}+\varepsilon\,(q-q^*) \end{bmatrix}, \tag{4.20}$$

where $\mathbf{E}^*, \mathbf{H}^*$, and q^* (two vectors and one scalar) are the Riemann solutions.

Similar to previous sections, we seek the relationships between the Riemann solutions to motivate the construction of HDG methods. Proposition 4.6 collects some important identities.

PROPOSITION 4.6. *The following hold for the Riemann solutions* $\mathbf{E}^*, \mathbf{H}^*$ *and* q^**:*

$$\begin{aligned} \mathbf{n}\times\mathbf{n}\times(\mathbf{E}^*-\mathbf{E}) &= \mathbf{n}\times(\mathbf{H}-\mathbf{H}^*), \\ (\mathbf{H}-\mathbf{H}^*)\cdot\mathbf{n} &= (q^*-q). \end{aligned}$$

and

$$\begin{aligned} \mathbf{n}\times\mathbf{n}\times\mathbf{E}^* &= \mathbf{n}\times\mathbf{n}\times\{\{\mathbf{E}\}\}+\frac{1}{2}[\![\mathbf{n}\times\mathbf{H}]\!], \\ \mathbf{n}\times\mathbf{n}\times\mathbf{H}^* &= -\{\{\mathbf{n}\times\mathbf{E}\}\}+\mathbf{n}\times\mathbf{n}\times\{\{\mathbf{H}\}\}, \\ \hat{\mathbf{H}}\cdot\mathbf{n} &= \{\{q\mathbf{n}+\mathbf{H}\}\}\cdot\mathbf{n}, \\ q^* &= \{\{q\}\}+\frac{1}{2}[\![\mathbf{H}\cdot\mathbf{n}]\!] \end{aligned}$$

Using the results in Proposition 4.6, the upwind flux (4.20) can be written either as

$$\mathbf{F}^*\cdot\mathbf{n} = \begin{bmatrix} -\mathbf{n}\times\mathbf{H}+\mathbf{n}\times\mathbf{n}\times(\mathbf{E}^*-\mathbf{E}) \\ \mathbf{n}\times\mathbf{E}^*+\varepsilon q^*\mathbf{n} \\ \varepsilon\mathbf{H}\cdot\mathbf{n}+\varepsilon\,(q-q^*) \end{bmatrix}, \tag{4.21}$$

or

$$\mathbf{F}^*\cdot\mathbf{n} = \begin{bmatrix} -\mathbf{n}\times\mathbf{H}^* \\ \mathbf{n}\times\mathbf{E}+\mathbf{n}\times\mathbf{n}\times(\mathbf{H}^*-\mathbf{H})+\varepsilon q^*\mathbf{n} \\ \varepsilon\mathbf{H}\cdot\mathbf{n}+\varepsilon\,(q-q^*) \end{bmatrix}, \tag{4.22}$$

or

$$\mathbf{F}^*\cdot\mathbf{n} = \begin{bmatrix} -\mathbf{n}\times\mathbf{H}^* \\ \mathbf{n}\times\mathbf{E}+\varepsilon q\mathbf{n}+\mathbf{n}\times\mathbf{n}\times(\mathbf{H}^*-\mathbf{H})+\varepsilon\left[(\mathbf{H}-\mathbf{H}^*)\cdot\mathbf{n}\right]\mathbf{n} \\ \varepsilon\mathbf{H}^*\cdot\mathbf{n} \end{bmatrix}. \tag{4.23}$$

We have used the property of Riemann solutions $\mathbf{E}^*, \mathbf{H}^*, q^*$ and the Godunov flux to construct different forms of the upwind fluxes (4.21)–(4.23) and identities in Proposition 4.6. One can observe from (4.21)–(4.23) that we in fact need only either the pair $(\mathbf{n}\times\mathbf{n}\times\mathbf{E}^*, q^*)$ or the pair $(\mathbf{n}\times\mathbf{n}\times\mathbf{H}^*, q^*)$ or $\mathbf{H}^*$ to compute the upwind flux. This motivates us to define the following two[1] (families of) HDG schemes for the time harmonic Maxwell equation based on two different, but equivalent, Godunov fluxes (4.21)–(4.22).

[1] Our analysis shows that the HDG local solver using the HDG flux (4.23) does not have a unique solution for q for the interior elements. A remedy similar to Section 5 can be done but we skip its discussion in this paper to keep the length of the paper reasonable.

4.2.1. HDG scheme based on $\left(\hat{\mathbf{E}}^t, \hat{q}\right)$. The starting point of the first HDG scheme is to define the HDG flux based on (4.21), i.e.,

$$\hat{\mathbf{F}}\cdot\mathbf{n} = \begin{bmatrix} -\mathbf{n}\times\mathbf{H} + \left(\mathbf{E}^t - \hat{\mathbf{E}}^t\right) \\ \mathbf{n}\times\hat{\mathbf{E}}^t + \varepsilon\hat{q}\mathbf{n} \\ \varepsilon\mathbf{H}\cdot\mathbf{n} + \varepsilon\left(q-\hat{q}\right) \end{bmatrix}. \tag{4.24}$$

Thus, the actual single-valued trace unknowns in our first HDG scheme are the tangent vector $\hat{\mathbf{E}}^t$ and the scalar $\hat{q}$.

Our next step is to determine the algebraic constraints (2.15b). Since $\mathbf{n}\times\hat{\mathbf{E}}^t + \varepsilon\hat{q}\mathbf{n}$ automatically fulfill the conservation property and $-\mathbf{n}\times\mathbf{H} + \left(\mathbf{E}^t - \hat{\mathbf{E}}^t\right)$ lives in the tangent plane, (2.15b) in this case reduces to

$$\left\langle [\![-\mathbf{n}\times\mathbf{H} + \left(\mathbf{E}^t - \hat{\mathbf{E}}^t\right)]\!], \boldsymbol{\mu}^t \right\rangle_e = 0, \quad \forall \boldsymbol{\mu}^t \in \boldsymbol{\Lambda}_h^t(e), \quad \forall e \in \mathcal{E}_h^o, \tag{4.25a}$$

$$\left\langle [\![\varepsilon\mathbf{H}\cdot\mathbf{n} + \varepsilon\left(q-\hat{q}\right)]\!], \lambda \right\rangle_e = 0, \quad \lambda \in \Lambda_h(e), \quad \forall e \in \mathcal{E}_h^o. \tag{4.25b}$$

One can observe that $\mathbf{E}^t - \hat{\mathbf{E}}^t$ and $q - \hat{q}$ are the mismatches between the trace unknowns and volume unknowns (in fact their traces) restricted on the mesh skeleton. These mismatches vanish for the exact solution, but converges to zero for the HDG solutions as the mesh (or solution order) is refined. This suggests that one can control these mismatches by introducing two penalty parameters τ^t and τ^n to form a penalized family of HDG fluxes as follows

$$\hat{\mathbf{F}}\cdot\mathbf{n} = \begin{bmatrix} -\mathbf{n}\times\mathbf{H} + \tau^t\left(\mathbf{E}^t - \hat{\mathbf{E}}^t\right) \\ \mathbf{n}\times\hat{\mathbf{E}}^t + \varepsilon\hat{q}\mathbf{n} \\ \varepsilon\mathbf{H}\cdot\mathbf{n} + \tau^n\varepsilon\left(q-\hat{q}\right) \end{bmatrix}. \tag{4.26}$$

The conservation algebraic constraints in this case read

$$\left\langle [\![-\mathbf{n}\times\mathbf{H} + \tau^t\left(\mathbf{E}^t - \hat{\mathbf{E}}^t\right)]\!], \boldsymbol{\mu}^t \right\rangle_e = 0, \quad \forall \boldsymbol{\mu}^t \in \boldsymbol{\Lambda}_h^t(e), \quad \forall e \in \mathcal{E}_h^o, \tag{4.27a}$$

$$\left\langle [\![\varepsilon\mathbf{H}\cdot\mathbf{n} + \tau^n\varepsilon\left(q-\hat{q}\right)]\!], \lambda \right\rangle_e = 0, \quad \forall e \in \mathcal{E}_h^o, \quad \forall \lambda \in \Lambda_h. \tag{4.27b}$$

Clearly, we recover the upwind HDG scheme by setting $\tau^t = \tau^n = 1$.

Next is the description of the local solver. Taking $\mathbf{v} = (\mathbf{e}, \mathbf{h}, v) \in \mathbf{V}_h(K) \otimes \mathbf{V}_h(K) \otimes V_h(K)$ as the test function, the local equation (2.15a) when applied to (4.19) becomes: find $(\mathbf{E}, \mathbf{H}, q) \in \mathbf{V}_h(K) \otimes \mathbf{V}_h(K) \otimes V_h(K)$ such that

$$(\nu\mathbf{E}, \mathbf{e})_K - (\mathbf{H}, \nabla\times\mathbf{e})_K + \sum_{i=1}^{3} \left\langle \left(\hat{\mathbf{F}}\cdot\mathbf{n}\right)_i, \mathbf{e}_i \right\rangle_{\partial K} = 0, \tag{4.28a}$$

$$-\left(\varepsilon\omega^2\mathbf{H}, \mathbf{h}\right)_K + (\mathbf{E}, \nabla\times\mathbf{h})_K - (q, \nabla\cdot(\varepsilon\mathbf{h}))_K + \sum_{i=4}^{6} \left\langle \left(\hat{\mathbf{F}}\cdot\mathbf{n}\right)_i, \mathbf{h}_i \right\rangle_{\partial K} = (\mathbf{f}, \mathbf{h})_K, \tag{4.28b}$$

$$-(\varepsilon\mathbf{H}, \nabla v)_K + \left\langle \left(\hat{\mathbf{F}}\cdot\mathbf{n}\right)_7, v \right\rangle_{\partial K} = 0, \tag{4.28c}$$

with $\left(\hat{\mathbf{F}}\cdot\mathbf{n}\right)_i, i = 1, \ldots, 7$ denoting the ith component of numerical flux (4.26).

The first HDG scheme consists of the local solver (4.28) and the algebraic equations (4.27), where the HDG flux is given in (4.26).

4.2.2. HDG scheme based on $\left(\hat{\mathbf{H}}^t, \hat{q}\right)$. In the second HDG scheme, we define the HDG flux based on (4.22), i.e.,

$$\hat{\mathbf{F}}\cdot\mathbf{n} = \begin{bmatrix} -\mathbf{n}\times\hat{\mathbf{H}}^t \\ \mathbf{n}\times\mathbf{E} - \mathbf{n}\times\mathbf{n}\times\left(\mathbf{H}-\hat{\mathbf{H}}^t\right) + \varepsilon\hat{q}\mathbf{n} \\ \varepsilon\mathbf{H}\cdot\mathbf{n} + \varepsilon\left(q-\hat{q}\right) \end{bmatrix}, \tag{4.29}$$

where $\hat{\mathbf{H}}^t := -\mathbf{n}\times\mathbf{n}\times\hat{\mathbf{H}}$, and $\hat{q}$ are now the single-valued unknown traces that need to be solved for. Our HDG flux (4.29) is exactly the proposed HDG flux for time-harmonic Maxwell equation in [46] with unity stabilization parameters. The beauty of our approach is to construct the HDG flux (4.29) by hybridizing the upwind scheme using the Godunov flux. On the one hand, our upwind HDG approach is (stabilization) parameter-free and hence removing the "usual complaint" that HDG schemes are parameter-dependent. On the other hand, one can view our approach as a constructive way to devise the parameter dependent HDG family in [46] by introducing two parameters τ^t and τ^n to penalize the deviation of $\hat{\mathbf{H}}^t$ and $\hat{q}$ from $\mathbf{H}$ and q, respectively, and rewrite (4.29) as

$$\hat{\mathbf{F}}\cdot\mathbf{n} = \begin{bmatrix} -\mathbf{n}\times\hat{\mathbf{H}}^t \\ \mathbf{n}\times\mathbf{E} - \tau^t\mathbf{n}\times\mathbf{n}\times\left(\mathbf{H}-\hat{\mathbf{H}}^t\right) + \varepsilon\hat{q}\mathbf{n} \\ \varepsilon\mathbf{H}\cdot\mathbf{n} + \tau^n\varepsilon\left(q-\hat{q}\right) \end{bmatrix}. \tag{4.30}$$

Clearly, when $\tau^t = \tau^n = 1$ the upwind HDG flux (4.29) is recovered.

It is obvious that the first three components of the HDG flux (4.30) automatically satisfy the conservation constraint (2.15b). For the next three components, note that $\mathbf{n}\times\mathbf{E} - \tau^t\mathbf{n}\times\mathbf{n}\times\left(\mathbf{H}-\hat{\mathbf{H}}^t\right)$ is a vector in the tangent plane while $\varepsilon\hat{q}\mathbf{n}$ is a vector along the normal vector. The latter automatically satisfies the conservation condition since $\hat{q}$ is single-valued, and hence will not appear in the conservation condition. Let us define the tangent component of the magnetic field $\mathbf{H}$ as $\mathbf{H}^t := -\mathbf{n}\times\mathbf{n}\times\mathbf{H}$. The conservation condition (2.15b) when applied to the HDG flux (4.30) reduces to the following algebraic constraints

$$\left\langle [\![\mathbf{n}\times\mathbf{E} + \tau^t\left(\mathbf{H}^t - \hat{\mathbf{H}}^t\right)]\!], \boldsymbol{\mu}^t\right\rangle_e = 0, \quad \forall\boldsymbol{\mu}^t\in\boldsymbol{\Lambda}_h^t(e), \forall e\in\mathcal{E}_h^o, \tag{4.31a}$$

$$\langle [\![\varepsilon\mathbf{H}\cdot\mathbf{n} + \tau^n\varepsilon\left(q-\hat{q}\right)]\!], \mu\rangle_e = 0, \quad \forall e\in\mathcal{E}_h^o, \quad \forall\mu\in\Lambda_h. \tag{4.31b}$$

The second HDG scheme consists of the local solver (4.28) and the algebraic equations (4.31), where the HDG flux is given in (4.30).

REMARK 4.7. *Given the understanding on the nature of HDG schemes established in this paper, one can introduce a new HDG scheme based on the HDG flux* (4.22) *by defining*

$$\varepsilon\tilde{\hat{q}}\ sgn(\mathbf{n}) := \varepsilon\mathbf{H}\cdot\mathbf{n} + \tau^n\varepsilon\left(q-\hat{q}\right),$$

which transform the HDG flux (4.22) *into*

$$\hat{\mathbf{F}}\cdot\mathbf{n} = \begin{bmatrix} -\mathbf{n}\times\hat{\mathbf{H}}^t \\ \mathbf{n}\times\mathbf{E} + \tau^t\left(\mathbf{H}^t - \hat{\mathbf{H}}^t\right) + \varepsilon\left(\mathbf{H}\cdot\mathbf{n}\right)\mathbf{n} + \tau^n\varepsilon\left(q - \tilde{\hat{q}}\ sgn(\mathbf{n})\right)\mathbf{n} \\ \varepsilon\tilde{\hat{q}}\ sgn(\mathbf{n}) \end{bmatrix}. \tag{4.32}$$

For this HDG flux, the first three and the seventh conservation conditions are automatically satisfied. We are left with three algebraic constraints, i.e. $\forall \boldsymbol{\mu} \in \boldsymbol{\Lambda}_h(e), e \in \mathcal{E}_h^o$,

$$\left\langle [\![\mathbf{n} \times \mathbf{E} + \tau^t \left(\mathbf{H}^t - \hat{\mathbf{H}}^t \right) + \varepsilon (\mathbf{H} \cdot \mathbf{n}) \mathbf{n} + \tau^n \varepsilon \left(q - \tilde{\hat{q}}\ sgn(\mathbf{n}) \right) \mathbf{n}]\!], \boldsymbol{\mu} \right\rangle_e = 0. \quad (4.33)$$

By construction, the HDG fluxes (4.22) *and* (4.32) *are equivalent though different in appearance. The number of the algebraic constraints in* (4.31) *is also the same as that in* (4.33) *since the tangent trace space* $\boldsymbol{\Lambda}_h^t$ *has two components while it is three for* $\boldsymbol{\Lambda}_h$.

Parallel to Lemma 3.5 and Corollary 3.6, the following results hold for two proposed HDG families.

LEMMA 4.8. *Assume* ε, ν *are positive and continuous across* $e \in \mathcal{E}_h^o$, *and* $\tau^t = \tau^n = 1$.

i) The tangent component of the trace solution $\hat{\mathbf{H}}^t$ *(or* $\hat{\mathbf{E}}^t$*) of the two proposed HDG schemes coincides with that of the Riemann solution in Proposition 4.6. Furthermore, the HDG fluxes are identical to the Godunov upwind flux* (4.20).

ii) The two proposed HDG schemes are equivalent to the standard upwind DG scheme.

Proof. The proofs of these assertions are similar to those of Lemma 3.5 and Corollary 3.6, so we leave out the details. ∎

4.2.3. Analysis. For simplicity in the exposition we will analyze our HDG scheme for the fully upwind case, i.e. $\tau^t = \tau^n = 1$. For the general case with $\tau^t, \tau^n > 0$, all the proofs will go through except that some terms will carry τ^t and τ^n. Since our second HDG scheme is the same as that proposed in [46], its analysis is ignored and the readers are referred to [46]. Thus, the analysis of the our first HDG scheme, *a new HDG scheme for time harmonic Maxwell equation*, is the main focus of this section. By construction, it is automatically locally conservative and consistent since it is equivalent to the upwind DG method as shown in Lemma 4.8.

In order to study the well-posedness of the local (solving for $\mathbf{E}, \mathbf{H}, q$ as a function of $\hat{\mathbf{E}}$ and $\hat{q}$) and global solvers (solving for $\hat{\mathbf{E}}$ and $\hat{q}$ on the mesh skeleton), we need to supply boundary conditions. For simplicity, we again consider the PEC boundary conditions

$$\mathbf{n} \times \mathbf{E} = \mathbf{0}, \text{ and } q = 0 \text{ on } \partial\Omega,$$

which is enforced through the hybrid variables, i.e.,

$$\mathbf{n} \times \hat{\mathbf{E}}^t = \mathbf{0}, \text{ and } \hat{q} = 0 \text{ on } \partial\Omega.$$

The local solver (4.28) with the HDG flux (4.21) equipped with the boundary conditions reads

$$(\nu \mathbf{E}, \mathbf{e})_K - (\mathbf{H}, \nabla \times \mathbf{e})_K + \left\langle -\mathbf{n} \times \mathbf{H} + \left(\mathbf{E}^t - \mathbf{1}_{\partial K \setminus \partial\Omega} \hat{\mathbf{E}}^t \right), \mathbf{e} \right\rangle_{\partial K} = 0, \quad (4.34a)$$

$$- \left(\varepsilon \omega^2 \mathbf{H}, \mathbf{h} \right)_K + (\mathbf{E}, \nabla \times \mathbf{h})_K - (q, \nabla \cdot (\varepsilon \mathbf{h}))_K + \left\langle \mathbf{1}_{\partial K \setminus \partial\Omega} \mathbf{n} \times \hat{\mathbf{E}}^t, \mathbf{h} \right\rangle_{\partial K} + \left\langle \mathbf{1}_{\partial K \setminus \partial\Omega} \varepsilon \hat{q} \mathbf{n}, \mathbf{h} \right\rangle_{\partial K} = (\mathbf{f}, \mathbf{h})_K, \quad (4.34b)$$

$$- (\varepsilon \mathbf{H}, \nabla v)_K + \left\langle \varepsilon \mathbf{H} \cdot \mathbf{n} + \varepsilon \left(q - \mathbf{1}_{\partial K \setminus \partial\Omega} \hat{q} \right), v \right\rangle_{\partial K} = 0, \quad (4.34c)$$

Similar to [46] we also assume that $\varepsilon\omega^2$ is not an eigenvalue for an eigenvalue problem defined by local solver (4.34) or by our HDG scheme with $\mathbf{f} = \mathbf{0}$. This

assumption is implicitly understood from now on to the end of the section. We are now in the position to study the well-posedness of the local solver.

LEMMA 4.9. *Assume that* $\varepsilon > 0$. *For a given value of* $\mathbf{f}$ *and* $\hat{\mathbf{H}}$, *the local solver* (4.34) *has a unique solution for* $\mathbf{E}, \mathbf{H}$ *and* q.

Proof. Since the local solver is a square linear system in finite dimensional space, it is sufficient to show that $\mathbf{E} = \mathbf{H} = \mathbf{0}$ and $q = 0$ is the only solution if $\mathbf{f} = \mathbf{0}$, $\hat{\mathbf{E}}^t = \mathbf{0}$, and $\hat{q} = 0$. Indeed, first, since $\varepsilon\omega^2$ is not an eigenvalue of the local solver (4.34), $\mathbf{H}$ must vanish. Second, taking $\mathbf{e} = \mathbf{E}, \mathbf{h} = \mathbf{H}$ and $v = q$, integrating by parts the second term in (4.34a) and the first term in (4.34c), and adding all equations in (4.34) yield

$$\|\mathbf{E}\|^2_{K,\nu} + \left\|\mathbf{E}^t\right\|^2_{\partial K} + \|q\|^2_{\partial K,\varepsilon} = 0,$$

which implies $\mathbf{E} = 0$ on K and $q = 0$ on ∂K. It follows from (4.34b), by integrating the third term by parts, that

$$(\varepsilon\mathbf{h}, \nabla q)_K = 0, \quad \forall \mathbf{h} \in \mathbf{V}_h(K),$$

which in turn shows that q is constant on K. Since $q = 0$ on ∂K, q must vanish, and this ends the proof. ∎

We next study the well-posedness of the global solver for $\hat{\mathbf{E}}^t$ and $\hat{q}$.

THEOREM 4.10. *Suppose* $\nu > 0$. *For a given value of* $\mathbf{f}$, *there is a unique solution for trace unknowns* $\hat{\mathbf{E}}^t$ *and* $\hat{q}$. *Consequently, there is a unique solution for the local volume unknowns* $\mathbf{E}$, $\mathbf{H}$, *and* q.

Proof. Similar to the proof of Lemma 4.9, we exploit the finite dimensionality and linearity of the square system determining $\hat{\mathbf{E}}^t$ and $\hat{q}$. The well-posedness of global solver is equivalent to show that the pair $\hat{\mathbf{E}}^t = \mathbf{0}$ and $\hat{q} = 0$ on $\mathcal{E}_h^o$ is the only solution if $\mathbf{f} = 0$. We proceed by taking $\mathbf{e} = \mathbf{E}, \mathbf{h} = \mathbf{H}$ and $v = q$ in the local solver (4.34). Next, integrating by parts the second term in (4.34a) and the first term in (4.34c), and adding the resulting equations of the all together we obtain

$$\|\mathbf{E}\|^2_{\Omega_h,v} + \sum_K \left\langle \left(\mathbf{E}^t - \mathbf{1}_{\partial K\setminus\partial\Omega}\hat{\mathbf{E}}^t\right), \mathbf{E}^t \right\rangle_{\partial K} + \left\langle \mathbf{1}_{\partial K\setminus\partial\Omega}\mathbf{n}\times\hat{\mathbf{E}}^t, \mathbf{H}\right\rangle_{\partial K} + \sum_K \left\langle \mathbf{1}_{\partial K\setminus\partial\Omega}\varepsilon\hat{q}\mathbf{n}, \mathbf{H}\right\rangle_{\partial K} + \left\langle \varepsilon\left(q - \mathbf{1}_{\partial K\setminus\partial\Omega}\hat{q}\right), q\right\rangle_{\partial K} = \|\mathbf{H}\|_{\Omega_h,\varepsilon\omega^2}. \quad (4.35)$$

On the other hand, taking $\boldsymbol{\mu}^t = \hat{\mathbf{E}}^t$ and $\lambda = \hat{q}$ in (4.25) and then adding the resulting equations lead to

$$\sum_K \left\langle -\mathbf{1}_{\partial K\setminus\partial\Omega}\mathbf{n}\times\mathbf{H}, \hat{\mathbf{E}}^t\right\rangle_{\partial K} + \left\langle \mathbf{1}_{\partial K\setminus\partial\Omega}\left(\mathbf{E}^t - \hat{\mathbf{E}}^t\right), \hat{\mathbf{E}}^t\right\rangle_{\partial K} + \sum_K \left\langle \mathbf{1}_{\partial K\setminus\partial\Omega}\varepsilon\mathbf{H}\cdot\mathbf{n}, \hat{q}\right\rangle_{\partial K} + \left\langle \mathbf{1}_{\partial K\setminus\partial\Omega}\varepsilon\left(q - \hat{q}\right), \hat{q}\right\rangle_{\partial K} = 0. \quad (4.36)$$

Next subtracting (4.36) from (4.35) yields

$$\|\mathbf{E}\|^2_{\Omega_h,v} + \sum_K \left\langle \mathbf{1}_{\partial K\setminus\partial\Omega}\left(\mathbf{E}^t - \hat{\mathbf{E}}^t\right), \mathbf{E}^t - \hat{\mathbf{E}}^t\right\rangle_{\partial K} + \left\langle \mathbf{1}_{\partial K\setminus\partial\Omega}\varepsilon\left(q - \hat{q}\right), q - \hat{q}\right\rangle_{\partial K} + \left\|\mathbf{E}^t\right\|^2_{\partial\Omega} + \|q\|^2_{\partial\Omega,\varepsilon} = \|\mathbf{H}\|_{\Omega_h,\varepsilon\omega^2}. \quad (4.37)$$

Since $\varepsilon\omega^2$ is not an eigenvalue of the eigenvalue problem defined by the HDG scheme with $\mathbf{f} = 0$, $\mathbf{H}$ must vanish. As a result, from (4.37), we infer that $\mathbf{E} = \mathbf{0}$ on Ω_h, $\hat{\mathbf{E}}^t = \mathbf{E}^t = \mathbf{0}$ on $\mathcal{E}_h^o$, $\hat{q} = q$ on $\mathcal{E}_h^o$, and $q = 0$ on $\partial\Omega$. It follows that q is continuous and has zero trace on $\partial\Omega$.

Now taking $v = q$ in (4.34c), using the fact that $\mathbf{H} = 0$, $\hat{q} = q$ on $\mathcal{E}_h^o$, and $q = 0$ on $\partial\Omega$, and then summing the resulting equations all together we have

$$(\varepsilon\mathbf{H}, \nabla q)_{\Omega_h} = 0, \quad \forall \mathbf{H} \in \mathbf{V}_h(\Omega_h),$$

which implies that q is piecewise constant. However, q is continuous and vanishes on $\partial\Omega$. This can only be true if q is identically zero. Consequently, $\hat{q} = 0$ on $\mathcal{E}_h^o$ as well. ∎

4.2.4. HDG schemes for vector wave equation. We have explicitly imposed the divergent free condition for the magnetic field in (4.19c), and hence it is necessary to introduce the Lagrange multiplier q in (4.19b) [46]. Though this formulation is more stable, especially when ω is small, we have one extra PDE with one extra unknown. If this is not desirable one can study the vector wave equation directly, i.e.,

$$\nu\mathbf{E} - \nabla \times \mathbf{H} = \mathbf{0} \text{ in } \Omega, \tag{4.38a}$$

$$\nabla \times \mathbf{E} - \varepsilon\omega^2\mathbf{H} = \mathbf{f} \text{ in } \Omega, \tag{4.38b}$$

which is a simplified version of (4.19). Indeed, one can show that the Godunov flux in this case reads

$$\mathbf{F}^* \cdot \mathbf{n} = \begin{bmatrix} -\mathbf{n} \times \mathbf{H} + \mathbf{n} \times \mathbf{n} \times (\mathbf{E}^* - \mathbf{E}) \\ \mathbf{n} \times \mathbf{E} + \mathbf{n} \times \mathbf{n} \times (\mathbf{H}^* - \mathbf{H}) \end{bmatrix},$$

which is, as expected, a simpler version of (4.20) by removing the last component and all the terms associated with the normal direction. It is also almost the same as the Godunov flux (4.3) for the time domain Maxwell equation. This observation immediately gives us two HDG fluxes without detailed arguments, i.e.,

$$\hat{\mathbf{F}} \cdot \mathbf{n} = \begin{bmatrix} -\mathbf{n} \times \mathbf{H} + \mathbf{n} \times \mathbf{n} \times \left(\hat{\mathbf{E}} - \mathbf{E}\right) \\ \mathbf{n} \times \hat{\mathbf{E}} \end{bmatrix}, \tag{4.39a}$$

and

$$\hat{\mathbf{F}} \cdot \mathbf{n} = \begin{bmatrix} -\mathbf{n} \times \hat{\mathbf{H}} \\ \mathbf{n} \times \mathbf{E} + \mathbf{n} \times \mathbf{n} \times \left(\hat{\mathbf{H}} - \mathbf{H}\right) \end{bmatrix}. \tag{4.39b}$$

We can construct two HDG schemes corresponding to these two HDG fluxes, the former of which is a new HDG scheme for vector wave equation (4.38) while the latter coincides with that proposed in [46]. Clearly, the analysis for time harmonic Maxwell equation in previous sections still holds by removing appropriate terms, and for that reason we leave out the unnecessary details here.

5. HDG schemes for Stokes equation. Consider the Stokes equation in the following first order velocity-pressure-gradient form (see, e.g, [44, 15]):

$$\nu^{-1}\mathbf{L} - \nabla\mathbf{u} = 0, \quad \text{in } \Omega \tag{5.1a}$$

$$-\nabla \cdot \mathbf{L} + \nabla q = \mathbf{f}, \quad \text{in } \Omega \tag{5.1b}$$

$$\nabla \cdot \mathbf{u} = 0, \quad \text{in } \Omega, \tag{5.1c}$$

$$\int_\Omega q \, d\Omega = 0. \tag{5.1d}$$

Let us define

$$\boldsymbol{\Sigma} := \mathbf{n}\otimes\left[(\mathbf{L}-\mathbf{L}^*)\cdot\mathbf{n}\right] + \frac{\left(\sqrt{2}-2\right)}{2}\left[\mathbf{n}\cdot(\mathbf{L}-\mathbf{L}^*)\cdot\mathbf{n}\right]\mathbf{n}\otimes\mathbf{n} - \frac{\sqrt{2}}{2}\mathbf{n}\otimes\mathbf{n}\,(q-q^*)\,,$$
$$\boldsymbol{\gamma} := \sqrt{2}\left[(\mathbf{u}-\mathbf{u}^*)\cdot\mathbf{n}\right]\mathbf{n} - \mathbf{n}\times\mathbf{n}\times(\mathbf{u}-\mathbf{u}^*)\,,$$
$$\alpha := -\frac{\sqrt{2}}{2}\mathbf{n}\cdot(\mathbf{L}-\mathbf{L}^*)\cdot\mathbf{n} + \frac{\sqrt{2}}{2}(q-q^*)\,.$$

Following the same exercise as above, one can compute $|\mathbf{A}|$ so that the Godunov flux in this case reads

$$\hat{\mathbf{F}}\cdot\mathbf{n} = \begin{bmatrix} -\mathbf{n}\otimes\mathbf{u} + \boldsymbol{\Sigma} \\ -\mathbf{L}\cdot\mathbf{n} + q\mathbf{n} + \boldsymbol{\gamma} \\ \mathbf{u}\cdot\mathbf{n} + \alpha \end{bmatrix}. \tag{5.2}$$

By inspection, the following result for the Riemann solutions $\mathbf{L}^*, \mathbf{u}^*$ and q^* is straightforward.

PROPOSITION 5.1. *There hold:*

$$\boldsymbol{\Sigma} = \mathbf{n}\otimes\left(\boldsymbol{\gamma} + \frac{\left(\sqrt{2}-2\right)}{2}\mathbf{n}\otimes\mathbf{n}\cdot\boldsymbol{\gamma}\right) = \mathbf{n}\otimes(\mathbf{u}-\mathbf{u}^*)\,, \tag{5.3a}$$

$$\alpha = -\frac{\sqrt{2}}{2}\boldsymbol{\gamma}\cdot\mathbf{n} = -(\mathbf{u}-\mathbf{u}^*)\cdot\mathbf{n}, \tag{5.3b}$$

$$\boldsymbol{\Sigma}\cdot\mathbf{n} = \frac{\sqrt{2}}{2}\mathbf{n}\otimes\mathbf{n}\cdot\boldsymbol{\gamma} = -\alpha\mathbf{n}, \tag{5.3c}$$

and the Godunov flux can be written as

$$\mathbf{F}^*\cdot\mathbf{n} = \begin{bmatrix} -\mathbf{n}\otimes\mathbf{u}^* \\ -\mathbf{L}\cdot\mathbf{n} + q\mathbf{n} + \sqrt{2}\left[(\mathbf{u}-\mathbf{u}^*)\cdot\mathbf{n}\right]\mathbf{n} - \mathbf{n}\times\mathbf{n}\times(\mathbf{u}-\mathbf{u}^*) \\ \mathbf{u}^*\cdot\mathbf{n} \end{bmatrix}. \tag{5.4}$$

As can be seen, $\mathbf{u}^*$ is the only quantity required to compute the upwind flux. This observation is the key to construct the HDG method. As for other PDEs discussed in this paper, we start our HDG construction by defining (5.4) as the HDG flux, i.e.,

$$\hat{\mathbf{F}}\cdot\mathbf{n} = \begin{bmatrix} -\mathbf{n}\otimes\hat{\mathbf{u}} \\ -\mathbf{L}\cdot\mathbf{n} + q\mathbf{n} + \sqrt{2}\left[(\mathbf{u}-\hat{\mathbf{u}})\cdot\mathbf{n}\right]\mathbf{n} - \mathbf{n}\times\mathbf{n}\times(\mathbf{u}-\hat{\mathbf{u}}) \\ \hat{\mathbf{u}}\cdot\mathbf{n} \end{bmatrix}, \tag{5.5}$$

with $\hat{\mathbf{u}}$ as the trace unknown that needs to be solved for.

Unlike the other PDEs for which we have started defining first the conservation condition and then the local solver, for Stokes case it is useful to discuss the local solver first as we will see. The reason is that additional condition has to be introduced to make the HDG method for Stokes equation well-defined, and this is best motivated through the local solver. To that end, taking $\mathbf{v} = (\mathbf{G}, \mathbf{v}, r)$ as the test function, the local equation (2.15a) when applied to (5.1) becomes: find $(\mathbf{L}, \mathbf{u}, q)$ such that

$$(\nu\mathbf{L}, \mathbf{G})_K + (\mathbf{u}, \nabla\cdot\mathbf{G})_K - \left\langle \mathbf{1}_{\partial K\setminus\partial\Omega}\mathbf{n}\otimes\hat{\mathbf{u}}, \mathbf{G}\right\rangle_{\partial K} = 0, \tag{5.6a}$$

$$(\mathbf{L}, \nabla\mathbf{v})_K - (q, \nabla\cdot\mathbf{v})_K + \langle -\mathbf{L}\cdot\mathbf{n} + q\mathbf{n}, \mathbf{v}\rangle_{\partial K} + \tag{5.6b}$$

$$\left\langle \sqrt{2}\left[\left(\mathbf{u} - \mathbf{1}_{\partial K\setminus\partial\Omega}\hat{\mathbf{u}}\right)\cdot\mathbf{n}\right]\mathbf{n} - \mathbf{n}\times\mathbf{n}\times\left(\mathbf{u} - \mathbf{1}_{\partial K\setminus\partial\Omega}\hat{\mathbf{u}}\right), \mathbf{v}\right\rangle_{\partial K} = (\mathbf{f}, \mathbf{v})_K\,, \tag{5.6c}$$

$$-(\mathbf{u}, \nabla r) + \left\langle \mathbf{1}_{\partial K\setminus\partial\Omega}\hat{\mathbf{u}}\cdot\mathbf{n}, r\right\rangle_{\partial K} = 0, \tag{5.6d}$$

where we have imposed the homogeneous Dirichlet boundary condition, $\mathbf{u} = \mathbf{0}$ on $\partial\Omega$, through the trace unknown $\hat{\mathbf{u}}$. Next, we use the energy method to study the well-posedness of the local solver. Since it is linear and finite dimensional, it is sufficient to show that $\mathbf{L} = \mathbf{0}$, $\mathbf{u} = \mathbf{0}$ and $q = 0$ is the only solution of the local solver if $\mathbf{f} = \mathbf{0}$ and $\hat{\mathbf{u}} = 0$. To begin, taking $\mathbf{G} = \mathbf{L}, \mathbf{v} = \mathbf{u}$ and $r = q$ in (5.6), integrating by parts the second term of (5.6a) and (5.6b), and then adding the resulting equations of (5.6) all together yield

$$\|\mathbf{L}\|^2_{K,\nu} + \|\mathbf{u}\cdot\mathbf{n}\|^2_{\partial K,\sqrt{2}} + \|\mathbf{n}\times\mathbf{n}\times\mathbf{u}\|^2_{\partial K} = 0$$

which implies that $\mathbf{L} = \mathbf{0}$ on K, $\mathbf{u}\cdot\mathbf{n} = 0$ and $\mathbf{n}\times\mathbf{n}\times\mathbf{u}$ on ∂K, and hence $\mathbf{u} = \mathbf{0}$ on ∂K. It follows that (5.6a), after integrating the second term of (5.6a) by parts, becomes

$$(\nabla\mathbf{u}, \mathbf{G})_K = 0, \quad \forall \mathbf{G} \in \mathbf{V}_h(K),$$

from which we infer that $\mathbf{u}$ must be a constant vector on K, in fact null vector since it vanishes on the boundary.

Similarly, integrating the second term of (5.6b) by parts and using the results $\mathbf{L} = 0$ and $\mathbf{u} = 0$ we obtain

$$(\nabla q, \mathbf{v})_K = 0, \quad \forall \mathbf{v} \in \mathbf{V}_h(K),$$

which shows that q must be a constant. At this point, one can observe that there is no extra information to prove the uniqueness of q, or equivalently $q = 0$. To resolve this issue, a natural idea is to equip the local solver (5.6) with a minimal condition to enforce the uniqueness. Similar to [44,15], we choose

$$\overline{q} = \rho, \text{ on } \partial K, \tag{5.7}$$

where $\overline{q}$ is the average of q on ∂K defined as $\overline{q} := |\partial K|^{-1}\langle q, 1\rangle_{\partial K}$, and ρ is a constant function belonging to

$$\overline{\Lambda}_h(\partial\Omega_h) := \left\{\lambda \in L^2(\partial\Omega_h) : \lambda|_{\partial K} \in \mathcal{P}^0(\partial K), \forall K \in \Omega_h\right\}.$$

Let us state the well-posedness result in Lemma 5.2.

LEMMA 5.2. *Suppose $\nu > 0$. Given $\hat{\mathbf{u}}$ and ρ, there exists a unique solution $(\mathbf{L}, \mathbf{u}, q)$ for the local solver (5.6)–(5.7).*

Proof. It is enough to show that $\hat{\mathbf{u}} = \mathbf{0}$ and $\rho = 0$ implies $\mathbf{L} = \mathbf{0}, \mathbf{u} = \mathbf{0}$ and $q = 0$. Using the above motivation for the augmented local solver (5.6)–(5.7) we need to only show $q = 0$, but it is clear since q is constant and have zero on ∂K according to (5.7). ∎

We next construct the global system of equations on the mesh skeleton to solve for $\hat{\mathbf{u}}$ and ρ. To this end, it is important to realize that the well-posedness of the augmented local solver (5.6)–(5.7) comes at an expense of introducing a new unknown ρ constant on each element boundary in addition to the trace unknown $\hat{\mathbf{u}}$. Since the HDG flux components corresponding to (5.1a) and (5.1c) automatically satisfy the conservation constraint (2.15b), we are left with three algebraic constraints (2.15b) in our HDG scheme for the trace unknown $\hat{\mathbf{u}}$, i.e., $\forall \boldsymbol{\mu} \in \boldsymbol{\Lambda}_h(e), \forall e \in \mathcal{E}^o_h$,

$$\left\langle [\![-\mathbf{L}\cdot\mathbf{n} + q\mathbf{n} + \sqrt{2}\,[(\mathbf{u}-\hat{\mathbf{u}})\cdot\mathbf{n}]\,\mathbf{n} - \mathbf{n}\times\mathbf{n}\times(\mathbf{u}-\hat{\mathbf{u}})]\!], \boldsymbol{\mu}\right\rangle_e = 0. \tag{5.8}$$

We still need one extra equation for ρ. To seek this equation we note that if we take r as a constant function so that $r|_{\partial K} = \overline{r|_{\partial K}} \in \overline{\Lambda}_h(\partial K)$, then (5.6d) reduces to

$$\left\langle \mathbf{1}_{\partial K\setminus\partial\Omega}\hat{\mathbf{u}}\cdot\mathbf{n}, r\right\rangle_{\partial K} = 0,$$

which implies

$$\left\langle \mathbf{1}_{\partial K\setminus\partial\Omega}\hat{\mathbf{u}}\cdot\mathbf{n}, \xi\right\rangle_{\partial K} = 0, \quad \forall \xi \in \overline{\Lambda}_h(\partial K), \tag{5.9}$$

since the trace operator from the space of constant functions on K to $\overline{\Lambda}_h(\partial K)$ is surjective. Since $\hat{\mathbf{u}}$ is viewed as one of the inputs (the forcing) for the local solver, (5.9) is the compatibility condition for $\hat{\mathbf{u}}$ and this is exactly the extra equation we are looking for. Thus, not only the usual conservation condition (5.8) but also the compatibility condition (5.9) constitutes the HDG equations on the mesh skeleton whose well-posedness is now discussed.

THEOREM 5.3. *Assume $\nu > 0$. The HDG scheme consists of the local solver (5.6)–(5.7) and the algebraic condition (5.8)–(5.9) has a unique solution $(\mathbf{L}, \mathbf{u}, q, \hat{\mathbf{u}}, \rho)$.*

Proof. We again employ the energy method as in previous sections. The task at hand is to show that $\mathbf{f} = \mathbf{0}$ implies $\mathbf{L} = \mathbf{0}$, $\mathbf{u} = \mathbf{0}, q = 0$, $\hat{\mathbf{u}} = \mathbf{0}$ and $\rho = 0$. Integrating by parts the second term of (5.6a) and (5.6b), adding the resulting equations of (5.6) all together, then summing over all elements give

$$\begin{aligned}\|\mathbf{L}\|^2_{\Omega_h,\nu} - \sum_K \left\langle \mathbf{1}_{\partial K\setminus\partial\Omega}\mathbf{n}\otimes\hat{\mathbf{u}}, \mathbf{L}\right\rangle_{\partial K} - \left\langle \sqrt{2}\left[\left(\mathbf{u} - \mathbf{1}_{\partial K\setminus\partial\Omega}\hat{\mathbf{u}}\right)\cdot\mathbf{n}\right], \mathbf{u}\cdot\mathbf{n}\right\rangle_{\partial K} \\ - \sum_K \left\langle \mathbf{n}\times\mathbf{n}\times\left(\mathbf{u} - \mathbf{1}_{\partial K\setminus\partial\Omega}\hat{\mathbf{u}}\right), \mathbf{u}\right\rangle_{\partial K} - \left\langle \mathbf{1}_{\partial K\setminus\partial\Omega}\hat{\mathbf{u}}\cdot\mathbf{n}, q\right\rangle_{\partial K} = 0.\end{aligned} \tag{5.10}$$

On the other hand, taking $\boldsymbol{\mu} = \hat{\mathbf{u}}$ in (5.8) and subtracting the resulting equation from (5.10) we arrive at

$$\|\mathbf{L}\|^2_{\Omega_h,\nu} + \sum_K \left\|\left(\mathbf{u} - \mathbf{1}_{\partial K\setminus\partial\Omega}\hat{\mathbf{u}}\right)\cdot\mathbf{n}\right\|^2_{\partial K,\sqrt{2}} + \sum_K \left\|\mathbf{n}\times\mathbf{n}\times\left(\mathbf{u} - \mathbf{1}_{\partial K\setminus\partial\Omega}\hat{\mathbf{u}}\right)\right\|^2_{\partial K} = 0,$$

which shows that $\mathbf{L}$ must vanish, i.e. $\mathbf{L} = \mathbf{0}$, on K. It also implies that $\mathbf{u}\cdot\mathbf{n} = \mathbf{1}_{\partial K\setminus\partial\Omega}\hat{\mathbf{u}}\cdot\mathbf{n}$ and $\mathbf{n}\times\mathbf{n}\times\mathbf{u} = \mathbf{1}_{\partial K\setminus\partial\Omega}\mathbf{n}\times\mathbf{n}\times\hat{\mathbf{u}}$ on ∂K. Thus, $\mathbf{u} = \mathbf{1}_{\partial K\setminus\partial\Omega}\hat{\mathbf{u}}$ on ∂K. In other words, $\mathbf{L} = 0$ on Ω_h, $\mathbf{u} = \hat{\mathbf{u}}$ on $\mathcal{E}_h^o$, and $\mathbf{u} = \mathbf{0}$ on $\mathcal{E}_h^\partial$. Since $\hat{\mathbf{u}}$ is single-valued on $\mathcal{E}_h^o$, $\mathbf{u}$ must be continuous across Ω_h.

Now integrating the second term of (5.6a) by parts we obtain

$$(\nabla\mathbf{u}, \mathbf{G})_{\Omega_h} = 0, \quad \forall \mathbf{G} \in \mathbf{V}_h(\Omega_h),$$

and hence $\mathbf{u}$ must be a constant. But $\mathbf{u}$ is continuous and vanishes on $\mathcal{E}_h^\partial$, it must vanish over Ω_h. As a result, $\hat{\mathbf{u}} = 0$ on $\mathcal{E}_h^o$.

Next, integrating the second term of (5.6b) by parts and using the results $\mathbf{L} = 0$ and $\mathbf{u} = 0$ we obtain

$$(\nabla q, \mathbf{v})_K = 0, \quad \forall \mathbf{v} \in \mathbf{V}_h(K),$$

which shows that q must be piecewise constant. On the other hand, if $\mathbf{v}$ is taken as a constant vector, it is clear from (5.6b) that $\overline{q} = 0$. Thus, $q = 0$ on K. It follows that ρ also vanishes on $\partial\Omega_h$ due to (5.7) and this ends the proof. ∎

REMARK 5.4. *As can be observed, though* (5.7) *is introduced to enforce the uniqueness of* q *locally on each element, and hence the local solver, it automatically enforces the uniqueness of* q *globally as shown in the proof of Theorem 5.3. This is the reason why we do not need to explicitly enforce* (5.1d) *in our HDG scheme.*

Though there are other HDG schemes such as those in [9], let us only discuss the similarity and difference between ours and that proposed in [44, 15] since they are related. Indeed, let us derive the HDG family in [44, 15] from ours. To that end, we first simplify our HDG flux (5.5) by removing $\sqrt{2}\left[(\mathbf{u}-\hat{\mathbf{u}})\cdot\mathbf{n}\right]\mathbf{n}$. Next, let us introduce a stabilization matrix $\mathscr{T}$ to penalize the deviation of the tangent velocity $\mathbf{n}\times\mathbf{n}\times(\mathbf{u}-\hat{\mathbf{u}})$ so that the HDG flux (5.5) now becomes

$$\hat{\mathbf{F}}\cdot\mathbf{n} = \begin{bmatrix} -\mathbf{n}\otimes\hat{\mathbf{u}} \\ -\mathbf{L}\cdot\mathbf{n} + q\mathbf{n} - \mathscr{T}\mathbf{n}\times\mathbf{n}\times(\mathbf{u}-\hat{\mathbf{u}}) \\ \hat{\mathbf{u}}\cdot\mathbf{n} \end{bmatrix}.$$

This is exactly the penalized HDG flux proposed in [44, 15] for the velocity-pressure-gradient form of the Stokes flow. Clearly, by taking $\mathscr{T}$ as the identity we obtain a simplified version of our upwind HDG flux (5.5) in which we omit $\sqrt{2}\left[(\mathbf{u}-\hat{\mathbf{u}})\cdot\mathbf{n}\right]\mathbf{n}$.

REMARK 5.5. *We note that there are other forms of the Stokes equations, see [15] for example. Following our HDG construction, we can similarly derive HDG methods for these forms as well. Since not much more benefit can be gained, we omit the details.*

6. A HDG framework for Friedrichs' system. We have used our unified HDG framework to constructively derive HDG schemes/families for three special PDEs in Sections 3, 4, and 5. Our intention has been to show that by employing our single abstract framework, namely hybridizing the upwind Godunov flux, one could derive different classes of HDG methods by exploiting the special structure of the underlying PDEs. This is then followed by the well-posedness analysis. As can be seen, though there are differences in the detailed manipulations, the construction and analysis are similar for all PDEs that we have considered. A natural question is whether we can unify not only the construction, as we have done, but also the analysis for a large abstract family of PDEs.

It is the purpose of this section that we generalize the analysis of our proposed upwind HDG framework for a large class of differential operator (2.1) of Friedrichs' type. We are interested in Friedrichs's systems since they embrace a large class of elliptic, parabolic, and hyperbolic PDEs. We start with the standard assumptions (see, e.g., [24, 20, 32]):

$$\mathbf{C}\in\left[L^{\infty}(\Omega)\right]^{m,m}, \tag{6.1a}$$

$$\mathbf{A}^k\in\left[L^{\infty}(\Omega)\right]^{m,m}, \quad k=1,\ldots,d, \quad \text{and} \quad \sum_{k=1}^{d}\partial_k\mathbf{A}^k\in\left[L^{\infty}(\Omega)\right]^{m,m}, \tag{6.1b}$$

$$\mathbf{A}^k=\left(\mathbf{A}^k\right)^T \text{ a.e. in } \Omega, \quad k=1,\ldots,d,, \tag{6.1c}$$

$$\mathbf{C}+\mathbf{C}^T+\sum_{k=1}^{d}\partial_k\mathbf{A}^k\geq 2\alpha_0\mathbf{I} \text{ a.e. in } \Omega, \tag{6.1d}$$

where $\alpha_0>0$ is some coercivity constant. In this paper, we restrict our analysis to the boundary condition defined by

$$\left(\mathbf{A}-|\mathbf{A}|\right)\mathbf{u}=\mathbf{0} \text{ on } \partial\Omega, \tag{6.1e}$$

and we assume that

$$\mathcal{N}\left(\mathbf{A}-|\mathbf{A}|\right)+\mathcal{N}\left(\mathbf{A}+|\mathbf{A}|\right)=\mathbb{R}^m,$$

with $\mathcal{N}$ denoting the nullspace of its argument.

With this simple setting, one can show that the abstract PDE (2.1) with boundary condition defined by (6.1e) is well-posed, i.e. $\mathcal{T}$ is an isomorphism from its domain to its range [19]. More general settings with other boundary conditions can be found in [23, 1, 2, 3].

The abstract HDG framework in Section 2 is still applicable for the Friedrichs' setting. In particular, the upwind HDG method for PDEs of Friedrichs' type consists of the local solver (2.15a), the conservation condition (2.15b) and the HDG flux (2.16). Let us now write (2.15a) explicitly as

$$-\sum_{k=1}^{d}\left(\mathbf{A}^k\mathbf{u},\partial_k\mathbf{v}\right)_K+\left(\mathbf{C}\mathbf{u},\mathbf{v}\right)_K+\left\langle\mathbf{A}\mathbf{u}+|\mathbf{A}|\left(\mathbf{u}-\hat{\mathbf{u}}\right),\mathbf{v}\right\rangle_{\partial K}=\left(\mathbf{f},\mathbf{v}\right)_K, \tag{6.2}$$

and similarly the explicit form of the conservation condition (2.15b) reads

$$\left\langle[\![\mathbf{A}\mathbf{u}+|\mathbf{A}|\left(\mathbf{u}-\hat{\mathbf{u}}\right)]\!],\boldsymbol{\mu}\right\rangle_e=\mathbf{0},\quad\forall\boldsymbol{\mu}\in\boldsymbol{\Lambda}_h\left(e\right),e\in\mathcal{E}_h^o. \tag{6.3}$$

We next describe how to enforce the boundary condition (6.1e) in our abstract HDG setting. As can be seen in previous sections, we have first reduced the number of trace unknowns using exact relationships of the Riemann solutions and exploiting the structure of the PDE under consideration, and then enforced the boundary condition directly on the reduced trace unknowns. However, at the abstract level of the HDG flux (2.16), it is not clear how to do so and we have to deal with the full trace unknown $\hat{\mathbf{u}}$. In particular, we still enforce the boundary condition through the trace unknown, i.e.,

$$\left(\mathbf{A}-|\mathbf{A}|\right)\hat{\mathbf{u}}=\mathbf{0}\text{ on }\mathcal{E}_h^\partial,$$

i.e., $\hat{\mathbf{u}}\in span\left\{\mathbb{R}^+\right\}$ where $\mathbb{R}^\pm$ are the collection of eigenvectors of $\mathbf{A}$ corresponding to positive and negative eigenvalues, respectively. We assume $span\left\{\mathbb{R}^+\right\}\cap span\left\{\mathbb{R}^-\right\}=\{\emptyset\}$. It is also sensible to require that

$$\left\langle\mathbf{A}\mathbf{u}+|\mathbf{A}|\left(\mathbf{u}-\hat{\mathbf{u}}\right),\boldsymbol{\mu}\right\rangle_e=\left\langle\mathbf{A}\hat{\mathbf{u}},\boldsymbol{\mu}\right\rangle_e,\quad\forall\boldsymbol{\mu}\in\boldsymbol{\Lambda}_h\left(e\right),e\in\mathcal{E}_h^\partial, \tag{6.4}$$

that is, the numerical flux must be the same of flux determined by the trace $\hat{\mathbf{u}}$ on the boundary $\partial\Omega$. Equivalently,

$$\left\langle\left(\mathbf{A}+|\mathbf{A}|\right)\left(\mathbf{u}-\hat{\mathbf{u}}\right),\boldsymbol{\mu}\right\rangle_e=0,\quad\forall\boldsymbol{\mu}\in\boldsymbol{\Lambda}_h\left(e\right),e\in\mathcal{E}_h^\partial,$$

which, after taking $\boldsymbol{\mu}=\mathbf{u}-\hat{\mathbf{u}}$, implies

$$\mathbf{u}-\hat{\mathbf{u}}\in span\left\{\mathbb{R}^-\right\},$$

but this can happen iff $\mathbf{u}=\hat{\mathbf{u}}$ on $\mathcal{E}_h^\partial$. That is, the condition (6.4) implies that $\mathbf{u}$ must also satisfy the boundary condition.

As a result, the local solver with the boundary condition incorporated can be written as

$$-\sum_{k=1}^{d}\left(\mathbf{A}^k\mathbf{u},\partial_k\mathbf{v}\right)_K+\left(\mathbf{C}\mathbf{u},\mathbf{v}\right)_K+\left\langle\mathbf{A}\mathbf{u}+\mathbf{1}_{\partial K\setminus\partial\Omega}|\mathbf{A}|\left(\mathbf{u}-\hat{\mathbf{u}}\right),\mathbf{v}\right\rangle_{\partial K}=\left(\mathbf{f},\mathbf{v}\right)_K. \tag{6.5}$$

We are now in the position to analyze the local solver.

LEMMA 6.1. *The local solver* (6.5) *is well-posed.*

Proof. It is sufficient to prove that $\mathbf{f} = \mathbf{0}$ and $\hat{\mathbf{u}} = \mathbf{0}$ implies $\mathbf{u} = \mathbf{0}$. To begin, in (6.5) taking $\mathbf{v} = \mathbf{u}$, and integrating the first term by parts we obtain

$$\frac{1}{2}\left(\left[\mathbf{C} + \mathbf{C}^T + \sum_{k=1}^{d} \partial_k \mathbf{A}^k\right]\mathbf{u}, \mathbf{u}\right)_K + \left\langle \frac{1}{2}\mathbf{A}\mathbf{u}, \mathbf{u}\right\rangle_{\partial K \cap \mathcal{E}_h^\partial} + \left\langle \left(\frac{1}{2}\mathbf{A} + |\mathbf{A}|\right)\mathbf{u}, \mathbf{u}\right\rangle_{\partial K \setminus \mathcal{E}_h^\partial} = 0,$$

which yields $\mathbf{u} = \mathbf{0}$ in K since the left hand side is non-negative owing to the coercivity condition (6.1d), the fact that $\mathbf{u} = \hat{\mathbf{u}}$ on $\mathcal{E}_h^\partial$, and $\frac{1}{2}\mathbf{A} + |\mathbf{A}| \geq 0$. ∎

The well-posedness of the global solver for $\hat{\mathbf{u}}$ is now established.

THEOREM 6.2. *Suppose* $|\mathbf{A}| + \frac{1}{2}\mathbf{A} > 0$ *a.e. on any* e. *There exist a unique trace solution* $\hat{\mathbf{u}}$ *for the HDG method defined by* (6.5) *and* (6.3).

Proof. It is sufficient to prove that $\hat{\mathbf{u}} = \mathbf{0}$ is the only solution to the global system if $\mathbf{f} = \mathbf{0}$. To that end, we again employ the energy approach by taking $\mathbf{v} = \mathbf{u}$ in (6.5), integrating the first term by parts, and summing over all elements K to arrive at

$$\frac{1}{2}\left(\left[\mathbf{C} + \mathbf{C}^T + \sum_{k=1}^{d} \partial_k \mathbf{A}^k\right]\mathbf{u}, \mathbf{u}\right)_{\Omega_h} + \sum_K \left\langle \frac{1}{2}\mathbf{A}\mathbf{u}, \mathbf{u}\right\rangle_{\partial K \cap \mathcal{E}_h^\partial} - \left\langle \frac{1}{2}\mathbf{A}\mathbf{u}, \mathbf{u}\right\rangle_{\partial K \cap \mathcal{E}_h^o} \\ \sum_K \langle \mathbf{A}\mathbf{u}, \mathbf{u}\rangle_{\partial K \cap \mathcal{E}_h^o} + \langle |\mathbf{A}|(\mathbf{u} - \hat{\mathbf{u}}), \mathbf{u}\rangle_{\partial K \cap \mathcal{E}_h^o} = 0. \quad (6.6)$$

On the other hand, taking $\boldsymbol{\mu} = \hat{\mathbf{u}}$ in (6.3), summing over all $e \in \mathcal{E}_h^o$, and then subtracting the resulting equation from (6.6) we obtain

$$\frac{1}{2}\left(\left[\mathbf{C} + \mathbf{C}^T + \sum_{k=1}^{d} \partial_k \mathbf{A}^k\right]\mathbf{u}, \mathbf{u}\right)_{\Omega_h} + \sum_K \left\langle \frac{1}{2}\mathbf{A}\mathbf{u}, \mathbf{u}\right\rangle_{\partial K \cap \mathcal{E}_h^\partial} - \left\langle \frac{1}{2}\mathbf{A}\mathbf{u}, \mathbf{u}\right\rangle_{\partial K \cap \mathcal{E}_h^o} \\ + \sum_K \langle \mathbf{A}(\mathbf{u} - \hat{\mathbf{u}}), \mathbf{u}\rangle_{\partial K \cap \mathcal{E}_h^o} + \langle |\mathbf{A}|(\mathbf{u} - \hat{\mathbf{u}}), \mathbf{u} - \hat{\mathbf{u}}\rangle_{\partial K \cap \mathcal{E}_h^o} = 0. \quad (6.7)$$

On the other hand, by inspection, the following identity is true for any e:

$$\langle \mathbf{A}(\mathbf{u} - \hat{\mathbf{u}}), \mathbf{u}\rangle_e = \frac{1}{2}\left[\langle \mathbf{A}\mathbf{u}, \mathbf{u}\rangle_e + \langle \mathbf{A}(\mathbf{u} - \hat{\mathbf{u}}), \mathbf{u} - \hat{\mathbf{u}}\rangle_e - \frac{1}{2}(\mathbf{A}\hat{\mathbf{u}}, \hat{\mathbf{u}})_e\right].$$

Hence, (6.7) becomes

$$\frac{1}{2}\left(\left[\mathbf{C} + \mathbf{C}^T + \sum_{k=1}^{d} \partial_k \mathbf{A}^k\right]\mathbf{u}, \mathbf{u}\right)_{\Omega_h} + \sum_K \left\langle \frac{1}{2}\mathbf{A}\mathbf{u}, \mathbf{u}\right\rangle_{\partial K \cap \mathcal{E}_h^\partial} - \left\langle \frac{1}{2}\mathbf{A}\hat{\mathbf{u}}, \hat{\mathbf{u}}\right\rangle_{\partial K \cap \mathcal{E}_h^o} \\ + \sum_K \left\langle \left(|\mathbf{A}| + \frac{1}{2}\mathbf{A}\right)(\mathbf{u} - \hat{\mathbf{u}}), \mathbf{u} - \hat{\mathbf{u}}\right\rangle_{\partial K \cap \mathcal{E}_h^o} = 0,$$

whose left hand side is non-negative due to various reasons. The first term is positive due to the coercivity condition (6.1d), the second term is clearly non-negative, i.e.,

$$\sum_K \left\langle \frac{1}{2}\mathbf{A}\mathbf{u}, \mathbf{u}\right\rangle_{\partial K \cap \mathcal{E}_h^\partial} = \sum_K \left\langle \frac{1}{2}|\mathbf{A}|\mathbf{u}, \mathbf{u}\right\rangle_{\partial K \cap \mathcal{E}_h^\partial} \geq 0,$$

since $\mathbf{u}$ satisfies the boundary condition. Since $\hat{\mathbf{u}}$ is single-valued on the skeleton, the third term vanishes

$$-\left\langle \frac{1}{2}\mathbf{A}\hat{\mathbf{u}}, \hat{\mathbf{u}} \right\rangle_{\partial K \cap \mathcal{E}_h^o} = 0.$$

The fourth term is non-negative is obvious. Consequently, we conclude that $\mathbf{u} = \mathbf{0}$ on Ω_h and $\hat{\mathbf{u}} = \mathbf{u} = \mathbf{0}$ on $\mathcal{E}_h$, and this completes the proof. □

Again, $\mathbf{u} - \hat{\mathbf{u}}$ is the discrepancy between the HDG solution $\mathbf{u}$ restricted on the skeleton and the trace unknown $\hat{\mathbf{u}}$. For exact solution this term vanishes. This suggests that one can construct a family of HDG schemes by penalizing this term. Doing so leads us to the following penalized HDG flux

$$\mathbf{F}^* \cdot \mathbf{n} = \mathbf{A}\mathbf{u} + \mathscr{T}\left(\mathbf{u} - \hat{\mathbf{u}}\right),$$

where $\mathscr{T}$ is some positive definite stabilization matrix. Clearly, when $\mathscr{T} = |\mathbf{A}|$, we recover our upwind HDG scheme.

REMARK 6.3. *We have applied our constructive HDG framework to Friedrichs' PDE systems with full coercivity condition (6.1d). In this light one can similarly develop an HDG framework for mutlifield systems with partial coercivity [22]. We nevertheless leave out the details here.*

We would like to also emphasize that the analysis of this section is mainly of theoretical interest, namely, a unified theory for the HDG framework is possible for a large class of PDEs. However, in practice one typically faces a particular PDE of interest, and in that case we suggest to follow our systematic construction of HDG schemes in Sections 3–5 to exploit the structure of the underlying PDE to minimize the number of trace unknowns, and hence arriving at the most economic HDG methods.

7. HDG schemes by hybridizing other numerical fluxes. Perhaps the most popular upwind flux is that of Godunov's with exact Riemann solutions, and we have used it to motivate a constructive derivation of the HDG framework. At the heart of our construction is the exploration of various identities satisfied by the exact Riemann solutions to devise HDG methods with least possible trace unknowns. A question that immediately arises is whether we can construct HDG method for other existing numerical fluxes, for example those summarized in [53, 36].

In this section, we restrict our derivation of HDG method for the Lax-Friedrichs numerical flux (LF) whose standard form is given by

$$\mathbf{F}^* \cdot \mathbf{n} = \frac{1}{2}\left[\mathbf{F}\left(\mathbf{u}^-\right) + \mathbf{F}\left(\mathbf{u}^+\right)\right] \cdot \mathbf{n}^- + \frac{1}{2}\max_i |\theta_i| \left(\mathbf{u}^- - \mathbf{u}^+\right). \tag{7.1}$$

Clearly, for scalar problem, i.e. $m = 1$, LF flux becomes the Godunov flux. This suggests us to hybridize the former in a similar manner as we have done for the latter. A natural idea is to consider the following hybridized version of the LF flux

$$\mathbf{F}^* \cdot \mathbf{n} = \mathbf{A}\mathbf{u} + \max_i |\theta_i| \left(\mathbf{u} - \mathbf{u}^*\right). \tag{7.2}$$

The hybridized LF flux is consistent with the upwind HDG flux in the sense that the former is identical to the latter for scalar problem. Moreover, it is easy to see that our hybridized LF flux (7.2) is identical to the original LF one (7.1) if pointwise conservation condition (2.13) is enforced.

Let us now explicitly derive the HDG scheme with LF flux for the convection-diffusion-reaction PDE and compare it with the hybridized Godunov counterpart.

(The construction for the Maxwell and Stokes equations are similar, and hence omitted.) For this case, it is easy to see that

$$\theta^{\max} := \max_i |\theta_i| = \frac{|\boldsymbol{\beta}\cdot\mathbf{n}| + \sqrt{|\boldsymbol{\beta}\cdot\mathbf{n}|^2 + 4}}{2},$$

and (7.2) becomes

$$\mathbf{F}^*\cdot\mathbf{n} = \begin{bmatrix} u\mathbf{n} + \theta^{\max}(\boldsymbol{\sigma} - \boldsymbol{\sigma}^*) \\ \boldsymbol{\beta}\cdot\mathbf{n}u + \boldsymbol{\sigma}\cdot\mathbf{n} + \theta^{\max}(u - u^*). \end{bmatrix} \tag{7.3}$$

Note that $u^*, \boldsymbol{\sigma}^*$ are no longer the exact Riemann solutions, but we still can use the conservation equation (2.13) to obtain the following identities

$$\theta^{\max}(\boldsymbol{\sigma}^* - \boldsymbol{\sigma}) = -\frac{\theta^{\max}}{2}[\![\boldsymbol{\sigma}]\!] + \frac{1}{2}[\![u\mathbf{n}]\!],$$
$$\theta^{\max}(u^* - u) = \frac{(\boldsymbol{\beta}\cdot\mathbf{n} - \theta^{\max})}{2}[\![u]\!] + \frac{1}{2}[\![\boldsymbol{\sigma}\cdot\mathbf{n}]\!].$$

Unlike the Godunov flux with exact Riemann solution in which we could find the relationship between u^* and $\boldsymbol{\sigma}^*$ (see (3.5)), we have not yet found a "clean" relationship between u^* and $\boldsymbol{\sigma}^*$ that does not require information from the neighbor element. As a result, it is not clear how to eliminate either u^* and $\boldsymbol{\sigma}^*$ before introducing the HDG flux.

In summary, the pure upwind flux with exact Riemann solution allows us to reduce the number of trace unknowns, but deviating from that, using the LF flux for example, does not seem to offer the same reduction. Thus, the hybridized LF (7.3), though looks much simpler than the Godunov counterpart (3.2), it yields more trace unknowns for HDG methods constructed using our framework, and hence more expensive. For nonlinear PDEs, it is nevertheless a better choice since we cannot reduce the number of trace unknowns for Godunov flux either.

8. Construction of other HDG variants. In this section, we will construct a simple variant of our HDG framework that allows us to recover other existing HDG methods. To that end, notice that we can write

$$\mathbf{A}\mathbf{u} + |\mathbf{A}|(\mathbf{u} - \hat{\mathbf{u}}) = \mathbf{A}\hat{\mathbf{u}} + (\mathbf{A} + |\mathbf{A}|)(\mathbf{u} - \hat{\mathbf{u}}).$$

This leads us to define a new family of HDG fluxes

$$\hat{\mathbf{F}}\cdot\mathbf{n} = \mathbf{A}\hat{\mathbf{u}} + \mathscr{T}(\mathbf{u} - \hat{\mathbf{u}}),$$

which becomes our upwind HDG flux when $\mathscr{T} = (\mathbf{A} + |\mathbf{A}|)$. Clearly, we can revisit all the examples in this paper with this HDG flux form to derive variants of HDG schemes for various type of PDEs. For example, we can rewrite the HDG flux (3.6) for the convection-diffusion-reaction PDE as

$$\hat{\mathbf{F}}\cdot\mathbf{n} = \begin{bmatrix} \hat{u}\mathbf{n}_1 \\ \hat{u}\mathbf{n}_2 \\ \hat{u}\mathbf{n}_3 \\ \boldsymbol{\beta}\cdot\mathbf{n}\hat{u} + \boldsymbol{\sigma}\cdot\mathbf{n} + \frac{1}{2}(\alpha + \boldsymbol{\beta}\cdot\mathbf{n})(u - \hat{u}) \end{bmatrix},$$

and deduce its penalized family as follows

$$\hat{\mathbf{F}}\cdot\mathbf{n}=\begin{bmatrix}\hat{u}\mathbf{n}_1\\ \hat{u}\mathbf{n}_2\\ \hat{u}\mathbf{n}_3\\ \boldsymbol{\beta}\cdot\mathbf{n}\hat{u}+\boldsymbol{\sigma}\cdot\mathbf{n}+\tau\left(u-\hat{u}\right)\end{bmatrix}. \tag{8.1}$$

A careful look at (8.1) shows that we have rediscovered the HDG family proposed in [42]. One can follow the same exercise to derive families of HDG methods of this type for other PDEs in a straightforward manner, so let us skip the details here.

9. HDG schemes for discontinuous material. In this section we present an extension of our HDG framework for linear PDEs with discontinuous material, i.e., $\mathbf{A}^k$ are possibly discontinuous across e. The Godunov fluxes still have exactly the same form as in (2.11) and (2.12), but $\mathbf{A}$ is computed using the information from the appropriate element under consideration. For example,

$$\mathbf{F}^*\cdot\mathbf{n}^-=\mathbf{F}\left(\mathbf{u}^-\right)\cdot\mathbf{n}^-+\left|\mathbf{A}^-\right|\left(\mathbf{u}^--\mathbf{u}^*\right). \tag{9.1}$$

One can then go through all the steps presented in this paper to derive the corresponding HDG family for each PDE of interest since the chief idea remains the same. For example, one first seeks various relations between the exact Riemann solution components in $\mathbf{u}^*$ to eliminate their dependencies so that the Godunov fluxes depend on the least number of components. One then defines the HDG flux by replacing these least components with the HDG trace unknowns. Together with the local solver (2.15a) and conservation constraint (2.15b), one obtains desirable HDG schemes. However, the arithmetic is more involved since we need to distinguish materials between neighbor elements. We omit the details here to avoid unnecessarily lengthy paper.

It is important to realize that most of the theory for Friedrichs also holds for this case. In particular, the well-posedness of the local solver remains true, but global solver is well-posed if we additionally assume that $\mathbf{A}^-+\mathbf{A}^+\leq 0$ on $e\in\mathcal{E}_h^o$. At this point, this assumption is merely mathematically convenient since using it allows us to conclude

$$-\left\langle\frac{1}{2}\mathbf{A}\hat{\mathbf{u}},\hat{\mathbf{u}}\right\rangle_{\partial K\cap\mathcal{E}_h^o}\geq 0, \tag{9.2}$$

and hence the proof of Theorem 6.2 goes through. Whether this assumption is practical is out of the scope of the paper. Clearly, one may find a proof that does not require (9.2) and in that case the assumption $\mathbf{A}^-+\mathbf{A}^+\leq 0$ can be completely discarded.

One can similarly define a penalized family of HDG flux with double-valued stabilization matrix $\mathscr{T}$, e.g.,

$$\hat{\mathbf{F}}\cdot\mathbf{n}^-=\mathbf{F}\left(\mathbf{u}^-\right)\cdot\mathbf{n}^-+\mathscr{T}^-\left(\mathbf{u}^--\hat{\mathbf{u}}\right).$$

HDG methods with double-valued stabilization parameters can be found, for example, in [9, 42].

10. HDG schemes for nonlinear PDEs. In this section we extrapolate our HDG schemes for linear PDEs to nonlinear ones. Specifically, based on the upwind HDG flux (2.6) we define HDG flux for nonlinear PDEs as

$$\hat{\mathbf{F}}\cdot\mathbf{n}=\mathbf{F}\left(\mathbf{u}\right)\cdot\mathbf{n}+\left|\mathbf{A}\right|\left(\mathbf{u}-\hat{\mathbf{u}}\right),$$

where $\mathbf{A}$ is now a function of $\mathbf{u}$, i.e.,

$$\mathbf{A} = \sum_{k=1}^{d} \partial_k \mathbf{F}^k(\mathbf{u})\, \mathbf{n}_k,$$

with $\mathbf{F}^k$ denoting the kth component of the flux $\mathbf{F}$.

Alternatively, one can follow the spirit of the Roe flux [51] to define the HDG flux as

$$\hat{\mathbf{F}} \cdot \mathbf{n} = \mathbf{F}(\mathbf{u}) \cdot \mathbf{n} + |\mathbf{A}(\hat{\mathbf{u}})| (\mathbf{u} - \hat{\mathbf{u}}), \tag{10.1}$$

in which $\mathbf{A}(\hat{\mathbf{u}})$ is computed using the trace unknown $\hat{\mathbf{u}}$, i.e.,

$$\mathbf{A}(\hat{\mathbf{u}}) = \sum_{k=1}^{d} \partial_k \mathbf{F}^k(\hat{\mathbf{u}})\, \mathbf{n}_k. \tag{10.2}$$

Clearly, if we use the Roe-average state in place of $\hat{\mathbf{u}}$ in (10.2) our HDG method, after eliminating $\hat{\mathbf{u}}$, is identical to the standard DG approach using Roe flux. However, using the Roe-average state in computing $|\mathbf{A}|$ requires extra state exchange for the neighboring states, and hence increasing communication time in parallel computation.

We end this section by presenting a nonlinear HDG scheme with a hybridized Lax-Friedrichs flux. Based on (7.2) and (10.1), we define a HDG flux of Lax-Friedrichs' type as

$$\hat{\mathbf{F}} \cdot \mathbf{n} = \mathbf{F}(\mathbf{u}) \cdot \mathbf{n} + \max_i |\theta_i(\mathbf{A}(\hat{\mathbf{u}}))| (\mathbf{u} - \hat{\mathbf{u}}), \tag{10.3}$$

where we denote by $\theta_i(\mathbf{A}(\hat{\mathbf{u}}))$ the ith eigenvalue of $\mathbf{A}(\hat{\mathbf{u}})$.

Alternatively, one can extrapolate the result in Section 8 to define the HDG flux as

$$\hat{\mathbf{F}} \cdot \mathbf{n} = \mathbf{F}(\hat{\mathbf{u}}) \cdot \mathbf{n} + \max_i |\theta_i(\mathbf{A}(\hat{\mathbf{u}}))| (\mathbf{u} - \hat{\mathbf{u}}), \tag{10.4}$$

or

$$\hat{\mathbf{F}} \cdot \mathbf{n} = \mathbf{F}(\hat{\mathbf{u}}) \cdot \mathbf{n} + |\mathbf{A}(\hat{\mathbf{u}})| (\mathbf{u} - \hat{\mathbf{u}}),$$

and these are exactly HDG methods proposed in [48, 41] for compressible Euler and Navier-Stokes equations.

11. Numerical results. It should be pointed out that there are vast existing numerical results for HDG methods on Laplace/Poisson equation [34], convection-diffusion equation [42, 43, 8, 18], Stokes equation [15, 9, 44], Euler and Navier-Stokes equations [47, 48, 40], Maxwell equation [46, 37, 38], acoustics and elastodynamics [45], Helmholtz equation [27, 17], and eigenvalue problem [14], to name a few. Instead of reproducing these results, let us present numerical results to compare our upwind HDG framework with some existing HDG schemes on transport equation, convection-diffusion equation, compressible Euler equation, and shallow water equation.

11.1. Steady convection (transport) equation. In this section, we apply our upwind HDG to convection equation of the form

$$\nabla \cdot (\boldsymbol{\beta} u) + \nu u = f, \quad \text{in } \Omega,$$

and compare its solutions with those of the upwind DG. As a numerical demonstration, we take an example from [31] in which $\Omega = (0,2)\times(0,1)$, $\boldsymbol{\beta} = (1+\sin(\pi y/2),2)$, $\nu = 0$, $f = 0$, and the inflow boundary condition

$$g = \begin{cases} 1 & x = 0, 0 \le y \le 1 \\ \sin^6(\pi x) & 0 < x \le 1, y = 0 \\ 0 & 1 \le x \le 2, y = 0 \end{cases}.$$

This problem admits an exact solution using the method of characteristics.

Figure 11.1(a) shows the mesh that we use for both HDG and DG schemes. To verify the theoretical result in Corollary 3.6, we compute the L^2-norm of the difference between the HDG trace solution $\hat{u}$ and the exact Riemann solution u^* (used in the DG upwind flux), and of the difference between the HDG solution u_{HDG} and the DG solution u_{DG}. Table 11.1 shows these differences for various solution orders $p = \{1,2,3,4,5\}$. As can be seen, the differences are (machine) zeros for all solution orders as expected by the theory.

We also show the HDG solution u with $p = 3$ in Figure 11.1(b) and its convergence against the exact solution at the outflow boundary $y = 1$ in Figure 11.1(c). As expected, as the solution order increases the HDG solution is more accurate in the smooth regions, but oscillates in regions with high gradient since we do not employ any limiter.

Recall that we have constructed HDG method by hybridizing the DG method (in fact the Godunov flux). This procedure could be understood as a redesign of the DG method. The beauty of this redesign is that the number coupled unknown is substantially reduced and the usual DG unknowns are recovered element by element independent of each other. It is therefore useful to compare the number of coupled of unknowns and the execution time for both methods. We do so for the above two dimensional transport equation on triangular meshes. The result is shown in Figure 11.1(d) in which we plot the ratio of DG and HDG coupled unknowns and similarly for the execution time. As can be seen, as the solution order increases these ratios increase as well. For the mesh ($h = 0.2$) in Figure 11.1(a) and its one level of refinement ($h = 0.1$), we gain (almost) an order of magnitude in solution time and the number of coupled unknowns for $p = 15$; also the finer the mesh is, the the more savings the HDG provides. Moreover, we have computed solution u in our HDG scheme in a serial manner, element-after-element. The time gain would be even more if we did it in parallel. These advantages are expected to more substantial for three dimensional problems.

TABLE 11.1
Transport equation: $\|\hat{u}-u^*\|_{L^2(\mathcal{E}_h^o)}$ *and* $\|u_{HDG}-u_{DG}\|_{L^2(\Omega)}$ *for various solution order* $p = \{1,2,3,4,5\}$.

p	1	2	3	4	5
$\|\hat{u}-u^*\|_{L^2(\mathcal{E}_h^o)}$	5.7×10^{-15}	1.6×10^{-14}	3.4×10^{-14}	4.1×10^{-14}	4.8×10^{-14}
$\|u_{\text{HDG}}-u_{\text{DG}}\|_{L^2(\Omega)}$	8.5×10^{-16}	3.1×10^{-15}	9.2×10^{-15}	1.1×10^{-14}	3.1×10^{-14}

11.2. Convection-diffusion equation. In this section we compare our upwind HDG and both upwind and centered trace HDG methods proposed in [42, Section 3.6.3] for the convection-diffusion equation, i.e. (3.1) with $\nu = 0$. We take $\boldsymbol{\beta} = (1,2)$

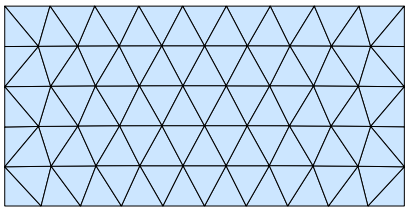

(a) Mesh with $h = 0.2$

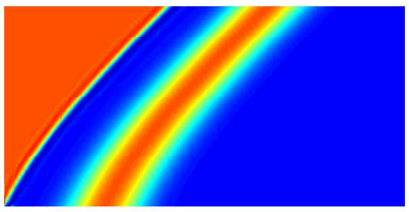

(b) HDG solution u with $p = 3$

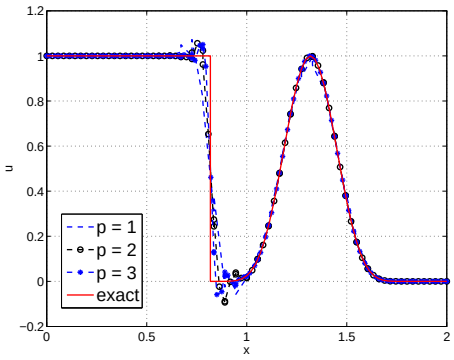

(c) HDG solution u restricted on $y = 1$

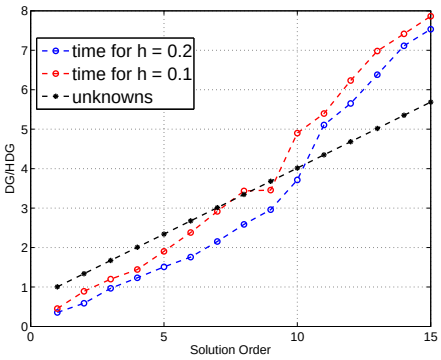

(d) upwind HDG versus upwind DG

FIG. 11.1. *Transport problem: the mesh with* $= 0.2$ *is in Figure 11.1(a), the HDG solution* u *with solution order* $p = 3$ *in Figure 11.1(b), HDG solution* u *restricted on the outflow boundary* $y = 1$ *in Figure 11.1(c), and the savings in time and number of coupled of unknowns of HDG relative to DG in Figure 11.1(d).*

and $\Omega = [0, 1]^2$. The right hand side f is chosen so that the exact solution is given by

$$u_e = \exp(x + y) \sin(\pi x) \sin(\pi y),$$

and the Dirichlet boundary are taken as the restriction of the exact solution on the domain boundary $\partial\Omega$. In Figure 11.2(a) we show a plot of $\nabla \cdot \boldsymbol{\beta}$ inside elements and $\boldsymbol{\beta}$ on element boundaries with $h = 0.2$, accompanied by our upwind HDG fourth order ($p = 3$) solution u in Figure 11.2(b), $\boldsymbol{\sigma}_x$ in Figure 11.2(c), and $\boldsymbol{\sigma}_y$ in 11.2(d).

What we are interested in this example is the behavior of these three methods for varying diffusion coefficients ε as the mesh is refined. Let us first examine the convergence rate as ε decreases. In Figures 11.3(a), 11.3(c), and 11.3(e) we present the observed convergence order of the three methods with $p = 3$ as the diffusion coefficient ε changes. As can be seen, the convergence for both u and $\hat{u}$ is optimal, with rate 4 and 3.5, respectively, for all methods when $\varepsilon > 10^{-2}$. When the equation is in convection-dominated regime, the behavior is different for the three methods. In particular, both upwind trace and centered trace HDG methods are unstable for $\varepsilon < 10^{-2}$, while it is for the upwind HDG. This behavior is expected for the upwind HDG by construction since it is equivalent to the standard upwind DG.

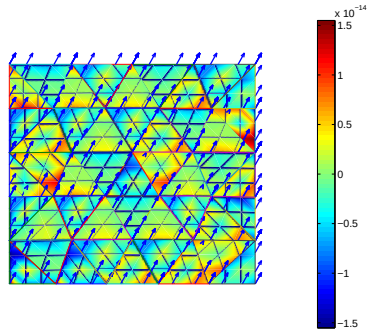

(a) $\boldsymbol{\beta}$ with $h = 0.2$

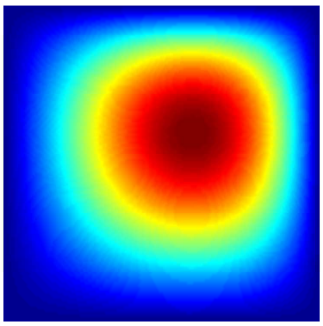

(b) uHDG solution u

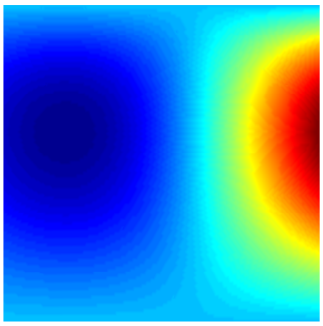

(c) uHDG solution $\boldsymbol{\sigma}_x$

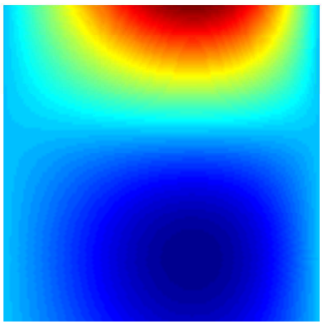

(d) uHDG solution $\boldsymbol{\sigma}_y$

FIG. 11.2. *Solution of the upwind HDG method for convection diffusion problem: Figure 11.2(a) is a plot of $\nabla \cdot \boldsymbol{\beta}$ inside elements and $\boldsymbol{\beta}$ on element boundaries with $h = 0.2$, Figure 11.2(b) the $p = 3$ solution u, Figure 11.2(c) the $p = 3$ solution $\boldsymbol{\sigma}_x$, and Figure 11.2(d) the $p = 3$ solution $\boldsymbol{\sigma}_y$.*

To gain some understanding on why the unstability may happen for the others let us recall that the stabilization for upwind trace HDG scheme is given by

$$\tau = (\varepsilon + |\boldsymbol{\beta} \cdot \mathbf{n}|) \frac{|\boldsymbol{\beta} \cdot \mathbf{n}| + \boldsymbol{\beta} \cdot \mathbf{n}}{2\,|\boldsymbol{\beta} \cdot \mathbf{n}|} = (\varepsilon + |\boldsymbol{\beta} \cdot \mathbf{n}|) \frac{1 + \ \mathrm{sgn}(\boldsymbol{\beta} \cdot \mathbf{n})}{2}$$

and

$$\tau = (\varepsilon + |\boldsymbol{\beta} \cdot \mathbf{n}|)$$

for the centered trace HDG scheme. In Figure 11.2(a), for edge e with $\boldsymbol{\beta} \cdot \mathbf{n} \lessapprox 0$ (negative but machine zero), then $\tau \approx 0$. On the other hand, though $\nabla \cdot \boldsymbol{\beta}$ is identically zero analytically, it is not numerically in our nodal implementation [28], in fact machine zero with positive and negative signs, as shown in Figure 11.2(a). Now recall from [42, Lemma 3.1 and Theorem 3.1] that a sufficient condition for the well-posedness is that $\nabla \cdot \boldsymbol{\beta} \geq 0$ and $\tau > \frac{1}{2}\boldsymbol{\beta} \cdot \mathbf{n}$. It follows that the well-posedness is not guaranteed in our implementation of the upwind and centered trace HDG methods. Nevertheless, when ε is sufficiently large, it does not seem to be a problem, but this does for $\varepsilon < 10^{-2}$.

Next, let us examine the dependence of actual L^2-errors on ε, especially when ε is large. As an example, we take $p = 3$ and $h = 0.05$ (two levels of refinement of the mesh in Figure 11.2(a)). In Figures 11.3(b), 11.3(d), and 11.3(f) are the L^2-errors for u and $\hat{u}$ of the three methods as the diffusion coefficient ε increases. As can be observed, the error in the trace unknown $\hat{u}$ for all methods is robust in ε, i.e., it is independent of ε. And so is for the error in u of the upwind and centered trace HDG methods. The error in u of the upwind HDG, however, increases as ε does.

In summary, our numerical results seem to suggest that either upwind or centered trace HDG method is preferred if the robustness with large ε (diffusion-dominated) is of importance. On the other hand, if the stable behavior for a wide range of ε is desired, the upwind HDG is likely to be a better choice.

11.3. Compressible Euler equation. The purpose of this section is to compare our proposed HDG flux (10.3) and Nguyen *et al.* flux (10.4) for nonlinear PDEs. To that end, we next consider the unsteady Euler equation in the conservative form

$$\frac{\partial \mathbf{u}}{\partial t} + \nabla \cdot \mathbf{F}(\mathbf{u}) = \mathbf{f}, \tag{11.1}$$

where the conservative state $\mathbf{u}$, and the x- and $y-$ components of the flux $\mathbf{F}$ are given by

$$\mathbf{u} := \begin{bmatrix} \rho \\ \rho u \\ \rho v \\ E \end{bmatrix}, \quad \mathbf{F}_x := \begin{bmatrix} \rho u \\ \rho u^2 + P \\ \rho uv \\ u(E+P) \end{bmatrix}, \quad \mathbf{F}_y := \begin{bmatrix} \rho v \\ \rho uv \\ \rho v^2 + P \\ v(E+P) \end{bmatrix}.$$

We assume that the pressure P satisfies the state equation

$$E = \frac{P}{\gamma - 1} + \frac{1}{2\rho}\left[(\rho u)^2 + (\rho v)^2\right],$$

with $\gamma = 1.4$ for monoatomic gas. Here, ρ is the density, u and v are the $x-$ and $y-$ components of velocity, and E denotes the total energy. The domain under consideration is $\Omega = [3.5, 5.5] \times [-1, 1]$.

For numerical example, we choose the forcing function $\mathbf{f}$ so that the exact solution is the following vortex [28]

$$\rho = \left[1 - \frac{(\gamma-1)}{16\gamma\pi^2}\beta^2 e^{2(1-R^2)}\right]^{\frac{1}{\gamma-1}}, \qquad u = 1 - \beta e^{(1-R^2)}\frac{(y-y_0)}{2\pi},$$
$$v = \beta e^{(1-R^2)}\frac{(x-x_0)}{2\pi}, \qquad P = \rho^\gamma,$$

with $R^2 = (x - t - x_0)^2 + (y - y_0)^2$, $x_0 = 0.5, y_0 = 0$, and $\beta = 5$. For simplicity, the exact solution is used to enforce the boundary condition.

Since the Euler equation is nonlinear, both the local solver (2.15a) and the conservative constraint are nonlinear too. For time discretization, we use the Crank-Nicholson method. Similar to [43, 41] we use Newton method to solve the resulting nonlinear algebraic equations. The HDG solution with our proposed hybridized flux (10.3) is shown in Figure 11.3 in which we plot the conservative variables $(\rho, \rho u, \rho v, E)$ after 100 time steps with stepsize 10^{-6}. The small step size is deliberately chosen so that the error is dominated by the spatial discretization by the HDG method. Also, 100 time steps is sufficient for convergence test that is discussed next.

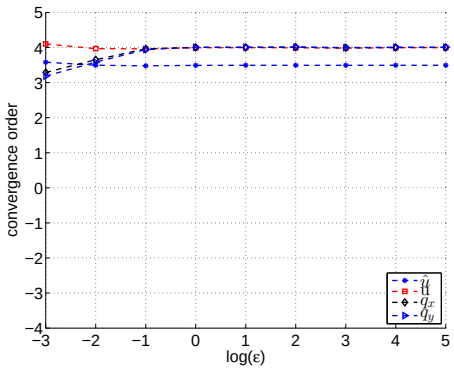

(a) Convergence of the upwind HDG

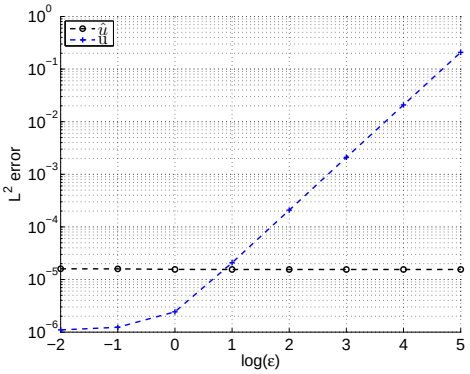

(b) Error of the upwind HDG

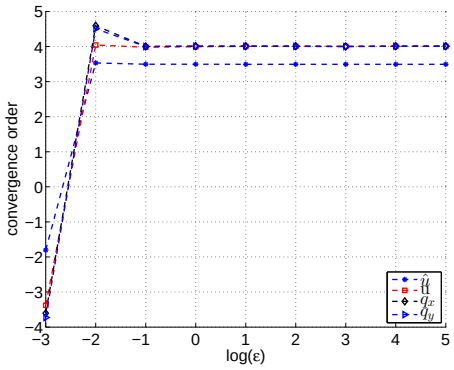

(c) Convergence of the upwind trace HDG

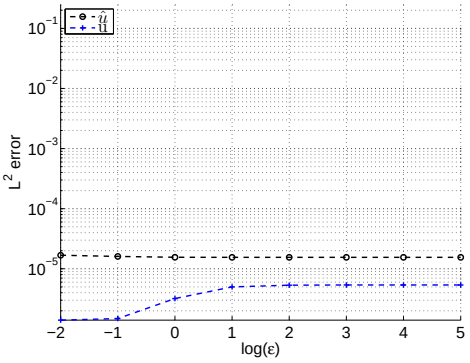

(d) Error of the upwind trace HDG

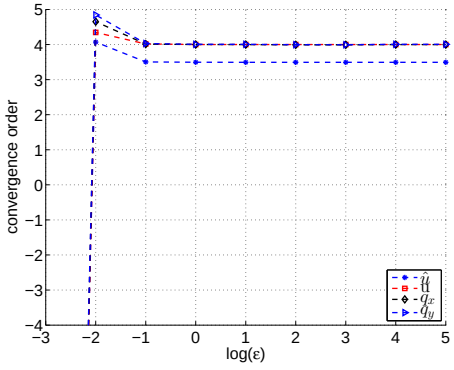

(e) Convergence of the centered trace HDG

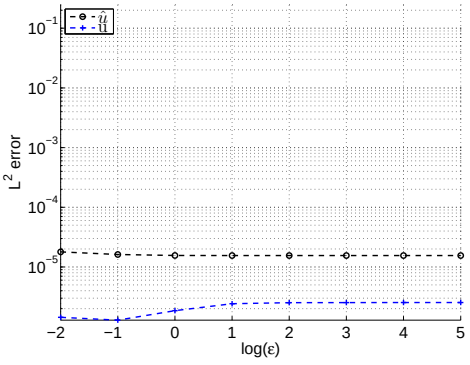

(f) Error of the centered trace HDG

FIG. 11.3. *Convection-diffusion equation: Figures 11.3(a) and 11.3(b) are the convergence order and L^2-errors of the upwind HDG method for $p = 3$, and similarly for the upwind trace HDG method in Figures 11.3(c) and 11.3(d), and the centered trace HDG method in Figures 11.3(e) and 11.3(f).*

In Figure 11.3, we present the convergence rate for HDG methods with our HDG flux (10.3) and Nguyen *et al.* flux (10.4) by refining the mesh with $h = \{0.125, 0.25, 0.5\}$.

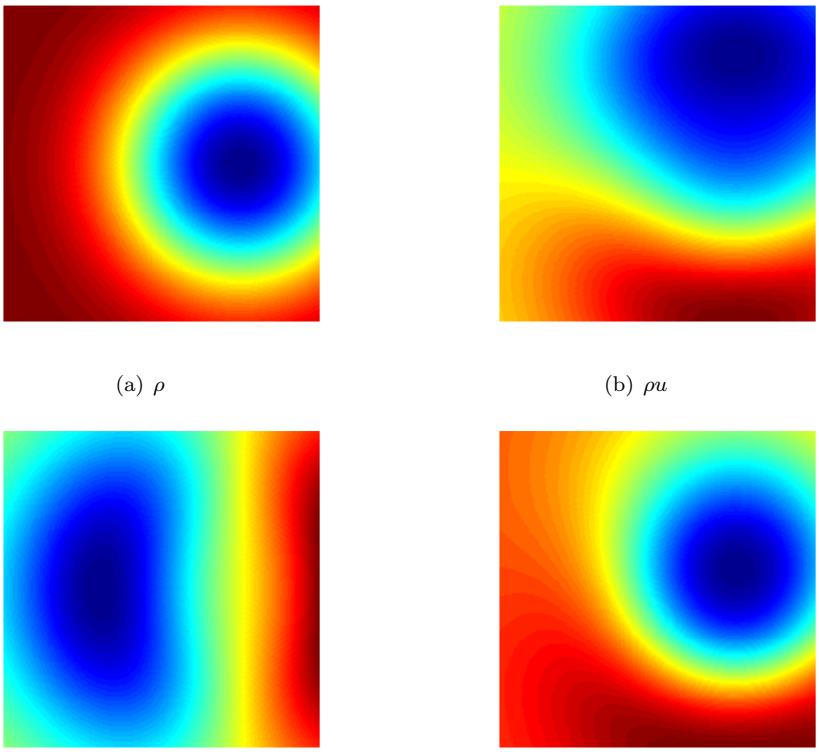

(a) ρ (b) ρu

(c) ρv (d) E

FIG. 11.4. *HDG solution with the Crank-Nicholson temporal discretization for the compressible Euler equation with time stepsize of* 10^{-6} *after* 100 *time steps.*

It is interesting to see that both methods give almost identical results. Moreover, the convergence is $p+1$ for all $p = \{2, 3, 4\}$, and hence optimal. We conclude that the two methods do not seem to different numerically.

11.4. Shallow water equation. The last example we consider in this paper is the shallow water equation written in the conservative form similar to (11.1), but now the flux $\mathbf{F}$ and the forcing function $\mathbf{f}$ are given by

$$\mathbf{F}_x := \begin{pmatrix} Hu \\ Hu^2 + \frac{1}{2}gH^2 \\ Huv \end{pmatrix}, \quad \mathbf{F}_y := \begin{pmatrix} Hv \\ Huv \\ Hv^2 + \frac{1}{2}gH^2 \end{pmatrix}, \text{ and } \mathbf{f} := \begin{pmatrix} 0 \\ -gb_x \\ -gb_y \end{pmatrix},$$

while the conservative variables $\mathbf{u}$ are defined as

$$\mathbf{u} := (H, Hu, Hv)^T.$$

Here, H is the water depth, u the depth average velocity component in x-direction, v the depth average velocity component in $y-$direction, b the bathymetry, and g the gravity acceleration.

Following [25] we take $\gamma = g = 2$ so that the vortex solution in Section 11.3 is also the exact solution for the shallow water equation with flat bathymetry ($b = b_x =$

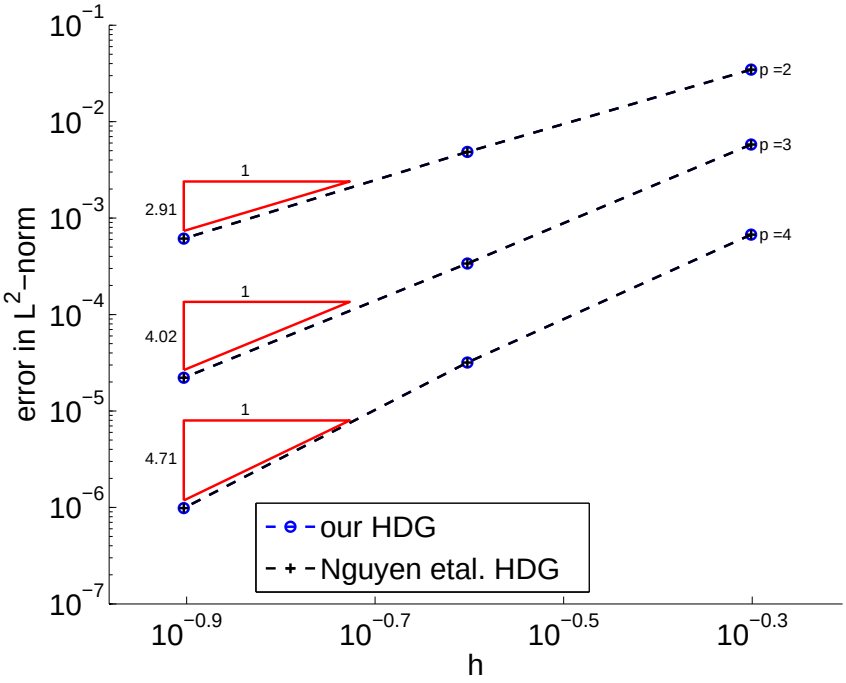

FIG. 11.5. *Compressible Euler equation: convergence rate for HDG methods with our HDG flux* (10.3) *and Nguyen et al. flux* (10.4).

$b_y = 0$). We choose this example to again compare the HDG methods with our HDG flux (10.3) and Nguyen *et al.* flux (10.4). The rest of the setting is same as that of the Euler equation. For example, we take $\Omega = [3.5, 5.5] \times [-1, 1]$, and use Crank-Nicholson temporal discretization with 100 time steps of stepsize 10^{-6}. In Figure 11.4, we again observe that both methods yield almost identical results. Furthermore, the convergence rate in this case is $p + \frac{1}{2}$ which is typical for hyperbolic equations using fluxes of Lax-Friedrichs' type.

The next example we like to apply our HDG method to is that considered in [52, 55], namely, the water drop problem with the initial water depth

$$H(x, y, 0) := 1 + 0.1 \exp\left[-100 (x - 0.5)^2 - 100 (y - 0.5)^2\right],$$

and the flow is initial at rest, i.e.,

$$Hu(x, y, 0) = Hv(x, y, 0) = 0.$$

We first consider the case with flat bottom, i.e., $b = b_x = b_y = 0$ and the domain of interest is $\Omega = [0, 1]^2$. An unstructured triangular mesh with the mesh size $h = 0.12$ is generated and we take $p = 6$. Wall (slip) boundary conditions are applied to the entire boundary $\partial\Omega$. Again, the Crank-Nicholson temporal discretization is employed with time step equal to 0.0005 and the simulation is run up to 2000 time steps. Presented in Figure 11.4 are the simulated water depth at various time instances $t = \{0, 0.15, 0.3, 0.5, 0.7, 1\}$. As can be seen, the water depth evolution is very complex. This is also confirmed in Figure 11.4 in which we plot the distribution of v (u is the

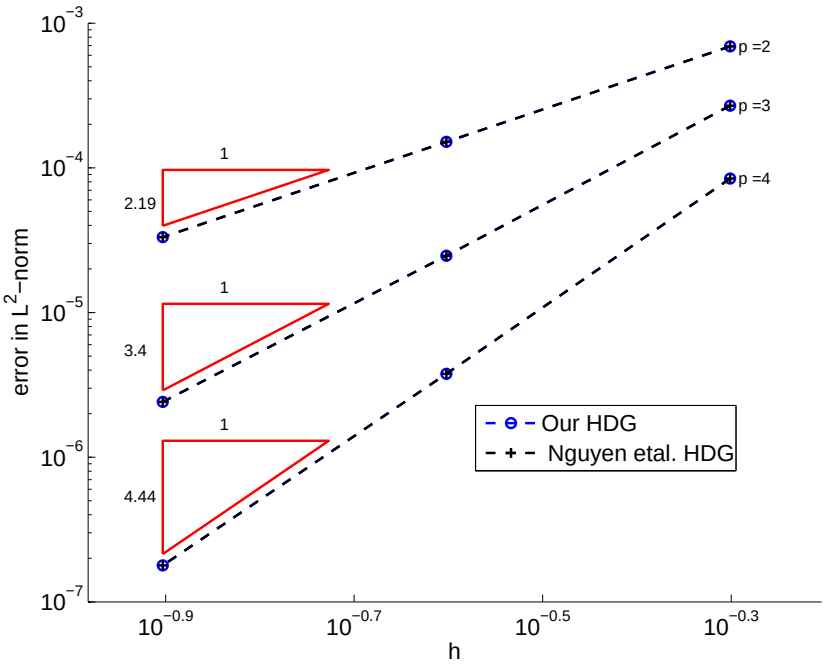

FIG. 11.6. *Shallow water equation: convergence rate for HDG methods with our HDG flux* (10.3) *and Nguyen et al. flux* (10.4).

same but rotated by 90 degrees) as a function of time. Though there is no analytical solution to compare with, our HDG results look comparable to those in [52, 55]. Note that we don't employ any special techniques to ensure the positivity-preserving and well-balanced properties.

Next we consider the case with non-flat bathymetry used in [55] with

$$b\,(x,y) := 0.5 \exp\left[-10\,(x-0.75)^2 - 10\,(y-0.5)^2\right].$$

The initial condition, boundary conditions, and time stepping scheme are the same as in the previous case but now with $g = 9.812$. We show the evolution of the water depth H after 600 time steps ($t = 0.3$) in Figure 11.4, while the velocities u and v are shown in Figures 11.4 and 11.4, respectively. As can be seen, due to the bathymetry, the $x-$ and $y-$ components of the velocity vector are completely different and very complex.

12. Conclusions. We have presented a unified framework for the emerging hybridized discontinuous Galerkin (HDG) methods. At the heart of our construction is the hybridization of the Godunov flux. In fact, we have shown that it is a natural recipe to constructively and systematically establish a unified HDG framework for a large class of PDEs including those of Friedrichs' type. The unification is fourfold. First, it provides a single constructive procedure to devise HDG schemes for elliptic, parabolic and hyperbolic PDEs. Second, it reveals the nature of the trace unknowns as the Riemann solutions. Third, it provides a parameter-free HDG framework, and hence eliminating the "usual complaint" that HDG is a parameter-dependent method.

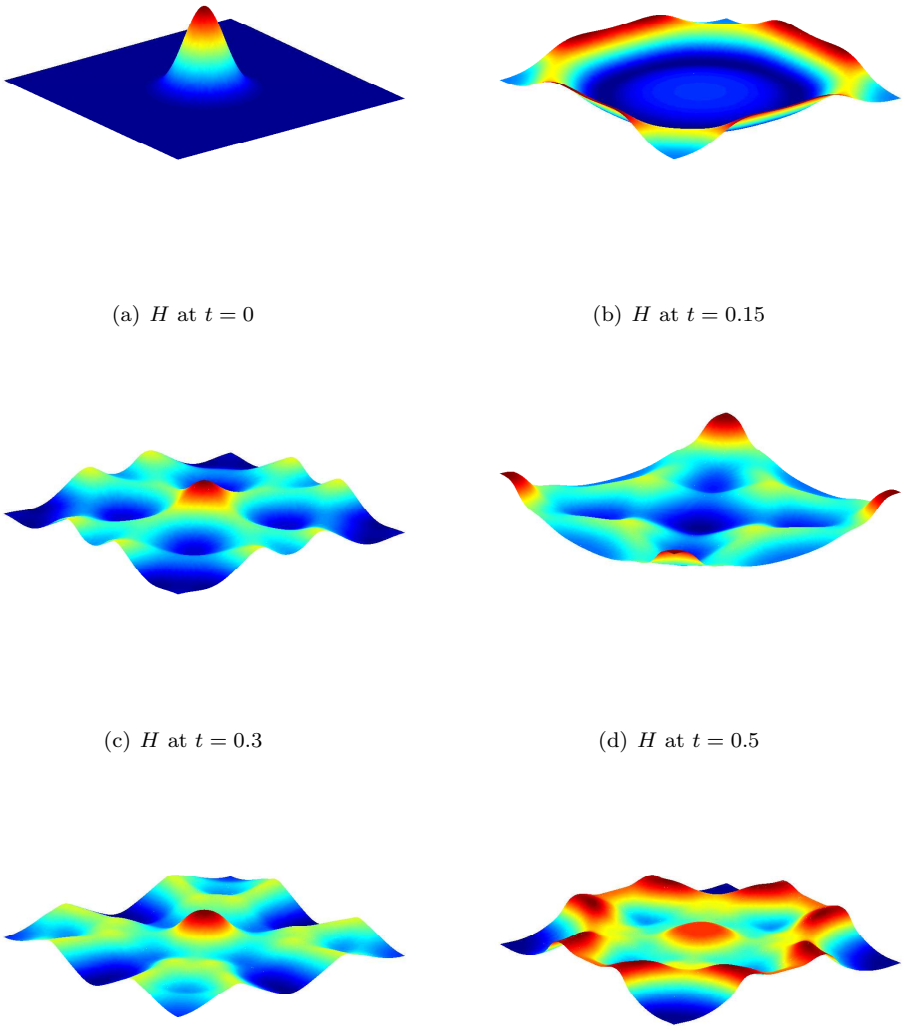

(a) H at $t = 0$ (b) H at $t = 0.15$

(c) H at $t = 0.3$ (d) H at $t = 0.5$

(e) H at $t = 0.7$ (f) H at $t = 1$

FIG. 11.7. *Evolution of the water depth H for flat bathymetry case.*

Fourth, it allows us to construct the existing HDG methods in a natural manner. In particular, using the unified framework we can rediscover most of the existing HDG methods and furthermore discover new ones.

We apply the proposed unified framework to three different PDEs: the convection-diffusion-reaction equation, the Maxwell equation in both frequency and time domains, and the Stokes equation. The purpose is to present a step-by-step construc-

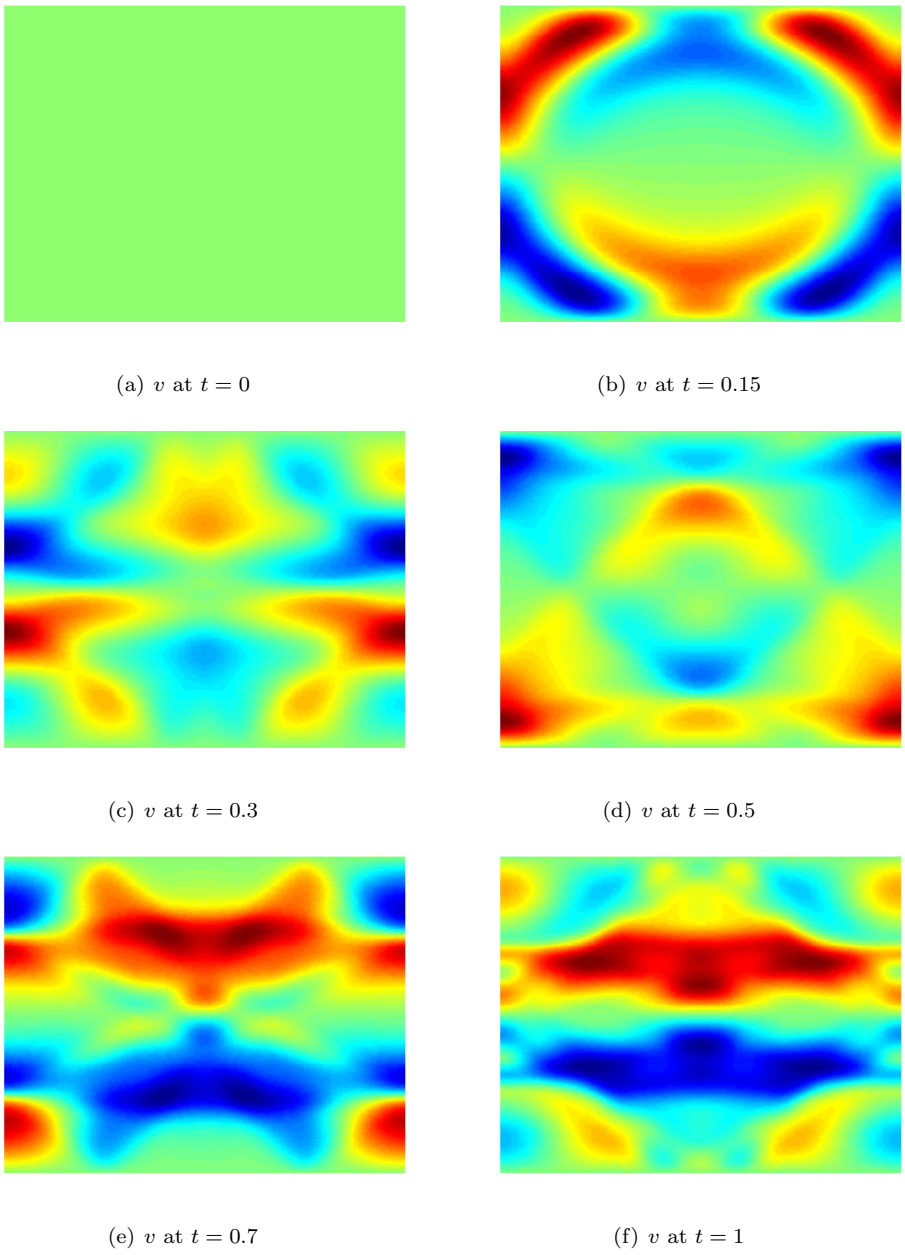

(a) v at $t = 0$ (b) v at $t = 0.15$

(c) v at $t = 0.3$ (d) v at $t = 0.5$

(e) v at $t = 0.7$ (f) v at $t = 1$

FIG. 11.8. *Evolution of depth average y-velocity v for flat bathymetry case.*

tion of various HDG methods, including the most economic ones with least trace unknowns, by exploiting the particular structure of the underlying PDEs. The well-posedness of the resulting HDG schemes, i.e. the existence and uniqueness of the HDG solutions, are proved. The well-posedness results are also extended and proved for abstract Friedrichs' systems. We also discuss variants of the proposed unified framework and extend them to the popular Lax-Friedrichs flux and to nonlinear PDEs.

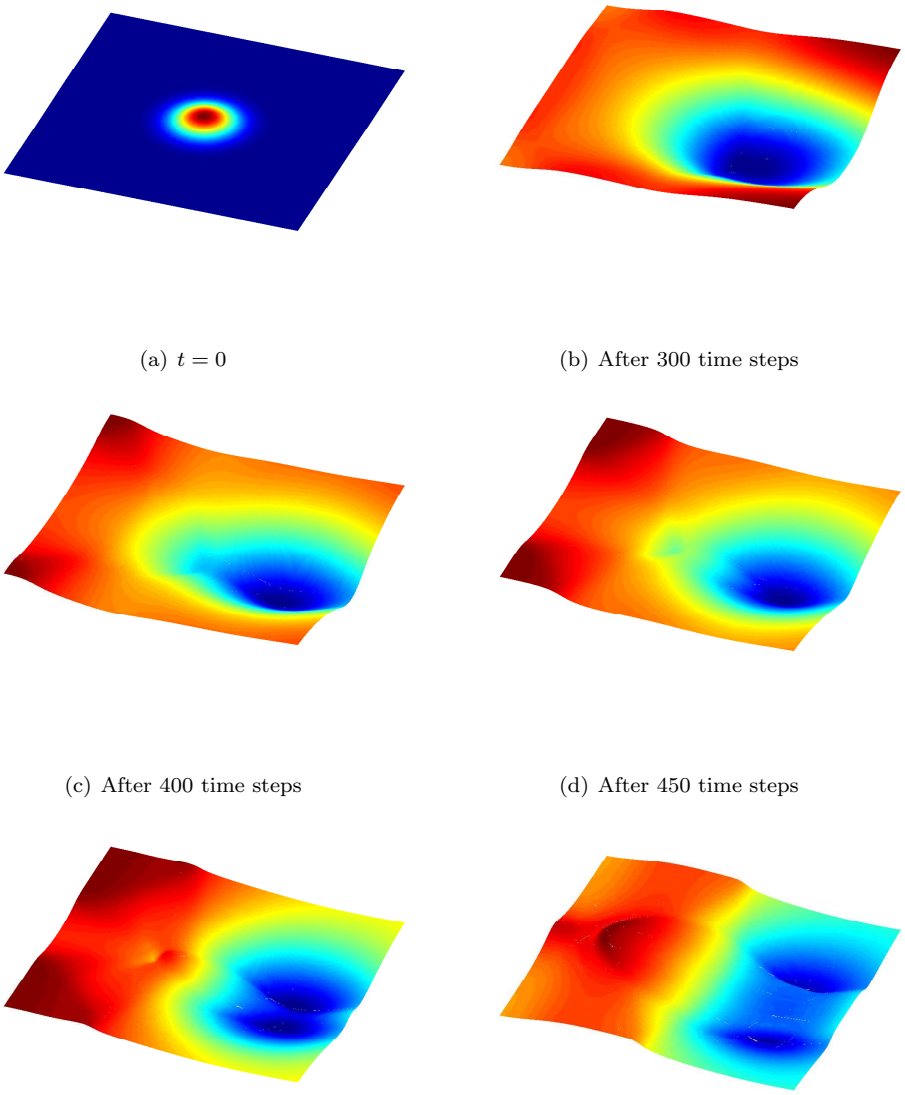

(a) $t = 0$ (b) After 300 time steps

(c) After 400 time steps (d) After 450 time steps

(e) After 500 time steps (f) After 600 time steps

FIG. 11.9. *Evolution of the water depth H for non-flat bathymetry case.*

Numerical results for transport equation, convection-diffusion equation, compressible Euler equation, and shallow water equation are presented to support the unification of the HDG methods.

REFERENCES

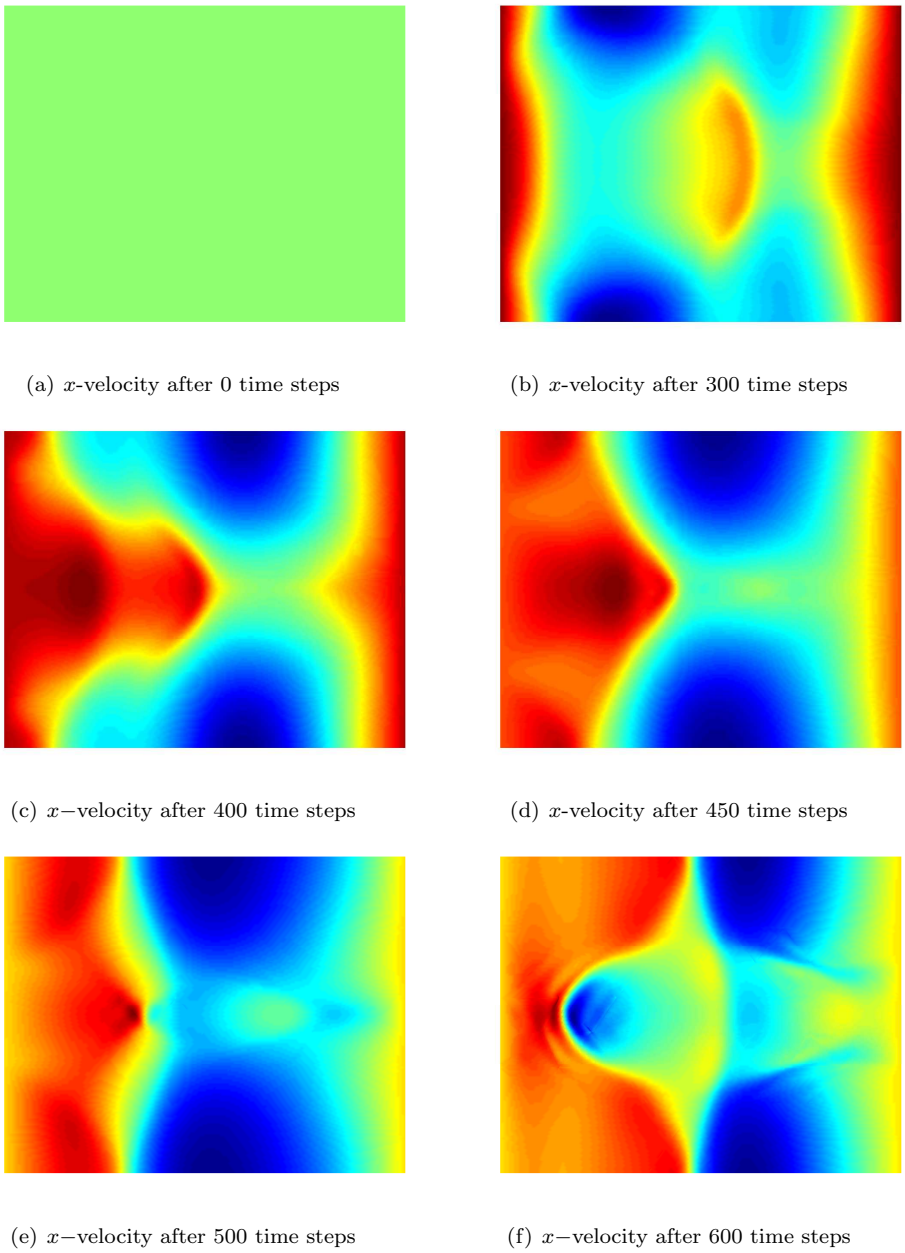

(a) x-velocity after 0 time steps

(b) x-velocity after 300 time steps

(c) $x-$velocity after 400 time steps

(d) x-velocity after 450 time steps

(e) $x-$velocity after 500 time steps

(f) $x-$velocity after 600 time steps

FIG. 11.10. *Evolution of depth average velocities u for non-flat bathymetry case.*

[1] NENAD ANTONIĆ AND KREVSIMIR BURAZIN, *Graph spaces of first-order linear partial differential operators*, Mathematical Communications, 14 (2009), pp. 135–155.
[2] ———, *Intrinsic boundary conditions for Friedrichs' systems*, Communications in Partial Differential Equations, 35 (2010), pp. 1690–1715.
[3] ———, *Boundary operator from matrix field formulation of boundary conditions for Friedrichs' systems*, Journal of Differential Equations, 250 (2011), pp. 2630–3651.
[4] A. BREUER, A. HEINECKE, S. RETTENBERGER, M. BADER A.A. GABRIEL, AND C. PELTIES, *Su-*

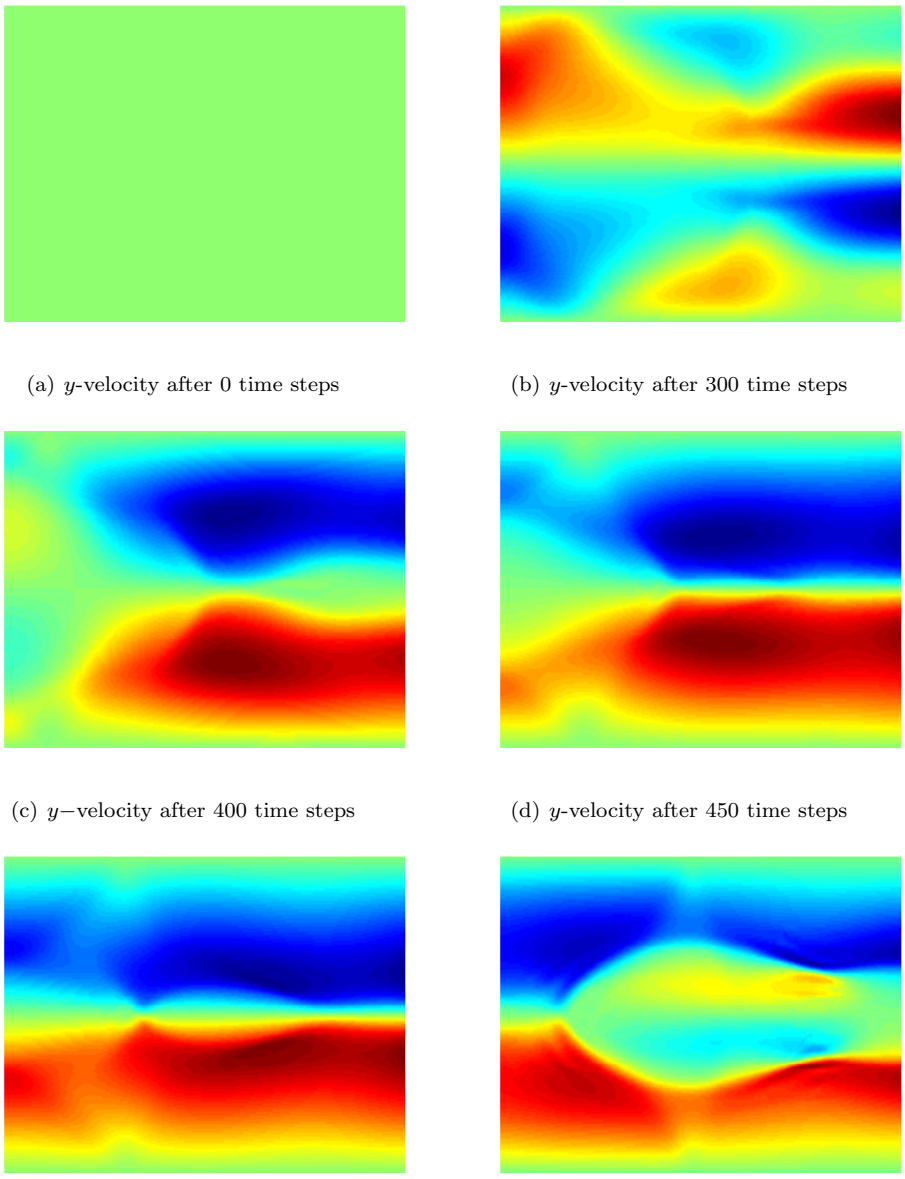

(a) y-velocity after 0 time steps

(b) y-velocity after 300 time steps

(c) $y-$velocity after 400 time steps

(d) y-velocity after 450 time steps

(e) $y-$velocity after 500 time steps

(f) $y-$velocity after 600 time steps

FIG. 11.11. *Evolution of depth average velocities v for non-flat bathymetry case.*

percomputing, Springer, 2013, ch. Sustained Petascale Performance of Seismic Simulations With SeisSol on SuperMUC, pp. 1–18.

[5] TAN BUI-THANH, CARSTEN BURSTEDDE, OMAR GHATTAS, JAMES MARTIN, GEORG STADLER, AND LUCAS C. WILCOX, *Extreme-scale UQ for Bayesian inverse problems governed by PDEs*, in SC12: Proceedings of the International Conference for High Performance Computing, Networking, Storage and Analysis, 2012. Gordon Bell Prize finalist.

[6] TAN BUI-THANH, LESZEK DEMKOWICZ, AND OMAR GHATTAS, *A unified discontinuous Petrov-*

Galerkin method and its analysis for Friedrichs' systems, SIAM J. Numer. Anal., 51 (2013), pp. 1933–1958.

[7] Tan Bui-Thanh and Omar Ghattas, *Analysis of an hp-non-conforming discontinuous Galerkin spectral element method for wave propagation*, SIAM Journal on Numerical Analysis, 50 (2012), pp. 1801–1826.

[8] B. Cockburn, B. Dong, J. Guzman, M. Restelli, and R. Sacco, *A hybridizable discontinuous Galerkin method for steady state convection-diffusion-reaction problems*, SIAM J. Sci. Comput., 31 (2009), pp. 3827–3846.

[9] B. Cockburn and J. Gopalakrishnan, *The derivation of hybridizable discontinuous Galerkin methods for Stokes flow*, SIAM J. Numer. Anal, 47 (2009), pp. 1092–1125.

[10] Bernardo Cockburn, Jay Gopalakrishnan, and Raytcho Lazarov, *Unified hybridization of discontinuous Galerkin, mixed, and continuous Galerkin methods for second order elliptic problems*, SIAM J. Numer. Anal., 47 (2009), pp. 1319–1365.

[11] B. Cockburn, J. Gopalakrishnan, and R. Lazarov, *Unified hybridization of discontinuous Galerkin, mixed, and continuous Galerkin methods for second order elliptic problems*, SIAM J. Numer. Anal., 47 (2009), pp. 1319–1365.

[12] Bernardo Cockburn, Jay Gopalakrishnan, and Francisco-Javier Sayas, *A projection-based error analysis of HDG methods*, Mathematics Of Computation, 79 (2010), pp. 1351–1367.

[13] Bernardo Cockburn, George E. Karniadakis, and Chi-Wang Shu, *Discontinuous Galerkin Methods: Theory, Computation and Applications*, Lecture Notes in Computational Science and Engineering, Vol. 11, Springer Verlag, Berlin, Heidelberg, New York, 2000.

[14] B. Cockburn, F. Li, N. C. Nguyen, and J. Peraire, *Hybridization and postprocessing techniques for mixed eigenfunctions*, SIAM J. Numer. Anal, 48 (2010), pp. 857–881.

[15] B. Cockburn, N. C. Nguyen, and J. Peraire, *A comparison of HDG methods for Stokes flow*, J. Sci. Comput., 45 (2010), pp. 215–237.

[16] B. Cockburn and C.-W. Shu, *The local discontinuous Galerkin finite element method for convection-diffusion systems*, SIAM Journal on Numerical Analysis, 35 (1998), pp. 2440–2463.

[17] J. Cui and W. Zhang, *An analysis of HDG methods for the Helmholtz equation*, IMA J. Numer. Anal., 34 (2014), pp. 279–295.

[18] H. Egger and J. Schoberl, *A hybrid mixed discontinuous Galerkin finite element method for convection-diffusion problems*, IMA Journal of Numerical Analysis, 30 (2010), pp. 1206–1234.

[19] Alexandre Ern and Jean-Luc Guermond, *Theory and Practice of Finite Elements*, vol. 159 of Applied Mathematical Sciences, Spinger-Verlag, 2004.

[20] ———, *Discontinuous Galerkin methods for Friedrichs' systems. Part I. General theory*, SIAM J. Numer. Anal., 44 (2006), pp. 753–778.

[21] ———, *Discontinuous Galerkin methods for Friedrichs' systems. Part II. Second-order elliptic PDEs*, SIAM J. Numer. Anal., 44 (2006), pp. 2363–2388.

[22] ———, *Discontinuous Galerkin methods for Friedrichs' systems. Part III. Multifield theories with partial coercivity*, SIAM J. Numer. Anal., 46 (2008), pp. 776–804.

[23] Alexandre Ern, Jean-Luc Guermond, and Gilbert Caplain, *An intrinsic criterion for the bijectivity of Hilbert operators related to Friedrichs' systems*, Communications in partial differential equations, 32 (2007), pp. 317–341.

[24] Kurt O. Friedrichs, *Symmetric positive linear differential equations*, Communications on pure and applied mathematics, XI (1958), pp. 333–418.

[25] Rajesh Gandham, David Medina, and Timothy Warburton, *GPU accelerated discontinuous Galerkin methods for shallow water equations*, arXiv, 1 (2014).

[26] S. K. Godunov, *A finite difference method for the computation of discontinuous solutions of the equations of fluid dynamics*, Mat. Sb., 44 (1959), pp. 357–393.

[27] R. Griesmaier and P. Monk, *Error analysis for a hybridizable discontinous Galerkin method for the Helmholtz equation*, J. Sci. Comput., 49 (2011), pp. 291–310.

[28] J. Hesthaven and T. Warburton, *High-order accurate methods for time-domain electromagnetics*, Comp. Mod. Engin. Sci., 5 (2004), pp. 395–408.

[29] Jan S. Hesthaven and Timothy Warburton, *Nodal high-order methods on unstructured grids. I. Time-domain solution of Maxwell's equations*, Journal of Computational Physics, 181 (2002), pp. 186–221.

[30] Jan S. Hesthaven and Timothy Warburton, *Nodal Discontinuous Galerkin Methods: Algorithms, Analysis, and Applications*, vol. 54 of Texts in Applied Mathematics, Springer, 2008.

[31] Paul Houston, Max Jensen, and Endre Süli, *hp-Discontinuous Galerkin finite element methods with least-squares stabilization*, Journal of Scientific Computing, 17 (2002), pp. 3–25.

[32] Max Jensen, *Discontinuous Galerkin methods for Friedrichs' systems with irregular solutions*, PhD thesis, University of Oxford, 2004.

[33] C. Johnson and J. Pitkäranta, *An analysis of the discontinuous Galerkin method for a scalar hyperbolic equation*, Mathematics of Computation, 46 (1986), pp. 1–26.

[34] R. M. Kirby, S. J. Sherwin, and B. Cockburn, *To CG or to HDG: A comparative study*, J. Sci. Comput., 51 (2012), pp. 183–212.

[35] P. LeSaint and P. A. Raviart, *On a finite element method for solving the neutron transport equation*, in Mathematical Aspects of Finite Element Methods in Partial Differential Equations, C. de Boor, ed., Academic Press, 1974, pp. 89–145.

[36] R. J. LeVeque, *Finite Volume Methods for Hyperbolic Problems*, Cambridge University Press, 2002.

[37] L. Li, S. Lanteri, and R. Perrrussel, *A hybridizable discontinuous Galerkin method for solving 3D time harmonic Maxwell's equations*, in Numerical Mathematics and Advanced Applications 2011, Springer, 2013, pp. 119–128.

[38] ———, *A hybridizable discontinuous Galerkin method combined to a Schwarz algorithm for the solution of 3D time harmonic Maxwell's equations*, Journal Computational Physics, 256 (2014), pp. 563–581.

[39] A. H. Mohammadian, V. Shankar, and W. F. Hall, *Computational of electromagmetic scattering and radiation using a time domain finite volume discretization procedure*, Comput. Phys. Commun., 68 (1991), pp. 175–196.

[40] D. Moro, N. C. Nguyen, and J. Peraire, *Navier-Stokes solution using hybridizable discontinuous Galerkin methods*, American Institute of Aeronautics and Astronautics, 2011-3407 (2011).

[41] N. C. Nguyen and J. Peraire, *Hybridizable discontinuous Galerkin methods for partial differential equations in continuum mechanics*, Journal Computational Physics, 231 (2012), pp. 5955–5988.

[42] N. C. Nguyen, J. Peraire, and B. Cockburn, *An implicit high-order hybridizable discontinuous Galerkin method for linear convection-diffusion equations*, Journal Computational Physics, 228 (2009), pp. 3232–3254.

[43] ———, *An implicit high-order hybridizable discontinuous Galerkin method for nonlinear convection-diffusion equations*, Journal Computational Physics, 228 (2009), pp. 8841–8855.

[44] ———, *A hybridizable discontinous Galerkin method for Stokes flow*, Comput Method Appl. Mech. Eng., 199 (2010), pp. 582–597.

[45] ———, *High-order implicit hybridizable discontinuous Galerkin method for acoustics and elastodynamics*, Journal Computational Physics, 230 (2011), pp. 3695–3718.

[46] ———, *Hybridizable discontinuous Galerkin method for the time harmonic Maxwell's equations*, Journal Computational Physics, 230 (2011), pp. 7151–7175.

[47] ———, *An implicit high-order hybridizable discontinuous Galerkin method for the incompressible Navier-Stokes equations*, Journal Computational Physics, 230 (2011), pp. 1147–1170.

[48] J. Peraire, N. C. Nguyen, and B. Cockburn, *A hybridizable discontinuous Galerkin for compressible Euler and Navier-Stokes equations*, American Institute of Aeronautics and Astronautics, 2010-363 (2010).

[49] D. A. Di Pietro and A. Ern, *Mathematical aspects of Discontinuous Galerkin methods*, Springer, 2012.

[50] W. H. Reed and T. R. Hill, *Triangular mesh methods for the neutron transport equation*, Tech. Report LA-UR-73-479, Los Alamos Scientific Laboratory, 1973.

[51] P. L. Roe, *Approximate riemann solvers, parametric vectors, and difference schemes*, Journal of Computational Physics, 43 (1981), pp. 357–372.

[52] O. San and K. Kara, *High-order accurate spectral difference method for shallow water equations*, International Journal of Research and Reviews in Applied Sciences, 6 (2011), pp. 41–54.

[53] Eleuterio F. Toro, *Riemann Solvers and Numerical Methods for Fluid Dynamics*, Springer, 1999.

[54] Lucas C. Wilcox, Georg Stadler, Carsten Burstedde, and Omar Ghattas, *A high-order discontinuous Galerkin method for wave propagation through coupled elastic-acoustic media*, Journal of Computational Physics, 229 (2010), pp. 9373–9396.

[55] Y. Xing and X. Zhang, *Positivity-preserving well-balanced discontinuous Galerkin methods for the shallow water equations on unstructured triangular meshes*, J. Sci. Comput., 57 (2013), pp. 19–41.